From *Columbia* to *Discovery*: Understanding the Impact Threat to the Space Shuttle (Abridged)

James D. Walker

Southwest Research Institute

San Antonio, Texas 78228

The work described in this talk was paid for by the American taxpayer through NASA and the Columbia Accident Investigation Board.

Lots of People

Photograph during *Columbia* investigation

Lots of people worked on the *Columbia* accident investigation and return to flight.

Some who directly helped with the impact-related material in this talk:

Donald J. Grosch (SwRI)
Sidney Chocron (SwRI)
Walt Gray (SwRI)
Justin Kerr (NASA/JSC)
Freeman Bertrand (Jacobs/Sverdrup)
Paul Parker (Boeing)
Mike Dunham (Boeing)

Southwest Research Institute

The *Columbia* Accident

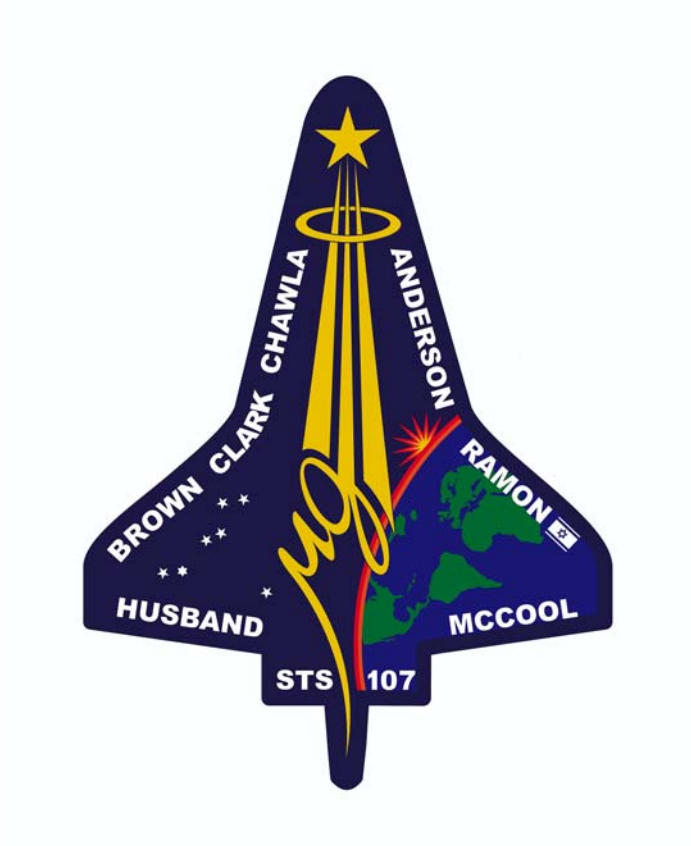

STS-107

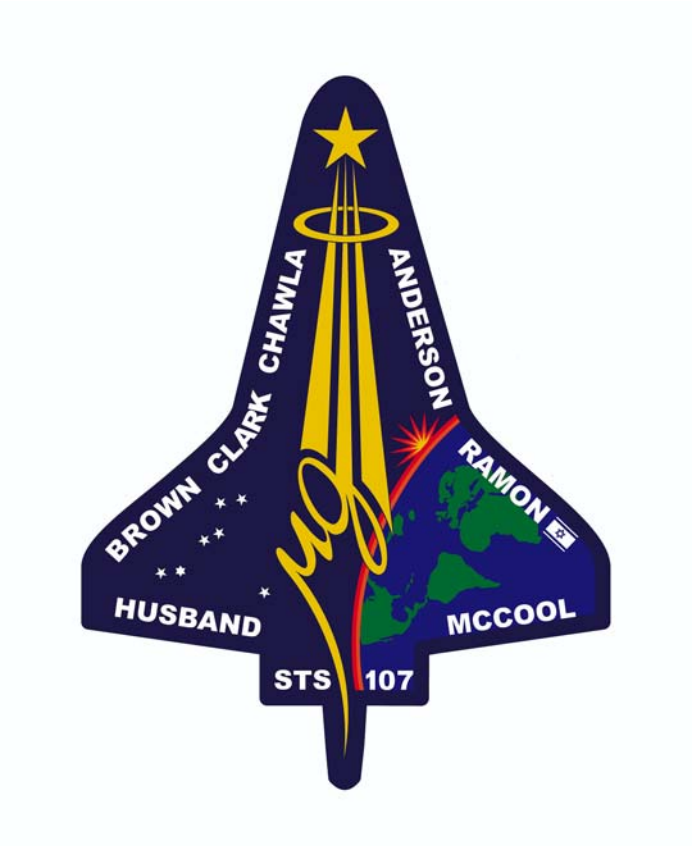

- 113th flight of the Space Shuttle Program
- 28th flight of *Columbia*
- *Columbia* was the first Shuttle to fly (April, 1981)
- Launched January 16, 2003
- Disintegrated on re-entry, February 1, 2003
- Crewed by
  - Rick Husband
  - William C. McCool
  - Michael P. Anderson
  - David M. Brown
  - Kalpana Chawla
  - Laurel Clark
  - Ilan Ramon

CAIB Report, Volume I

- Volume 1 of the Columbia Accident Investigation Report was published August 26, 2003
- It can be found at the CAIB web site: www.caib.us
- The conclusions were that there were two causes of the loss of the *Columbia*:
  - A physical cause
  - An organizational cause
- SwRI was involved in identifying the physical cause, discussed in Chapter 3 of the Volume I with more details in Volume II and a NASA report.

Columbia Accident Investigation Board Report, Volume II, Appendix D.12 (Oct. 2003)

APPENDIX D.12

Impact Modeling

Submitted by James D. Walker
Southwest Research Institute

EXECUTIVE SUMMARY

After the loss of the Orbiter *Columbia* during reentry on February 1, 2003, Southwest Research Institute (SwRI) was contracted by the Columbia Accident Investigation Board (CAIB) to perform impact modeling in support of the investigation. At the SwRI site, the CAIB in conjunction with the NASA Accident Investigation Team (NAIT) was performing impact tests against thermal protection system structures, including thermal tiles and fiberglass and reinforced carbon carbon (RCC) leading edges. To complement the extensive modeling work being carried out by the NAIT, the CAIB wished to support an independent analysis of the impact event.

model was developed to model the panel and an analytic boundary condition was developed to model the pressure load supplied by the impacting foam. Once again, central to the load delivered and the stresses calculated is the normal component of the foam impact velocity. Comparison with the two tests performed against RCC panels led to estimates of failure stresses within the panel material. Parametric studies were performed with the model to investigate the question of impact location and to investigate the effect of foam impactors with rotational velocity. It was shown that a nonzero rotation velocity for the foam impactor nearly always increased the stresses on both the panel face and the rib of the panel. Computations were performed to determine the most severe loads within the framework of impact location

Bipod Ramp Foam Insulation

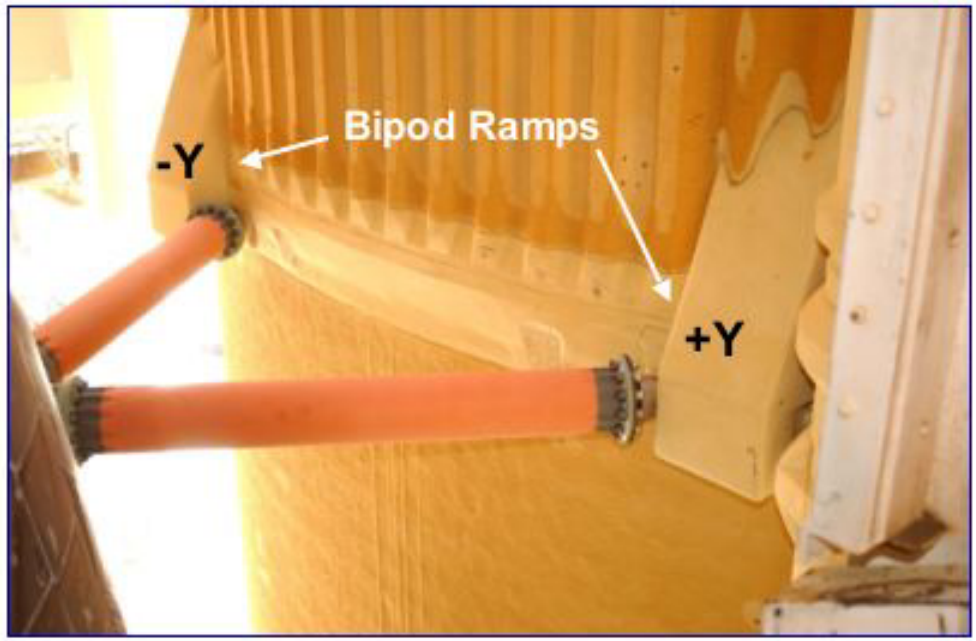

Foam Impact on STS-107

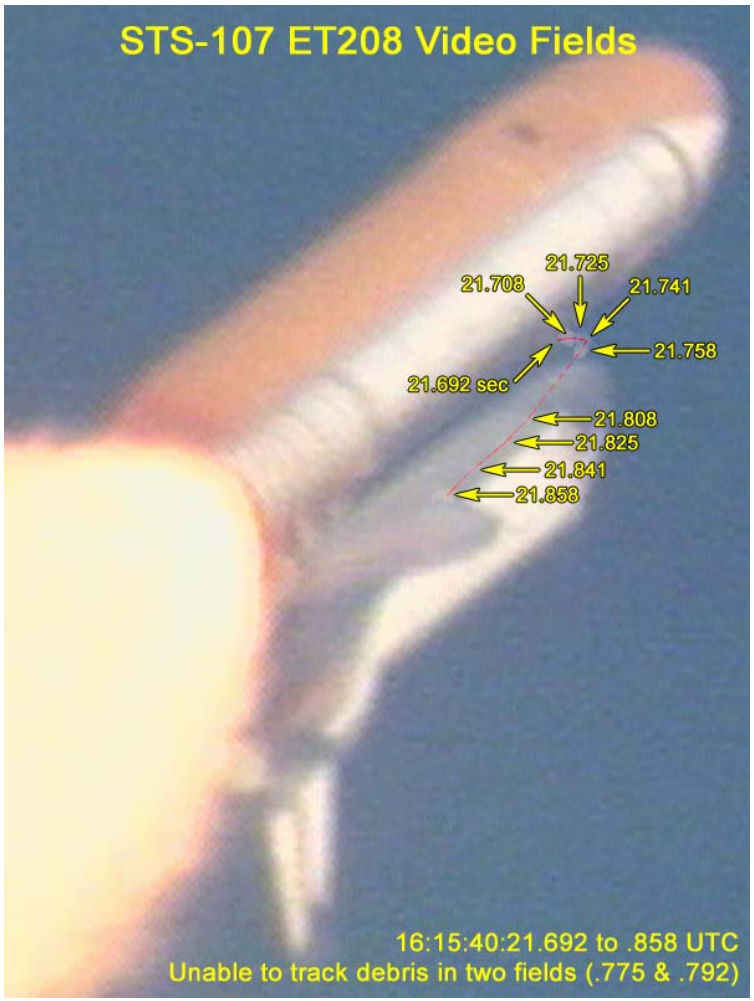

- 81.7 seconds into flight, the bipod ramp foam insulation broke away.
- The shuttle was at 66,000 ft.
- The shuttle velocity was mach 2.46 (1580 mph).
- The foam traversed the 58 feet between the bipod connection and the left wing in 0.16 seconds.
- The refined estimate of the impact velocity was 775 ft/s (528 mph).
- Estimated foam mass: 1.67 pounds.
- Estimated size: 21” × 11.5” × 5.5”

Possible Impact Locations

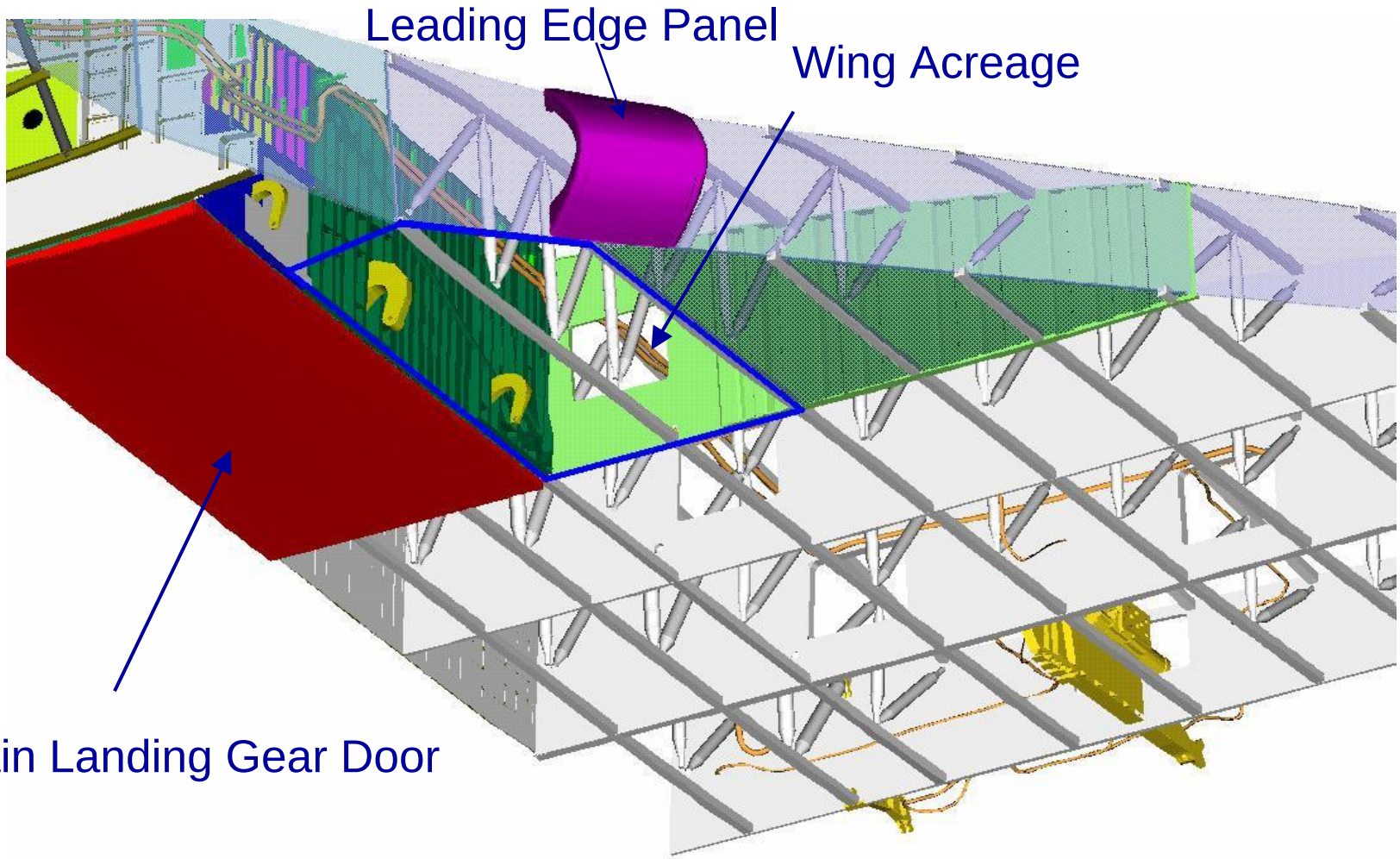

Shifting Focus

Modular Auxiliary Data System Recorder

- Early telemetry showed first anomalies in left main landing gear bay.
- Upon recovery of the Modular Auxiliary Data System recorder on March 19, 2003, analysis of the data led attention to the leading edge.

Main Landing Gear Door

Main Landing Gear Door from *Enterprise*

SwRI Large Compressed Gas Gun

- 500 gallon tank, 275 psi working pressure, 10-inch diameter by 35-foot long barrel.
- Typically used to launch large, irregularly-shaped projectiles.
- Helium or Nitrogen is used as the driver gas.

Launching Foam

Main Landing Gear Door Tests

- Performed 5 impact tests on the left Main Landing Gear Door.
- These impacts demonstrated that at the speed (775 ft/s) and angles of impact on the tiles (up to 13°) the foam barely damages the tiles.

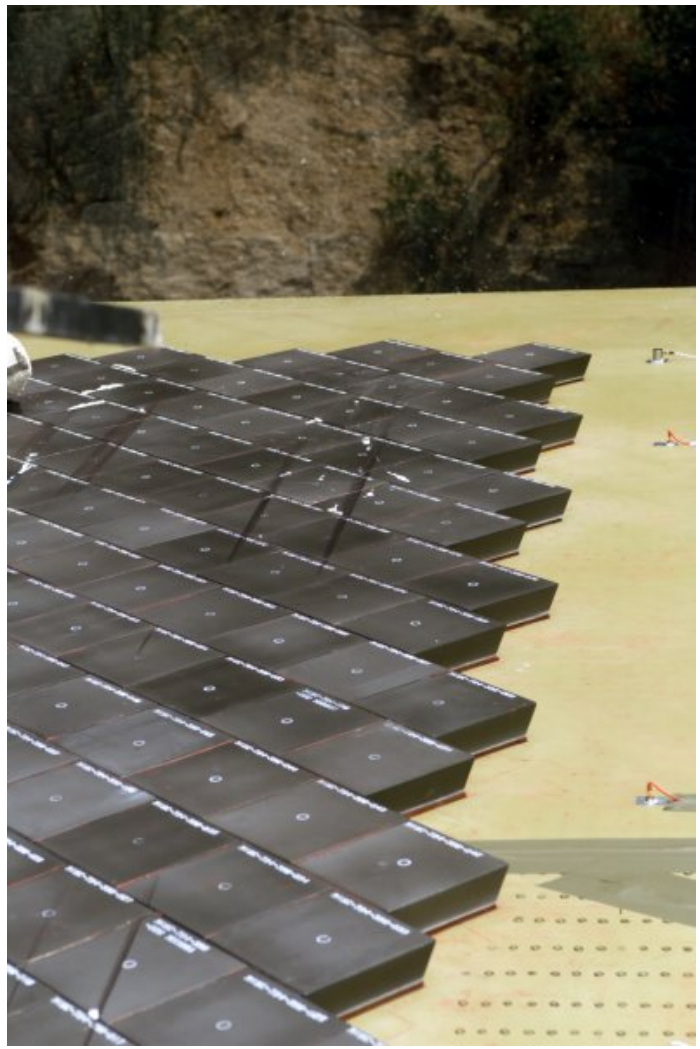

Tile and Foam Modeling

Foam Insulation Compression Tests

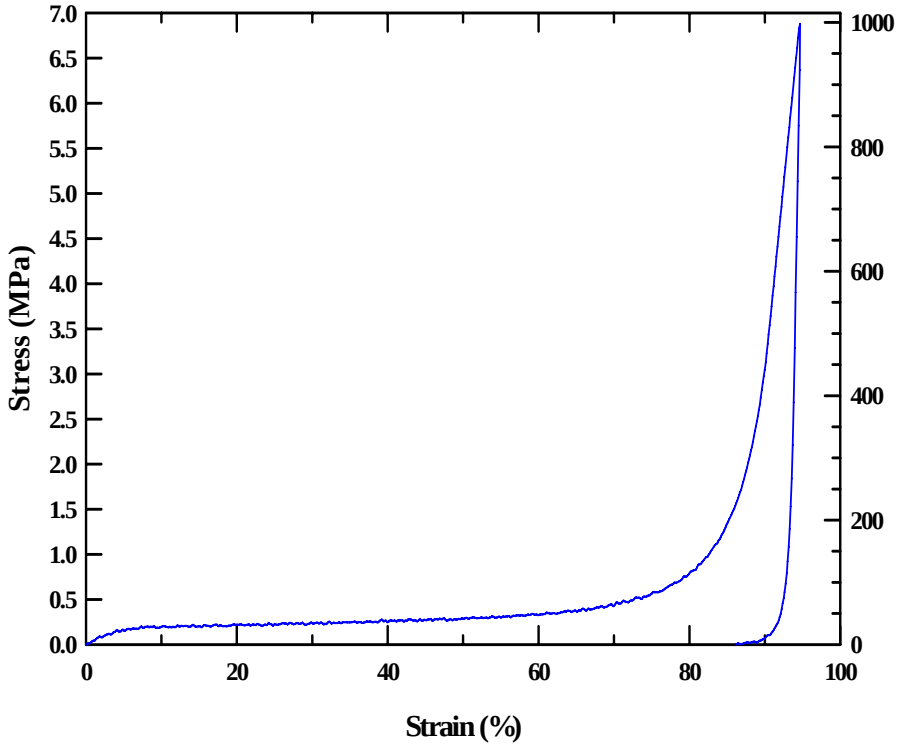

Stress-strain curve for sample 1

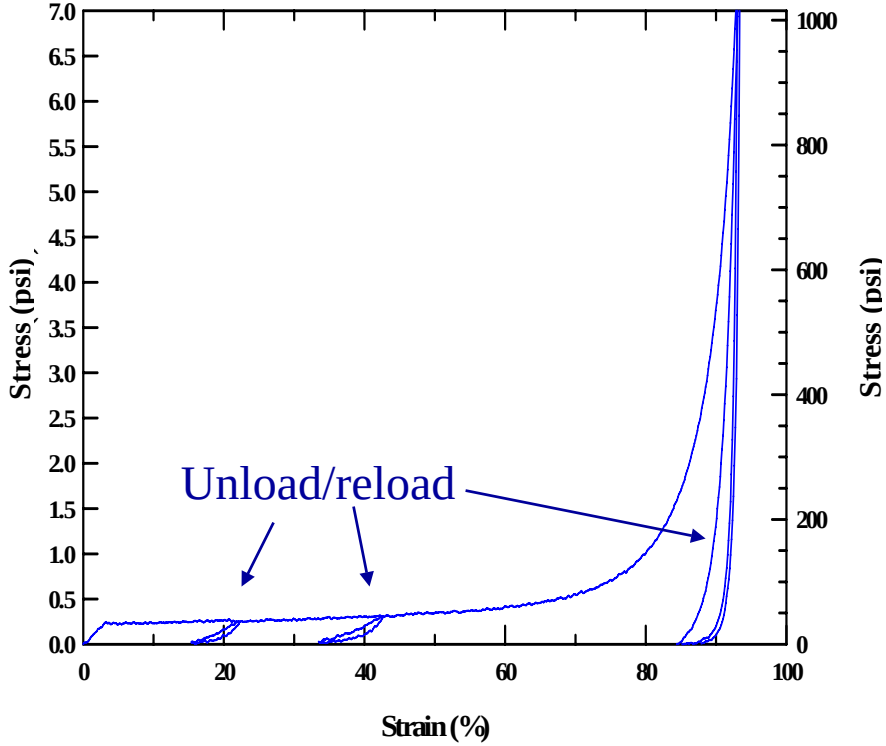

Stress-strain curve for sample 2

Transverse compression tests on roughly 2” cube tile samples taken from tile MISC-794-400-120

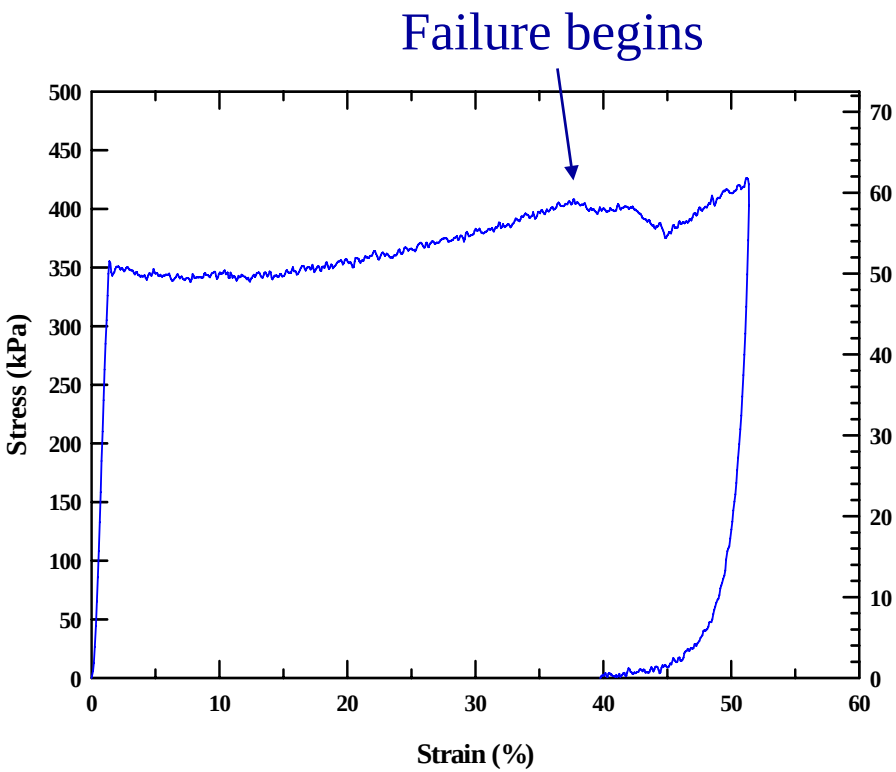

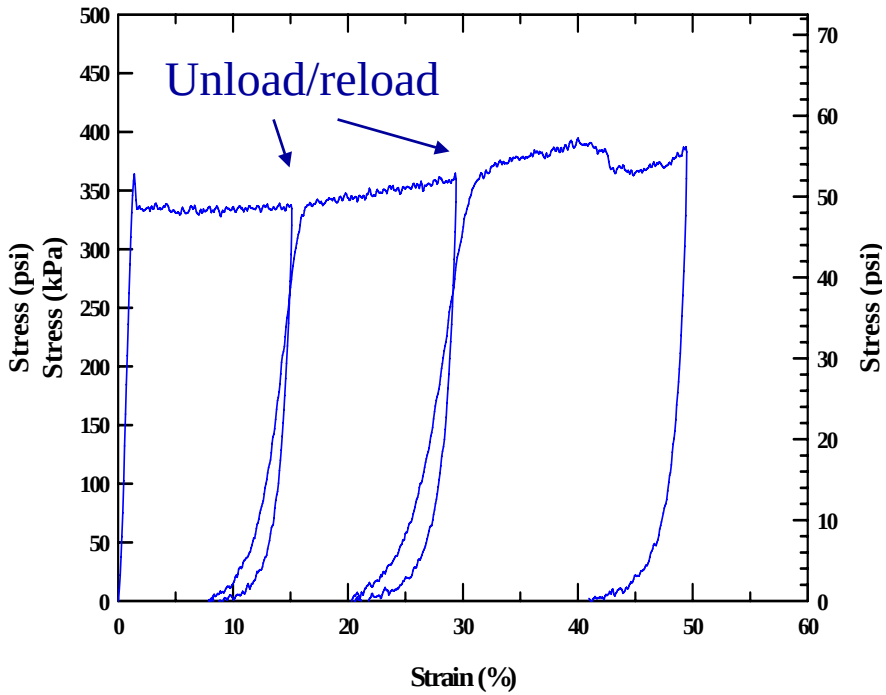

Crushing begins at 345 kPa (50 psi)

New EOS Model for Foam Insulation

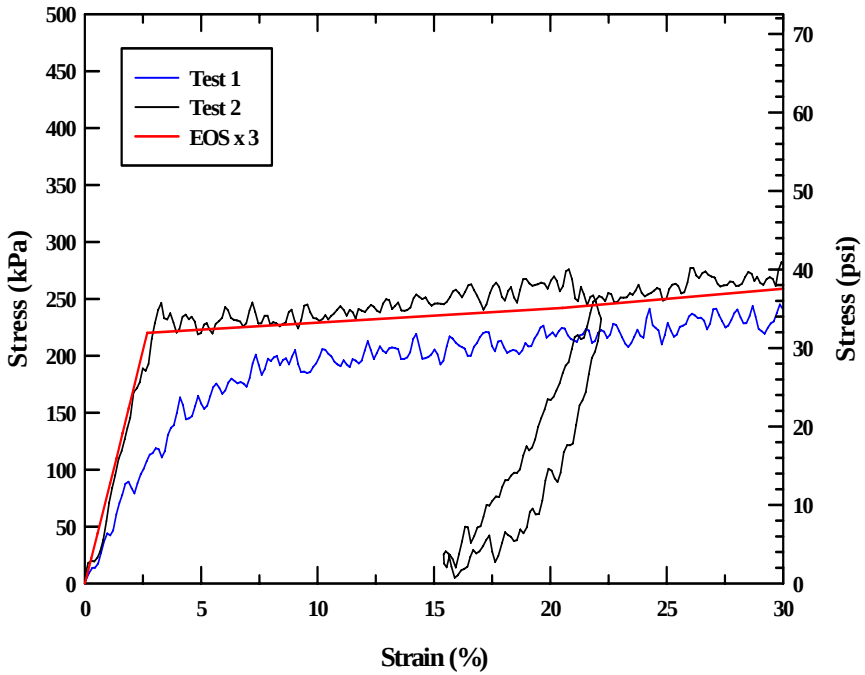

Enlargement of low strain region, blue and black are data, red is model

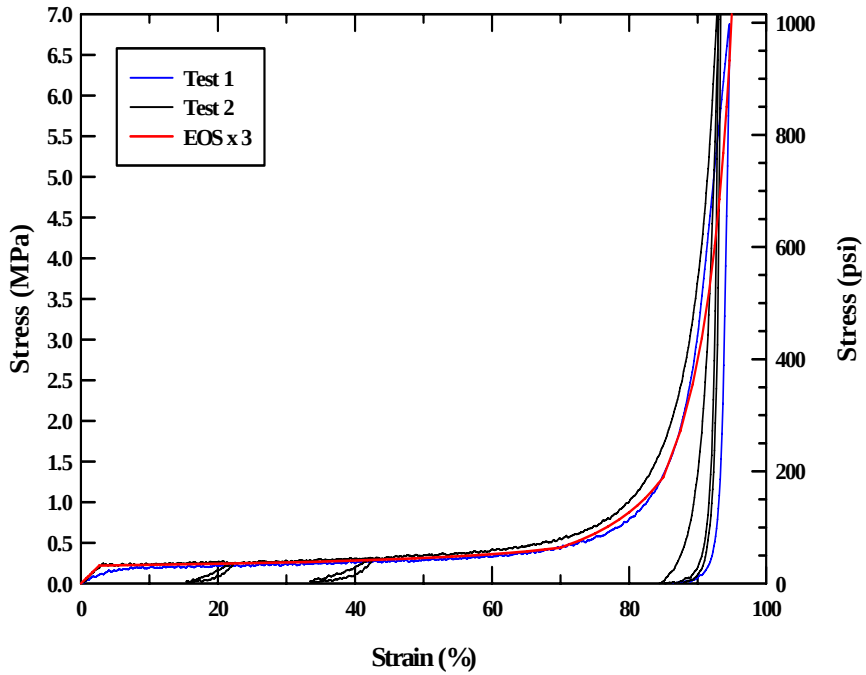

Full stress-strain curve, blue and black are data, red is model

Foam density is 0.03844 gm/cm^3 (2.4 lb/ft^3), initial crushup stress is 220 kPa (32 psi)

New EOS Model for Thermal Tile

Stress if yield did not occur; however, material model incorporates a yield at 400 kPa (58 psi)

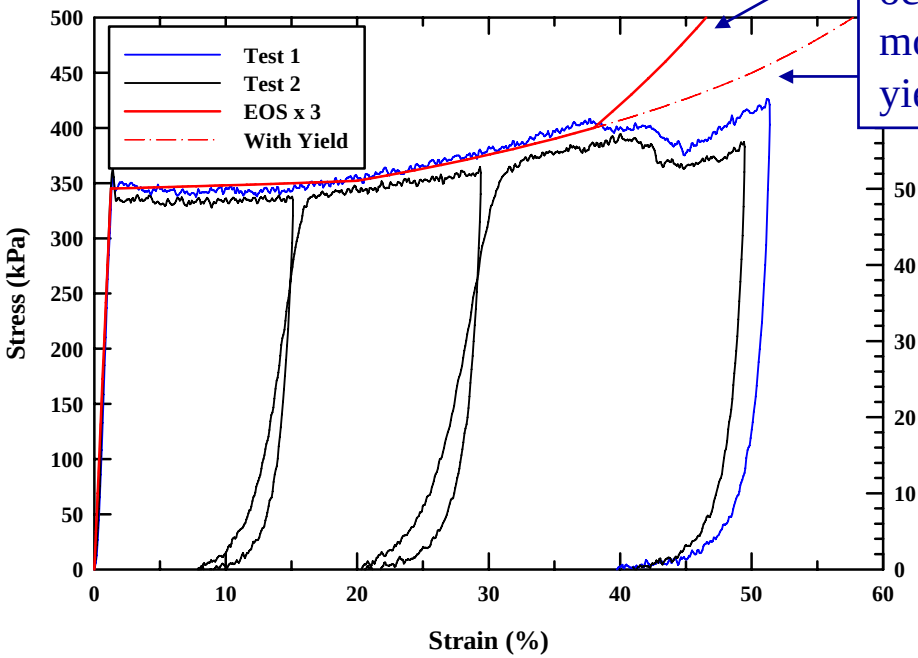

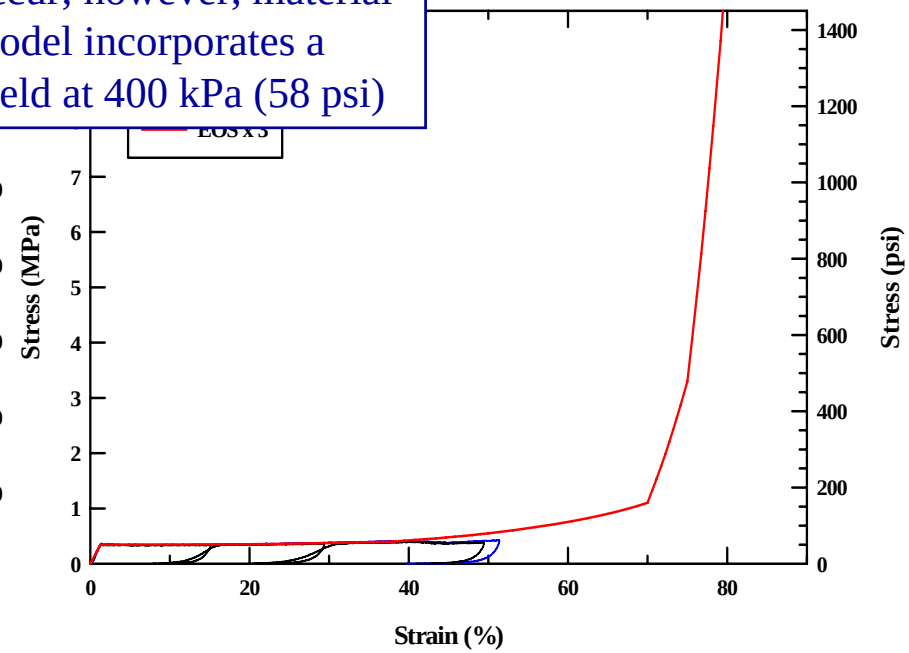

Enlargement of low strain region, blue and black are data, red is model

Full stress-strain curve, blue and black are data, red is model

Tile density is 0.18 gm/cm^3 (11.2 lb/ft^3), initial crushup stress is 345 kPa (50 psi)

Computations

Computations

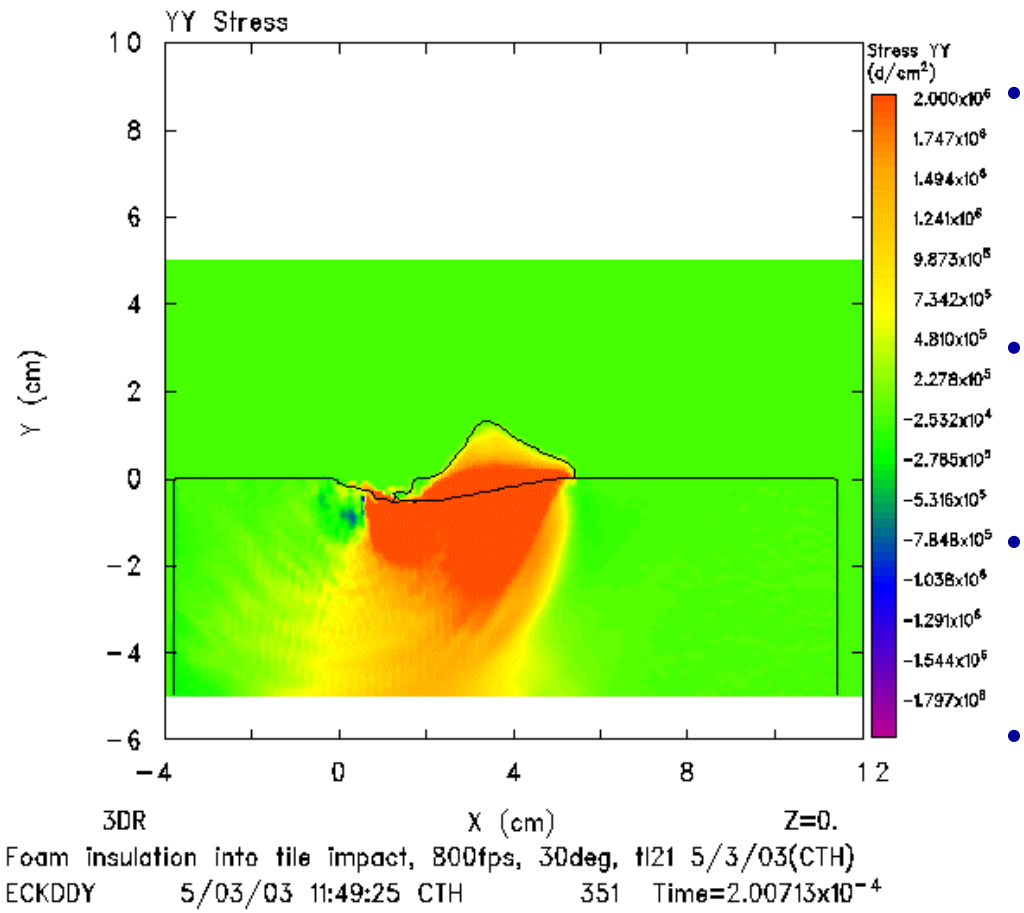

- Most computations were performed in 2D plane strain – however, there was excellent agreement between 2D plane strain and 3D.
- The normal stress was examined along the surface of the tile gages (“tracers”) spaced 0.5 cm apart.
- The gage readings show the normal stress in the *y* direction at the respective location.
- Computations performed in CTH with new material models.

How Damage/No Damage was Decided

No Damage for 700 ft/s Impact at 15º Impact Angle

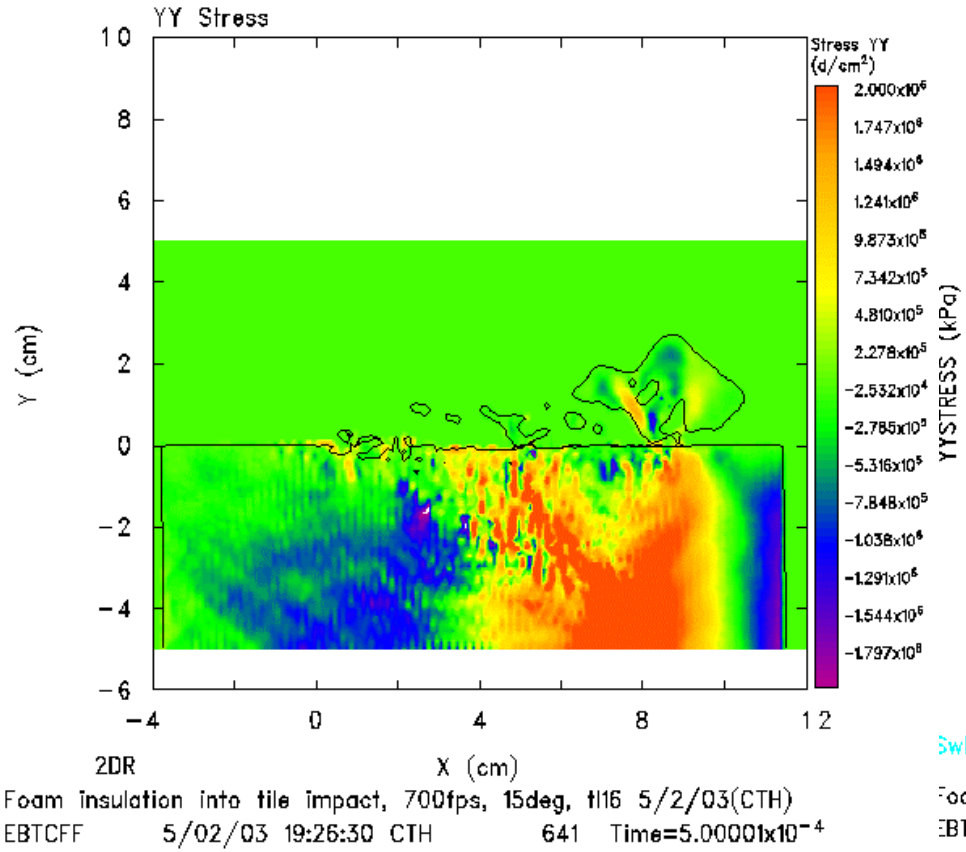

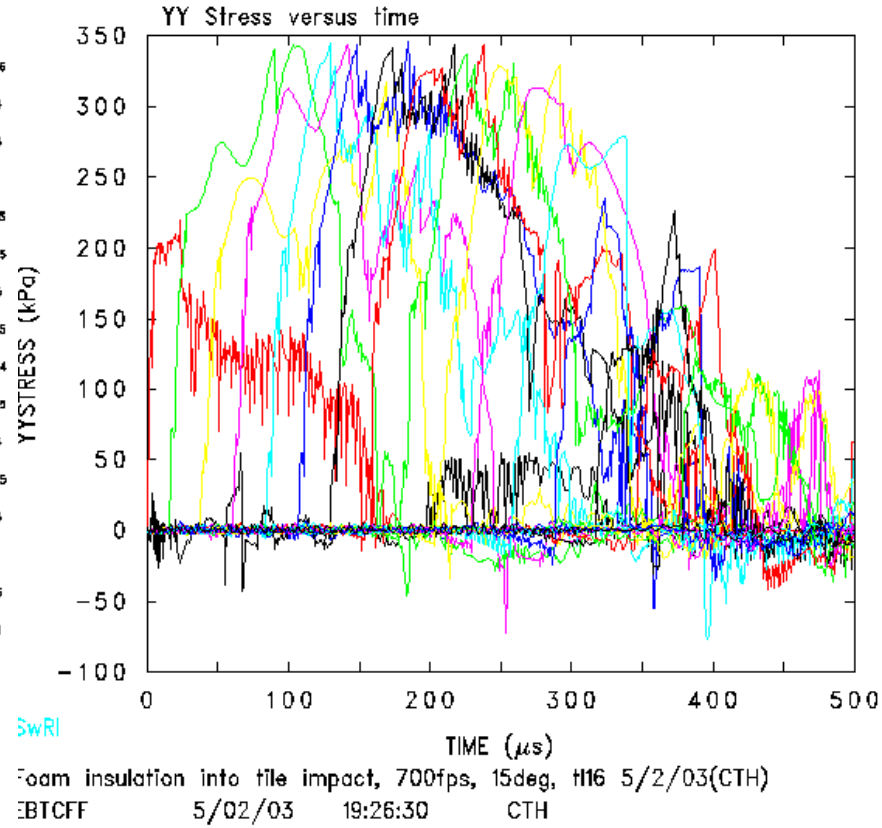

Tile surface mostly flat after impact; normal stresses are below 345 kPa (50 psi) tile crushup level

Crater for 700 ft/s Impact at 23º Impact Angle

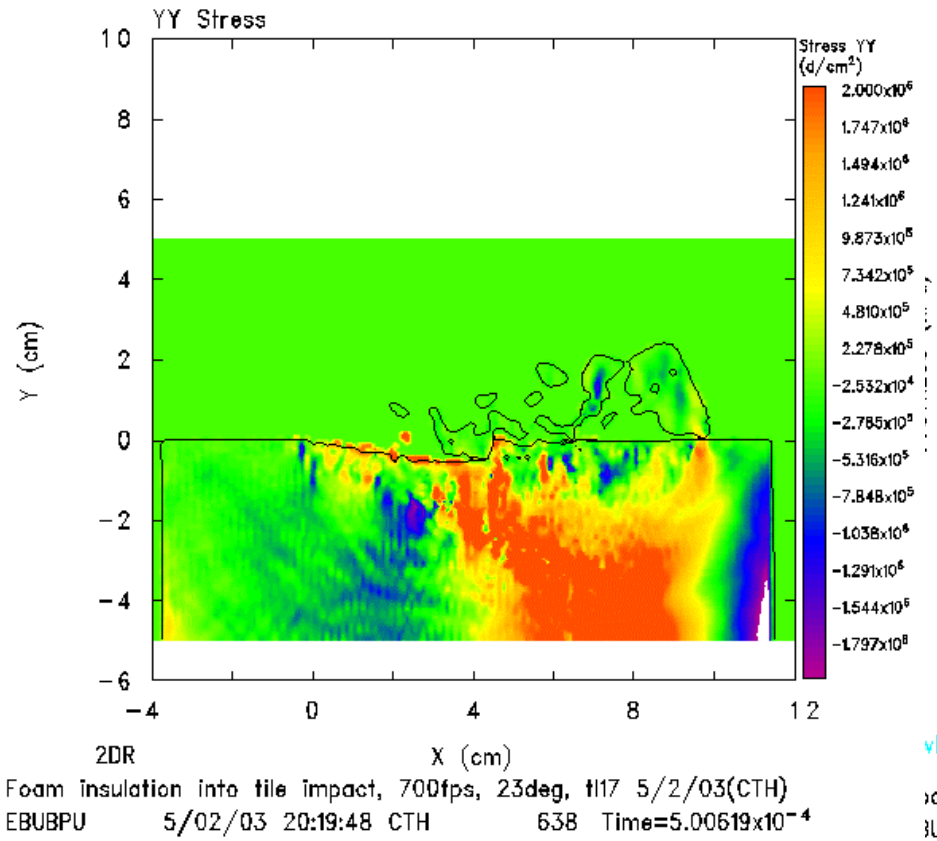

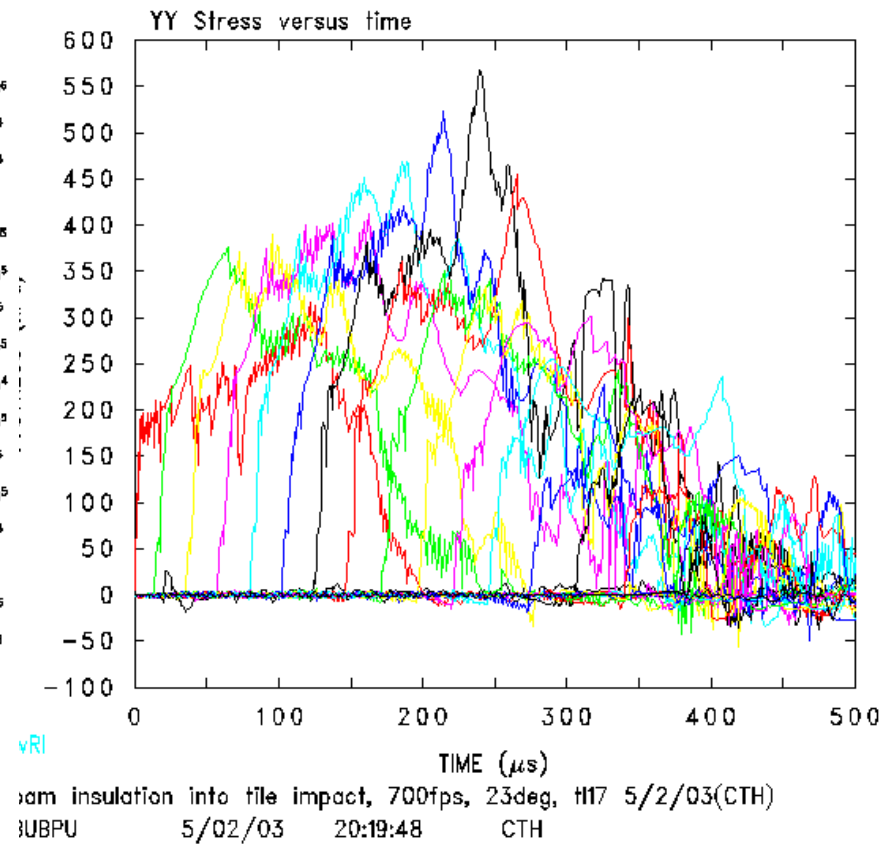

Crater (indention) seen in target; normal stresses are above 345 kPa (50 psi) tile crushup and 400 kPa (58 psi) tile yield/failure

Results on Damage/No Damage Transition Region

Damage/No Damage Transition

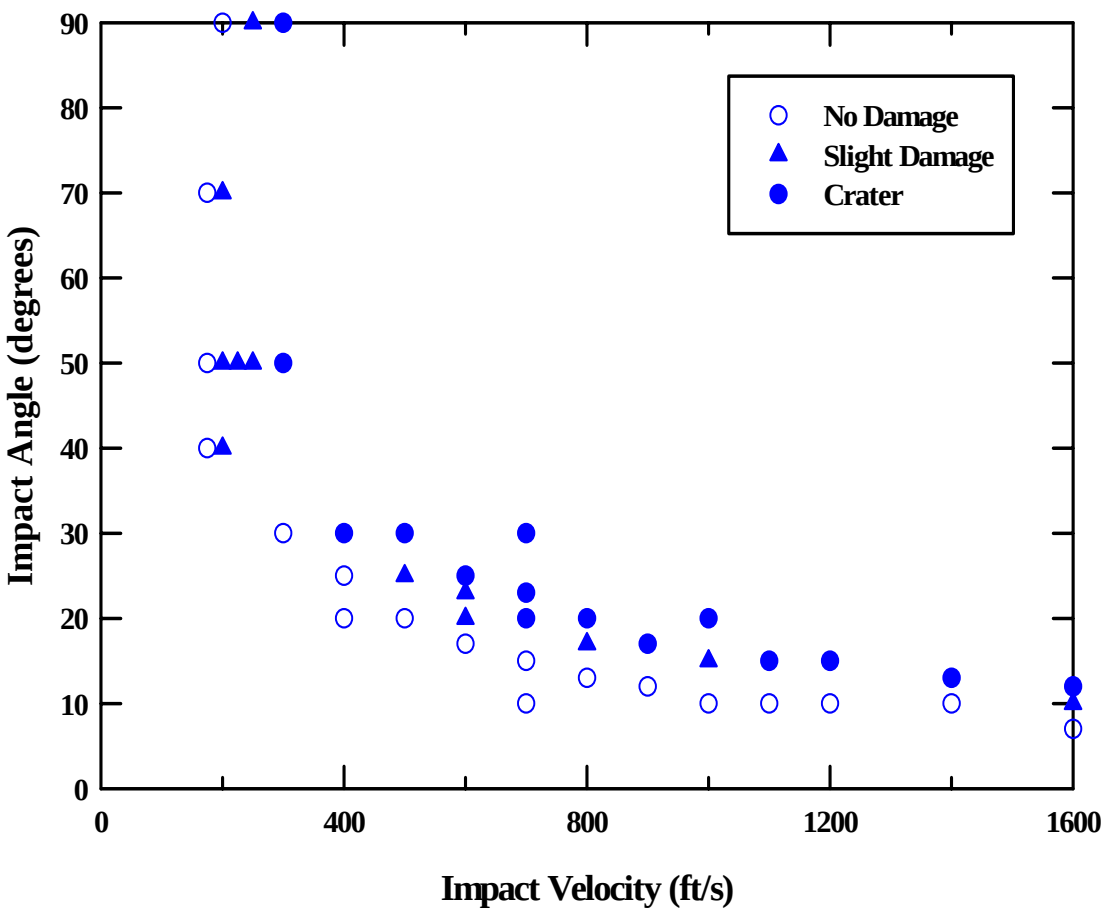

- Many CTH computations were performed using new EOS with 1” cubes of foam insulation impacting a tile.
- These computations allowed a determination of where the transition from no damage to damage occurred, in terms if impact velocity and impact angle.
- Figure shows results of computations.

Theory

- It is possible to determine the impact velocity at 90 degrees (flyer plate) at which the thermal tile just begins to crush. The velocity is given by

$$V_{crush} = u_{et} + u_{ef} + \frac{\sigma_{crush-t} - \sigma_{crush-f}}{\rho_{ef}\left(c_{1f} + u_{ef}\right)}$$

where σ is stress, *c* is sound speed, subscript *t* refers to tile, *f* to foam, *e* to elastic, and

$$u_e = \sigma_{crush} / \rho_0 c_0, \qquad \rho_e = \rho_0 / (1 - u_e / c_e)$$

- When computed, V_{crush} = 68.2 m/s (224 ft/s). This value was confirmed by 1D CTH computations.

Theory

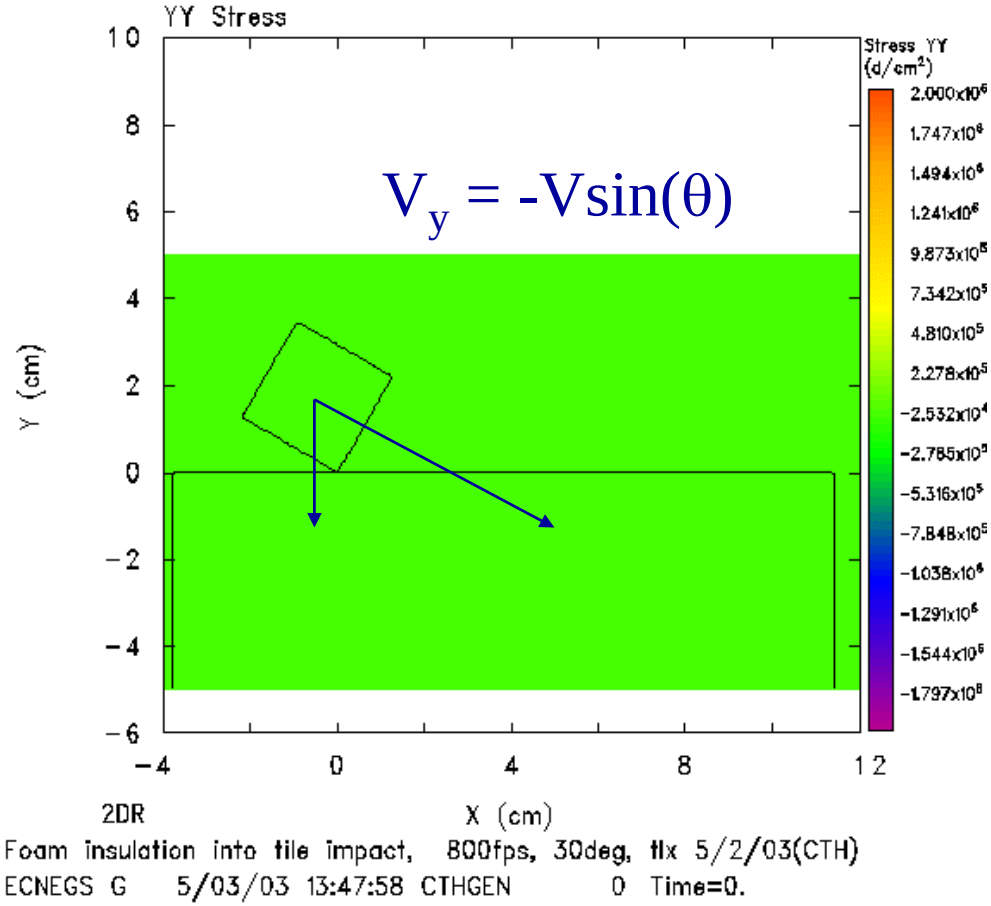

$$V_y = -V\sin(\theta)$$

- When foam impacts the tile at an angle, the horizontal and downward components of the velocity interact nearly separately if the interface remains relatively flat.
- Thus, crushing of the thermal tile would be expected when

$$V = \frac{V_{crush}}{\sin(\theta)}$$

Damage/No Damage Transition

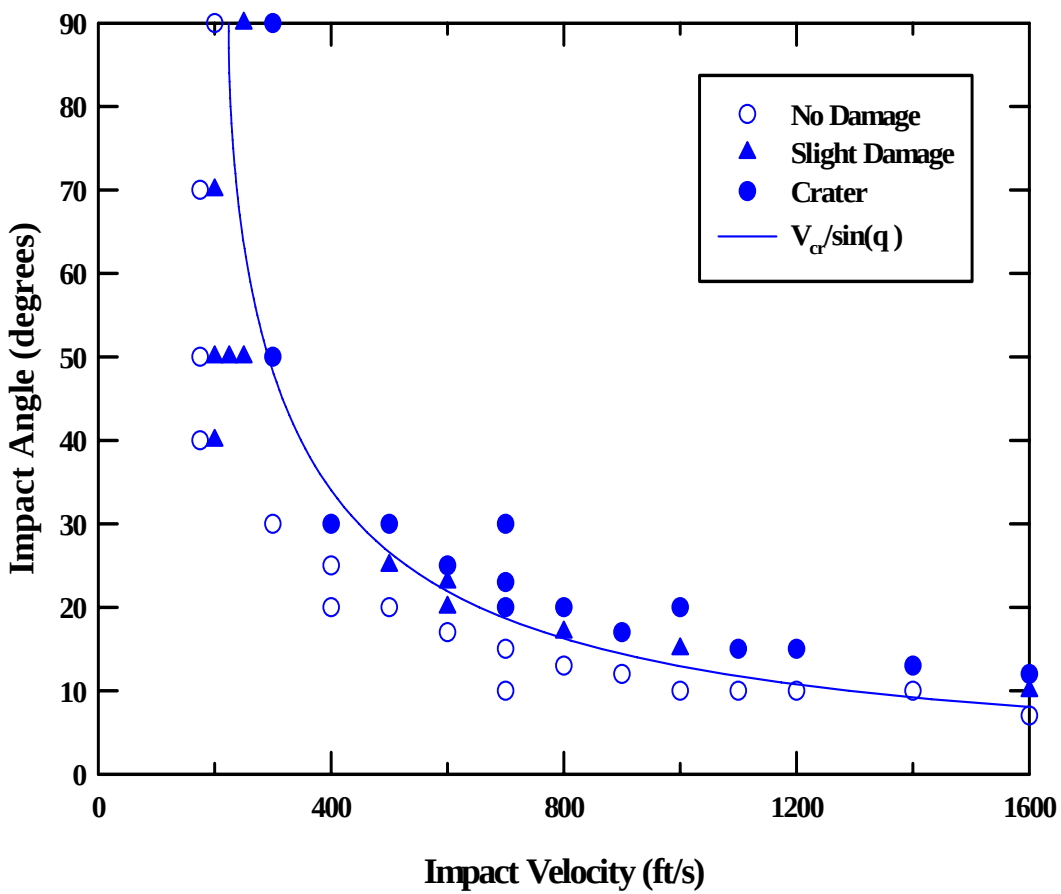

- When the computed V_{crush} = 68.2 m/s (224 ft/s) is used, good agreement is obtained with the computational results.

Damage/No Damage Transition

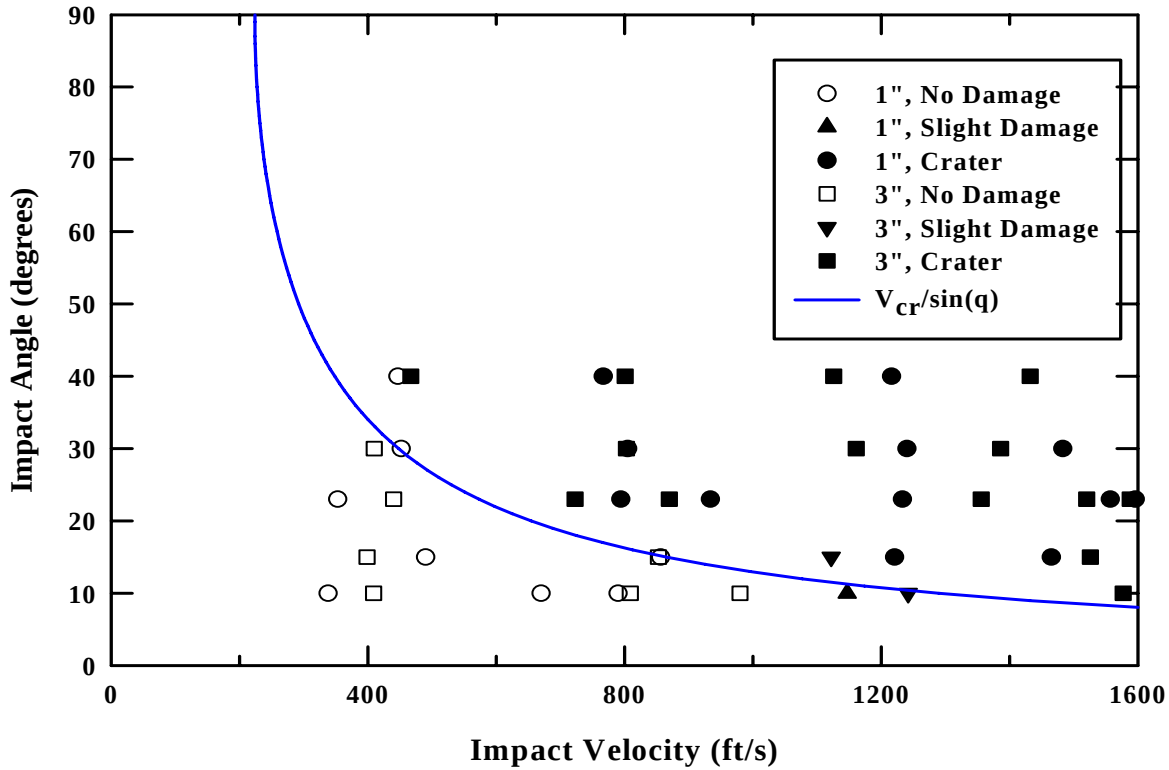

1999 foam impact data with 1” square cross section

Damage/No Damage Transition

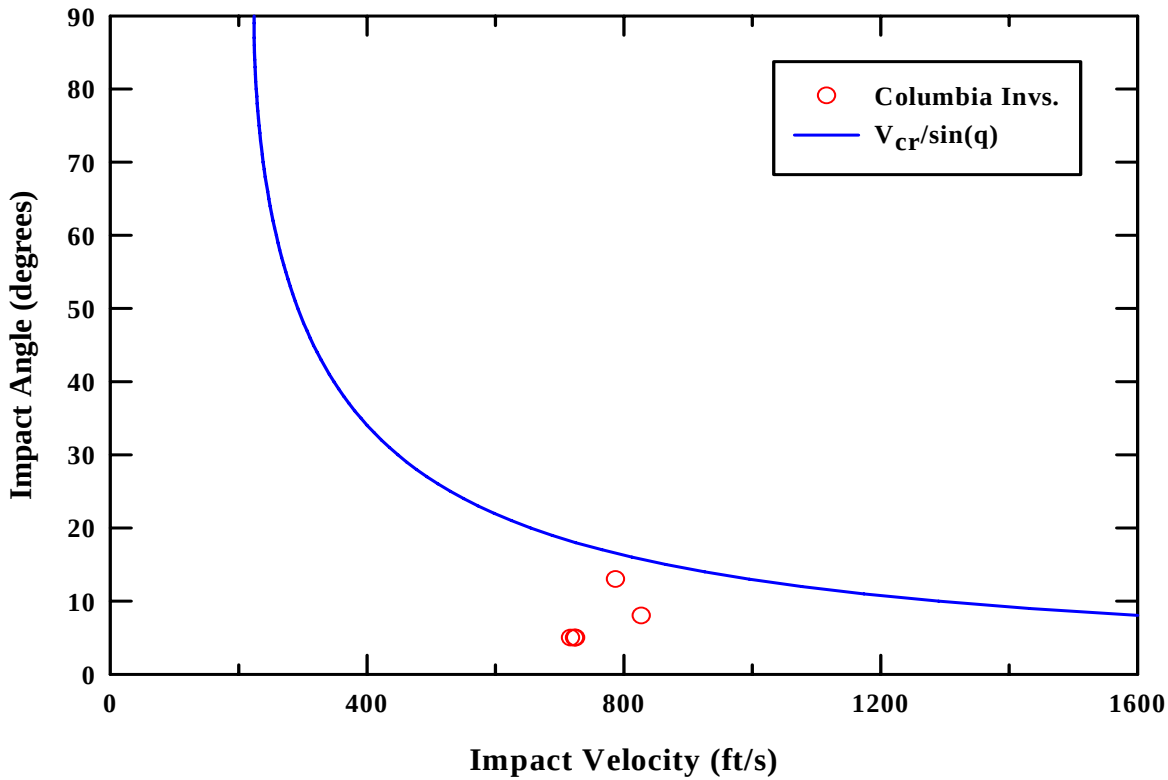

Five impact tests during Columbia investigation (minimal damage)

Damage/No Damage Transition

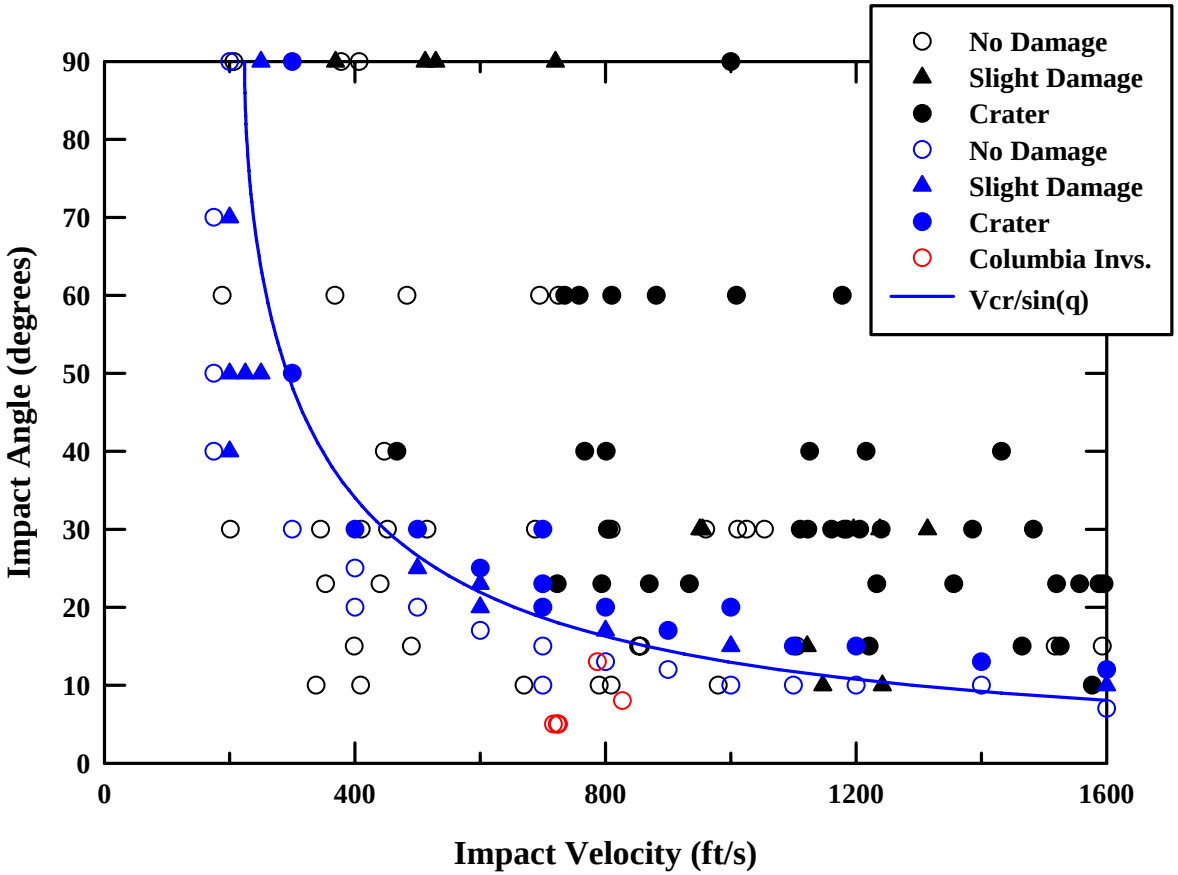

- All the foam data is plotted from Rand's 1979 report, SwRI's 1999 report and the Columbia investigation; there is good agreement with the theoretical curve.

RCC Panels 6 and 8 Tests

Final Estimates of Foam Path

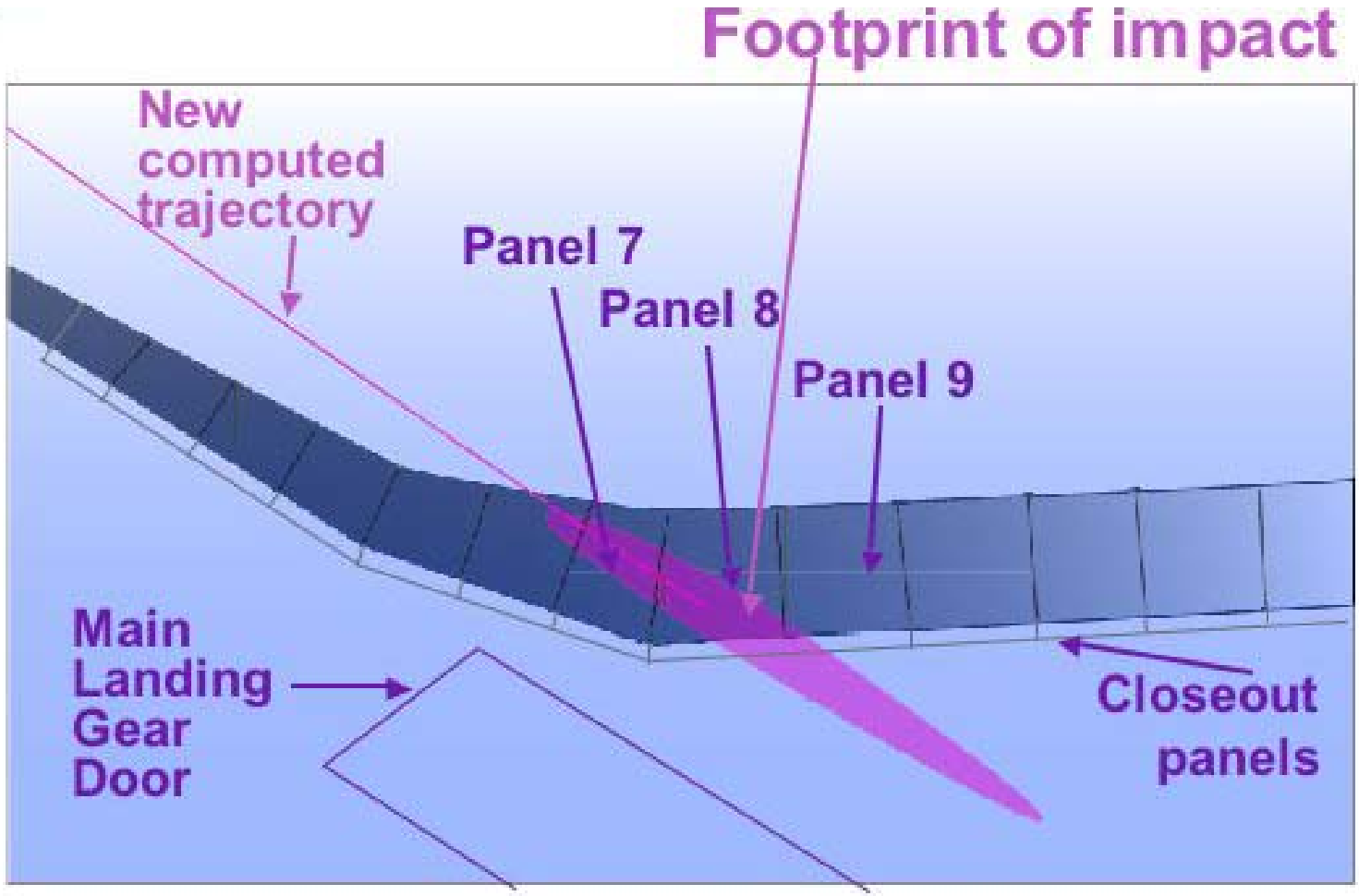

Leading Edge Test Article

Leading Edge Structural Subsystem

Test Article

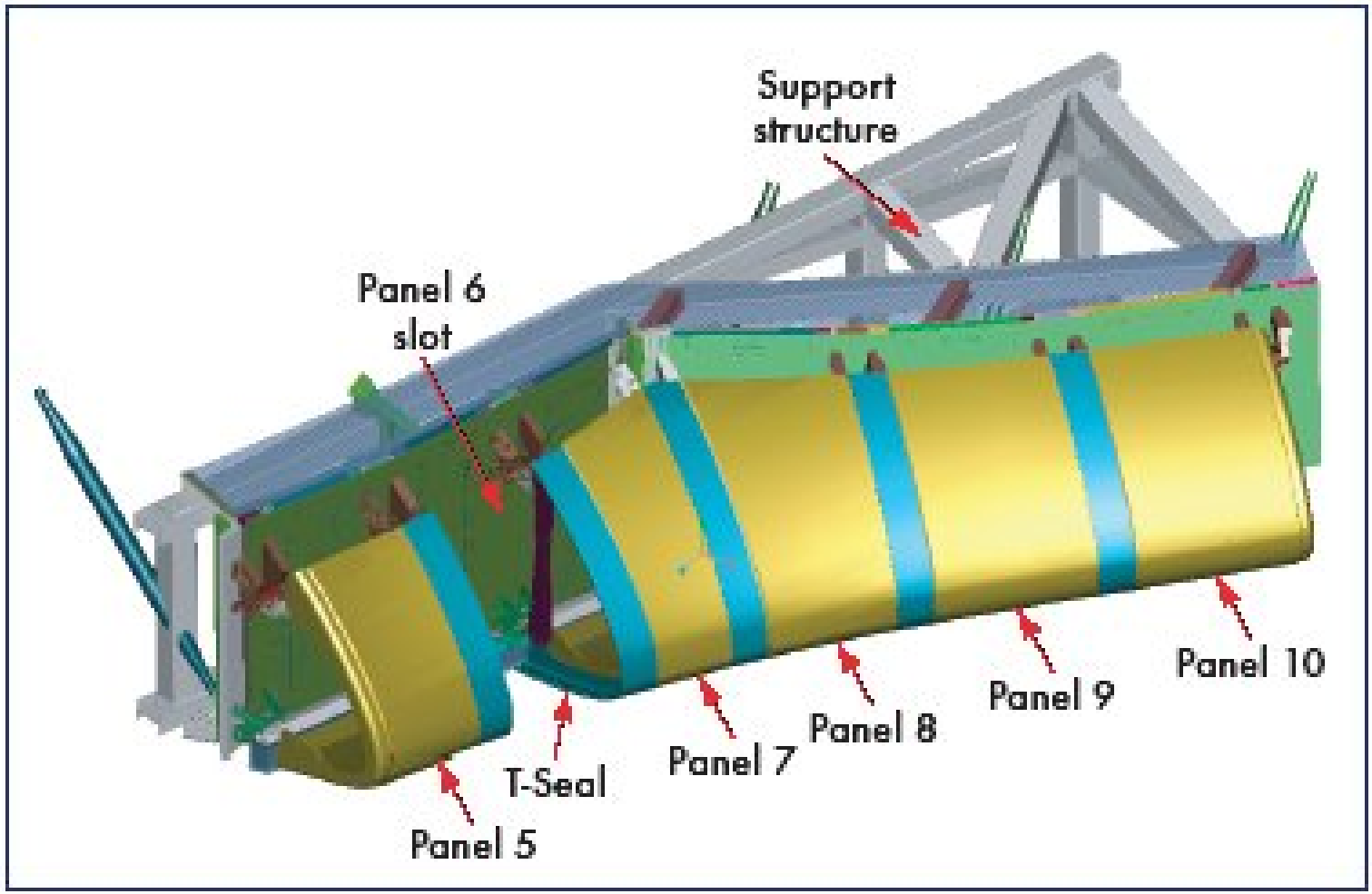

Interior Cameras and Gages

- Up to 16 high-speed video cameras were used per test (up to 8 outside of the target, up to 8 inside the target).
- Up to 250 channels of strain gage, accelerometer and load cell data were collected.

Exterior Cameras

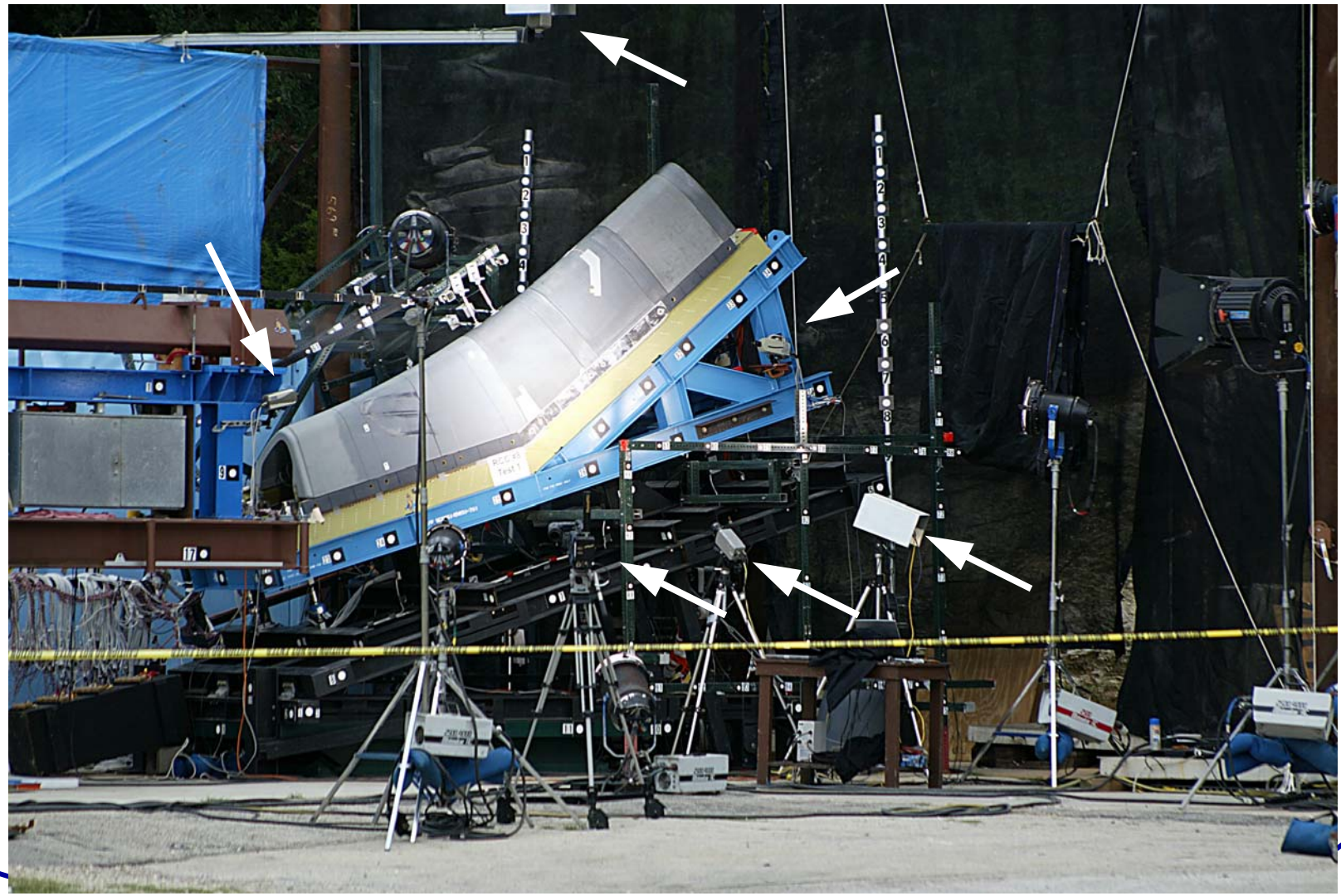

RCC Panel 6 Test

- RCC Panel 6 had flown 30 flights on *Discovery*.
- The test resulted in a cracked rib.
- Damage thought insufficient to cause the loss of the vehicle.

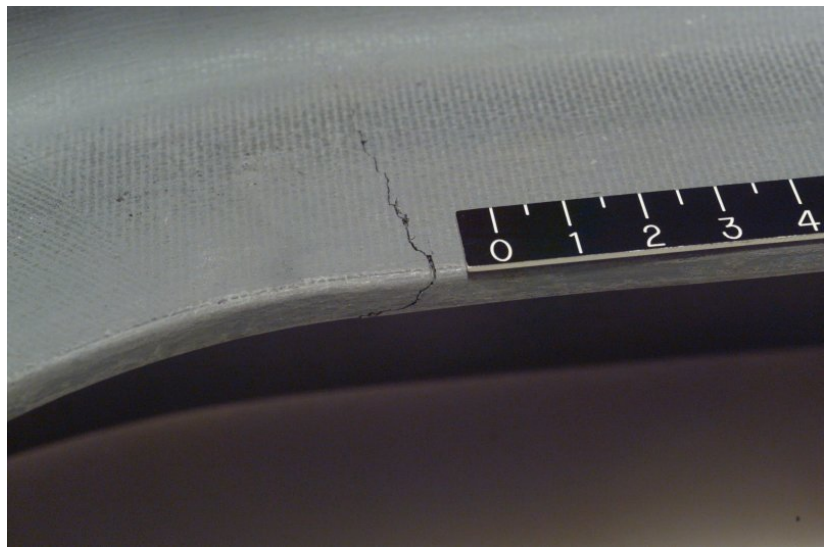

RCC Panel 8

RCC Panel 8

- RCC Panel 8 had flown 26 missions on *Atlantis*.

RCC Panel 8

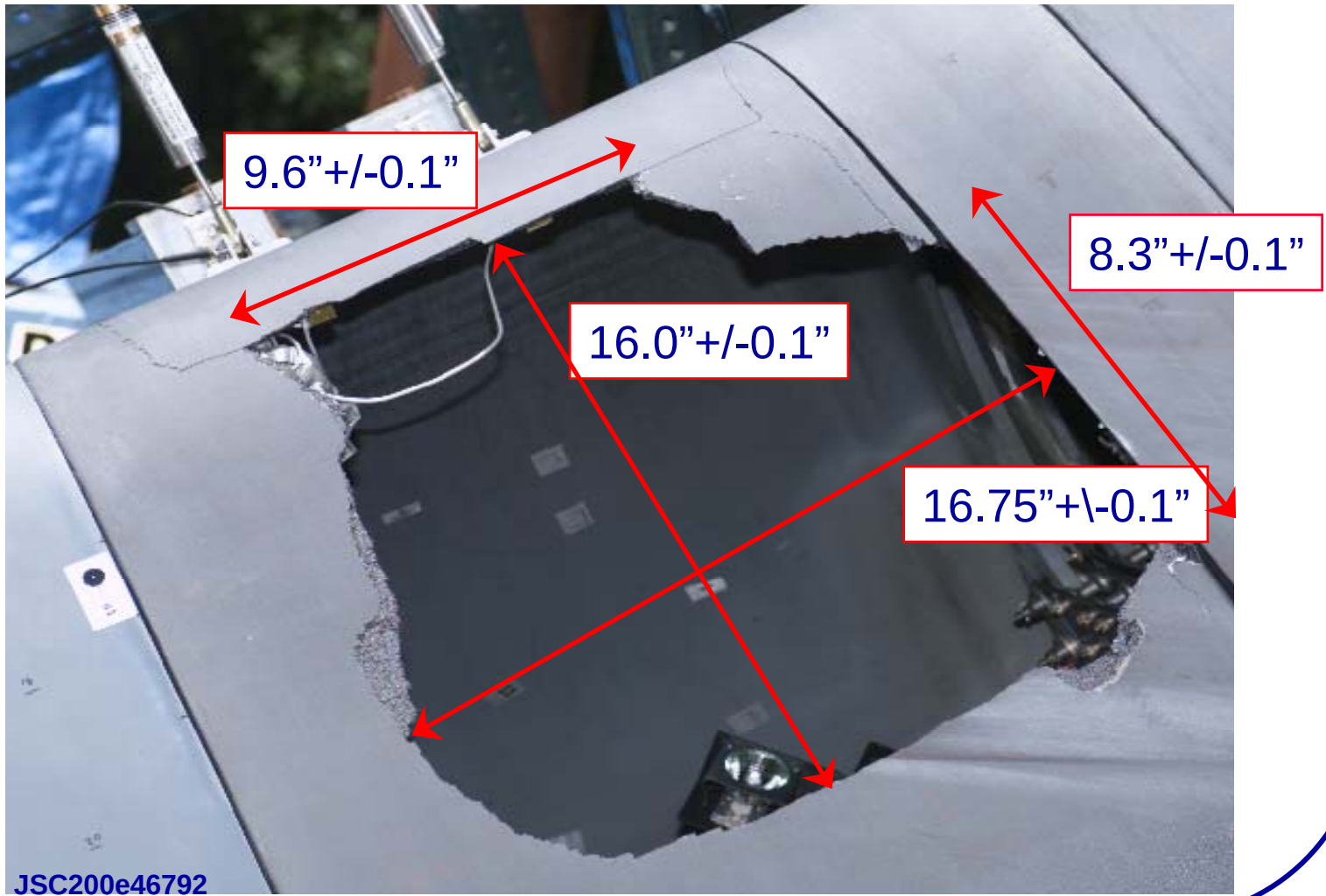

Modeling Foam Insulation Impact on RCC Panels 6 and 8

Experimental Results RCC Panel 6

Replicating RCC Panel 6 Test

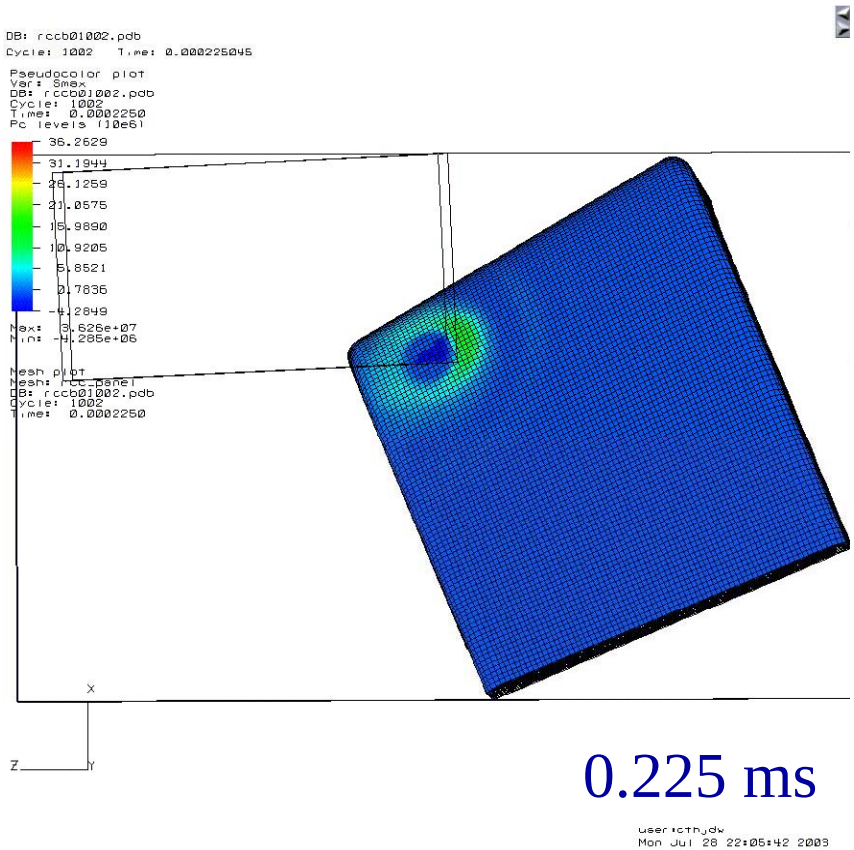

0.225 ms

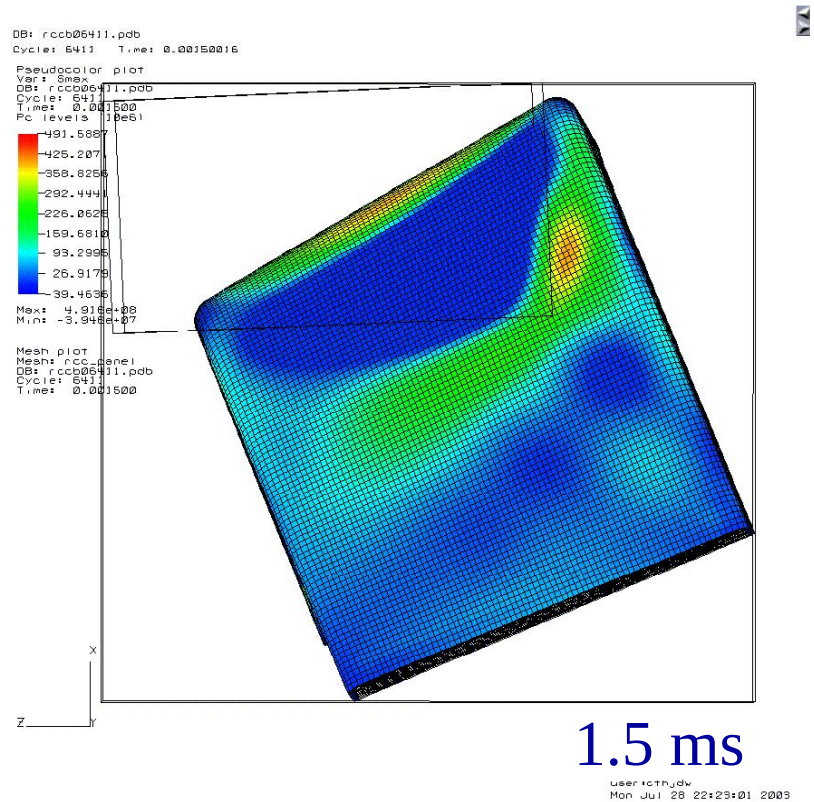

1.5 ms

- The impact point 0.83” left from the 5-6 T-seal, 18.7” up from the carrier panel.
- Flight direction: α=5.5° (bottom to top), β=2.5° (away from center).
- The impact velocity was 768 ft/s, computation carried out to 5 ms.

Replicating RCC Panel 6 Test

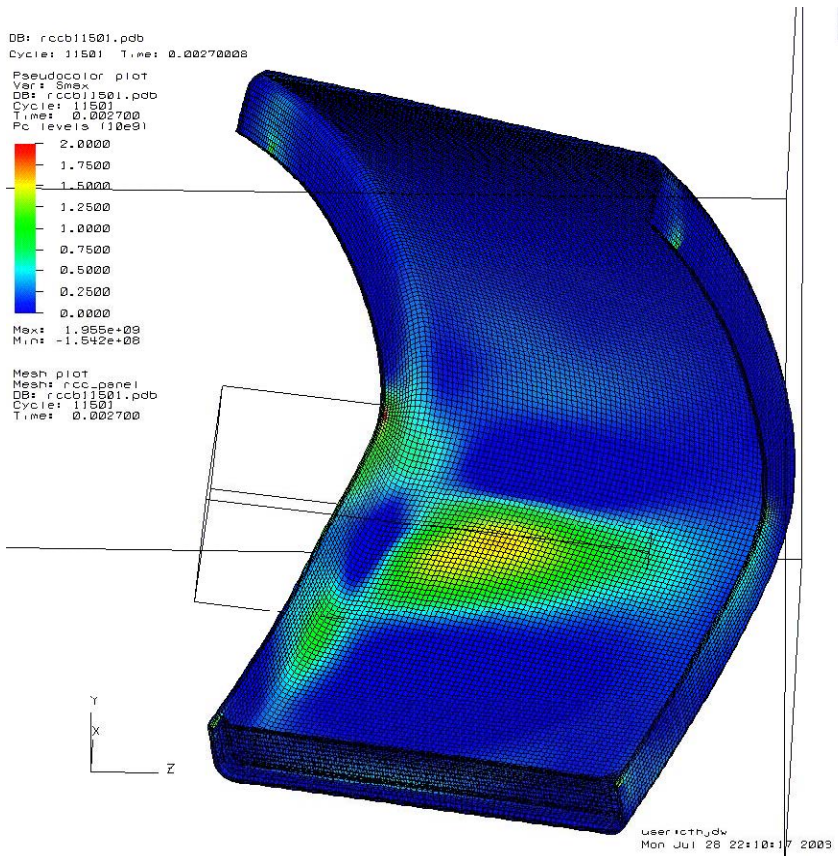

2.7 ms

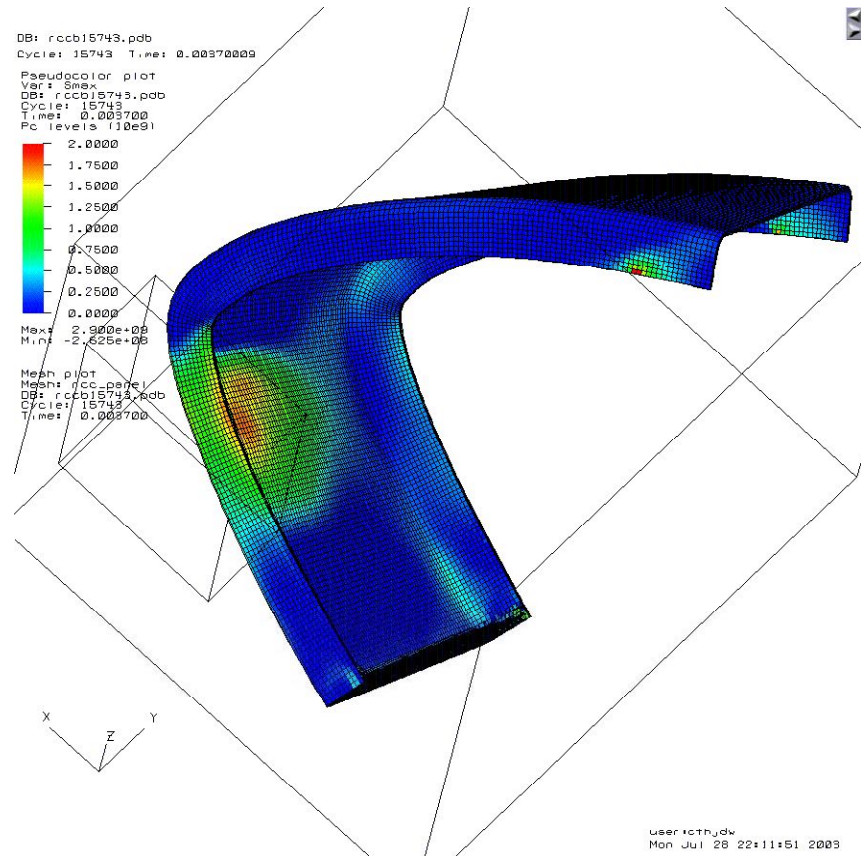

3.7 ms

Experimental Results RCC Panel 8

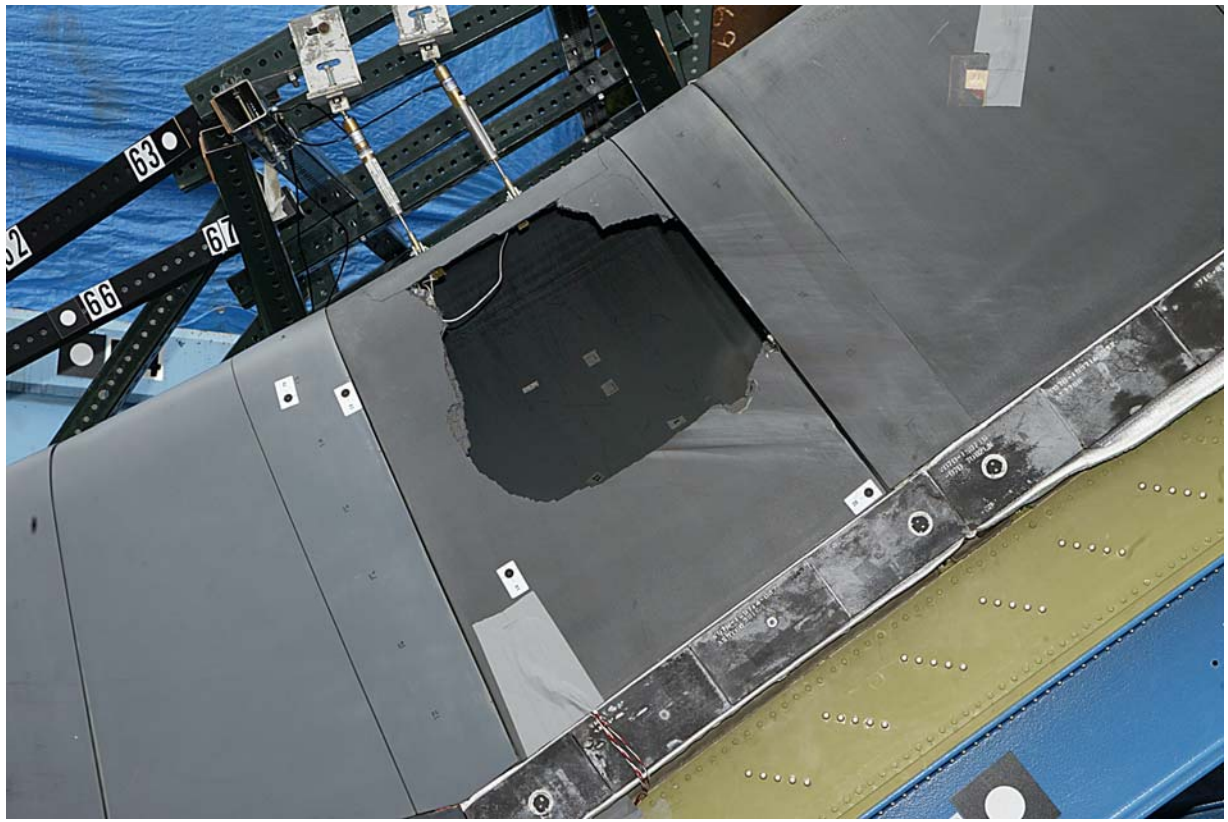

Replicating RCC Panel 8 Test

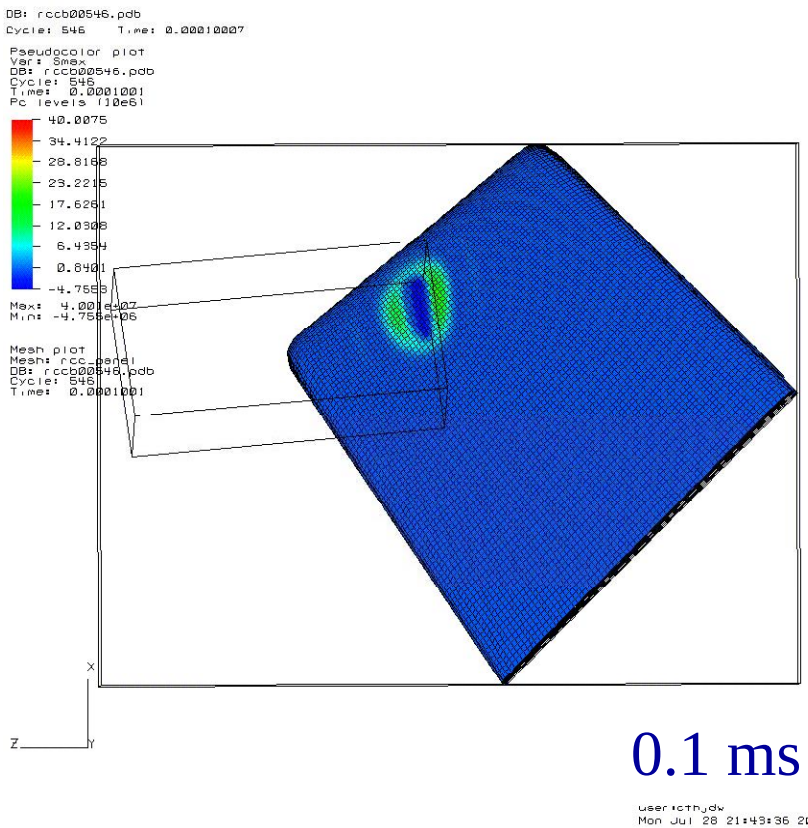

0.1 ms

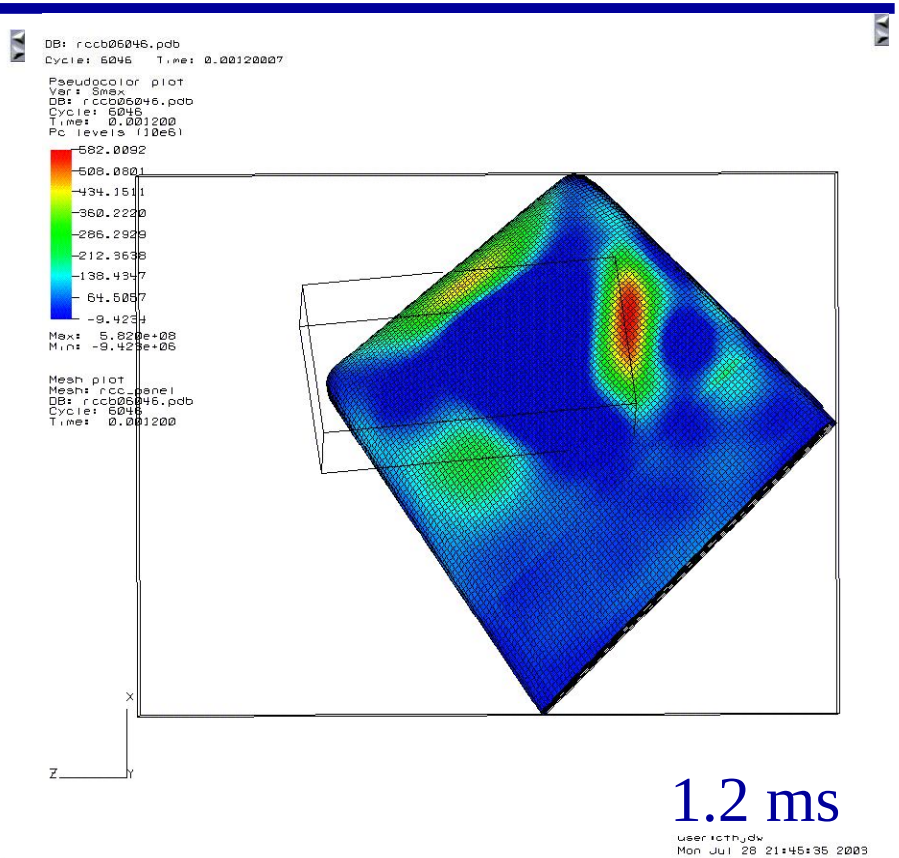

1.2 ms

- The impact point 7.3” left from the 7-8 T-seal, 25.5” up from the carrier panel.
- Flight direction: α=5.5° (bottom to top), β=5.0° (away from center), 30° clocking.
- The impact velocity was 777 ft/s, computation carried out to 5 ms.

Replicating RCC Panel 8 Test

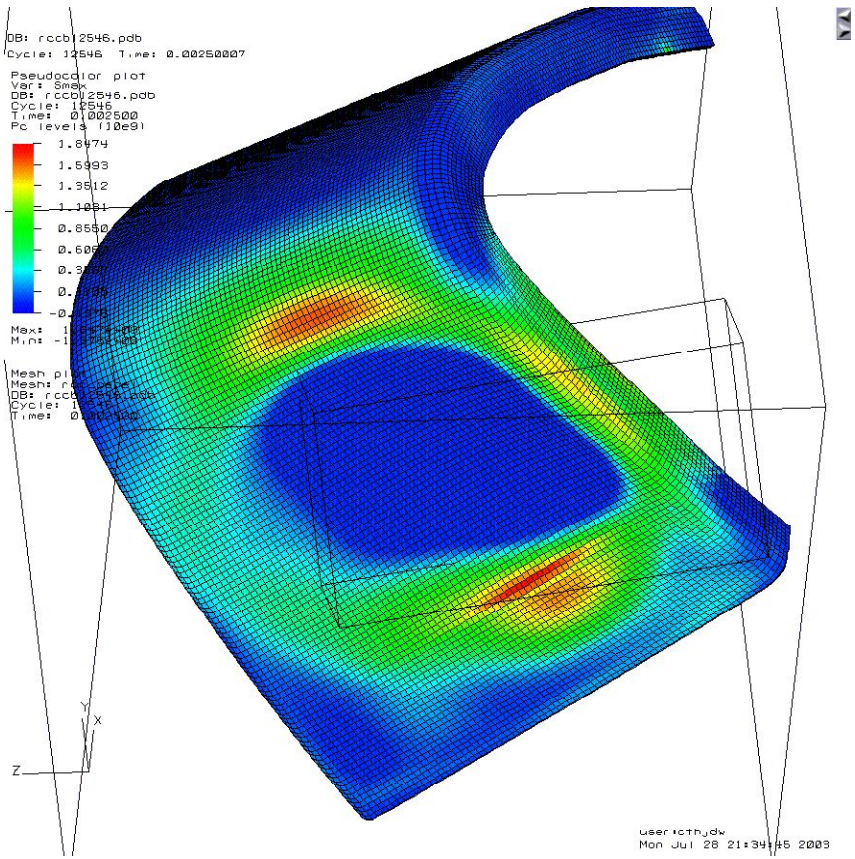

2.5 ms

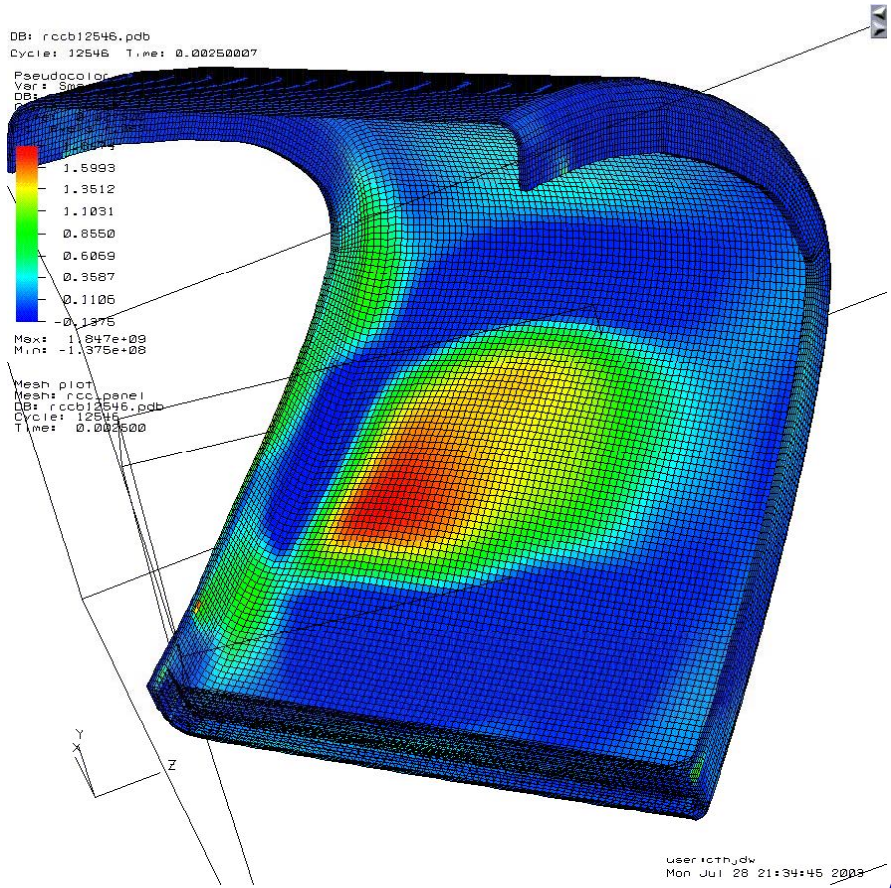

2.5 ms

Loading Footprint

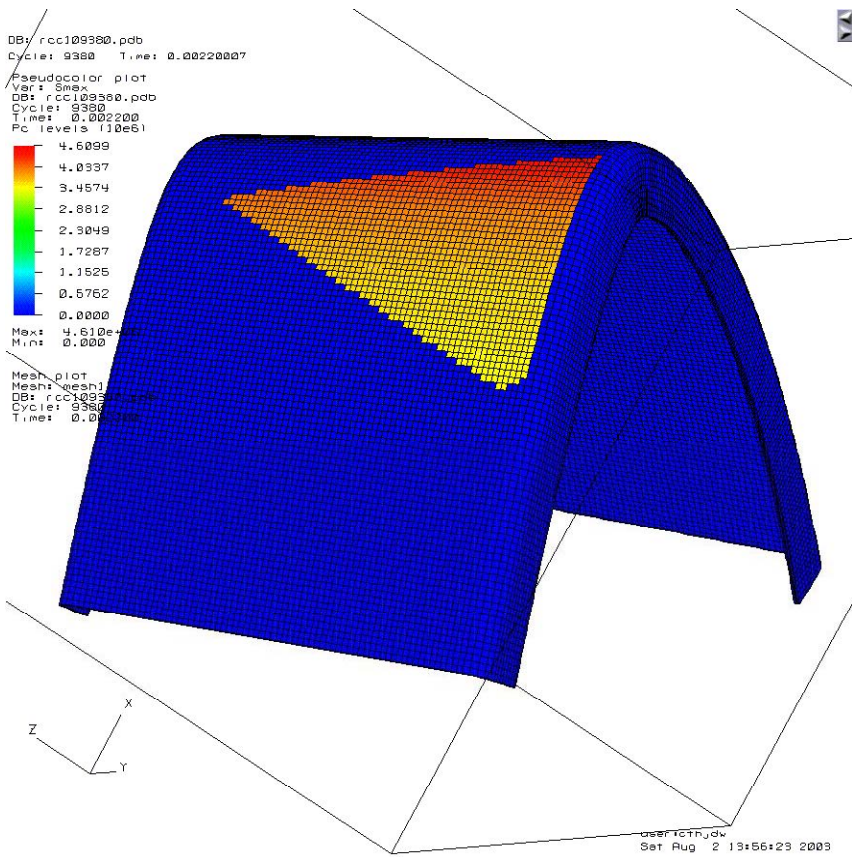

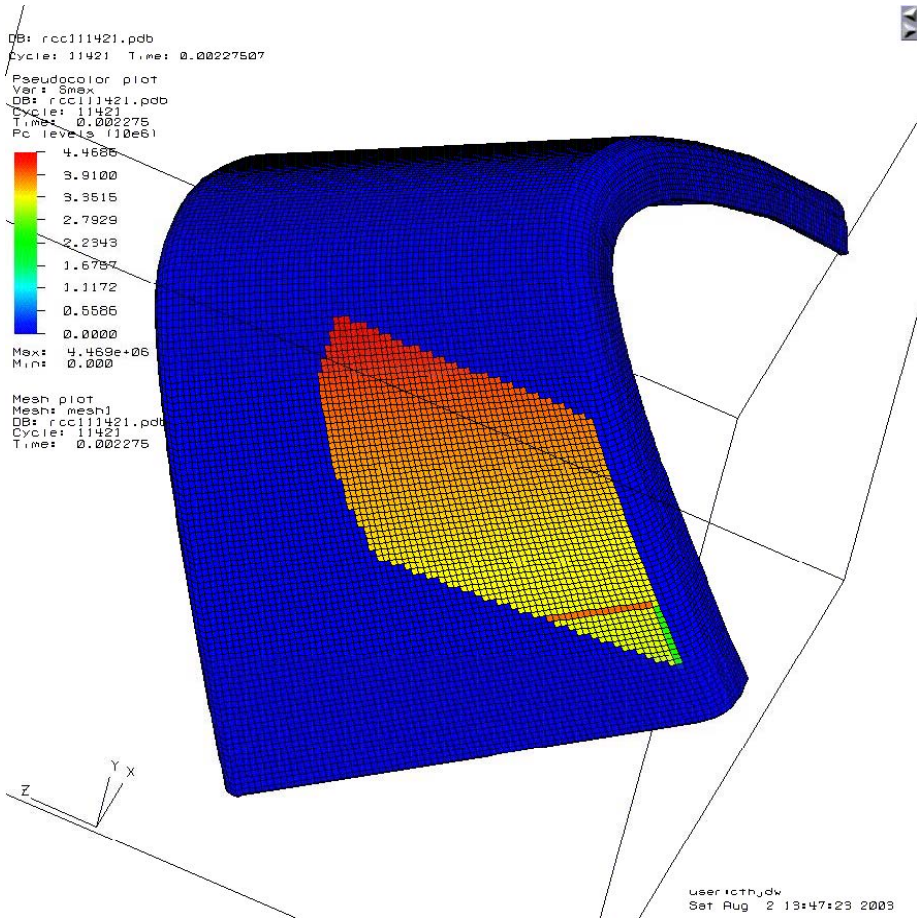

RCC panel 6 impact

RCC panel 8 impact

Stresses RCC Panels 6 and 8

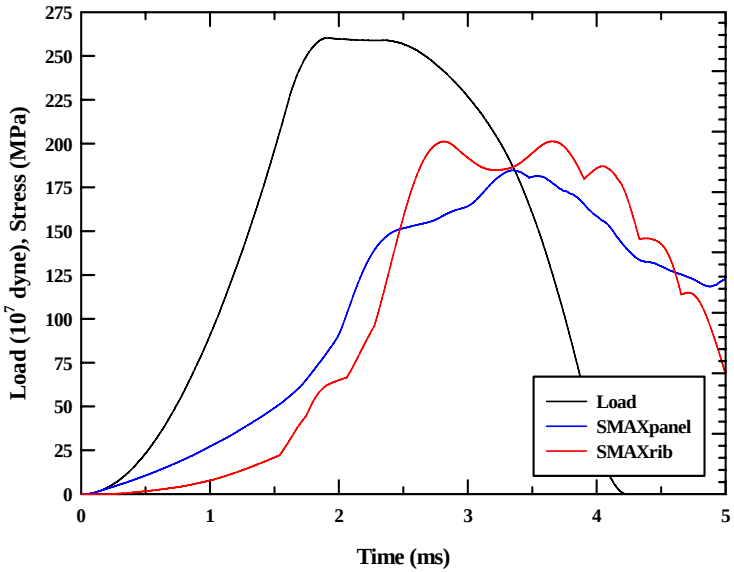

RCC Panel 6

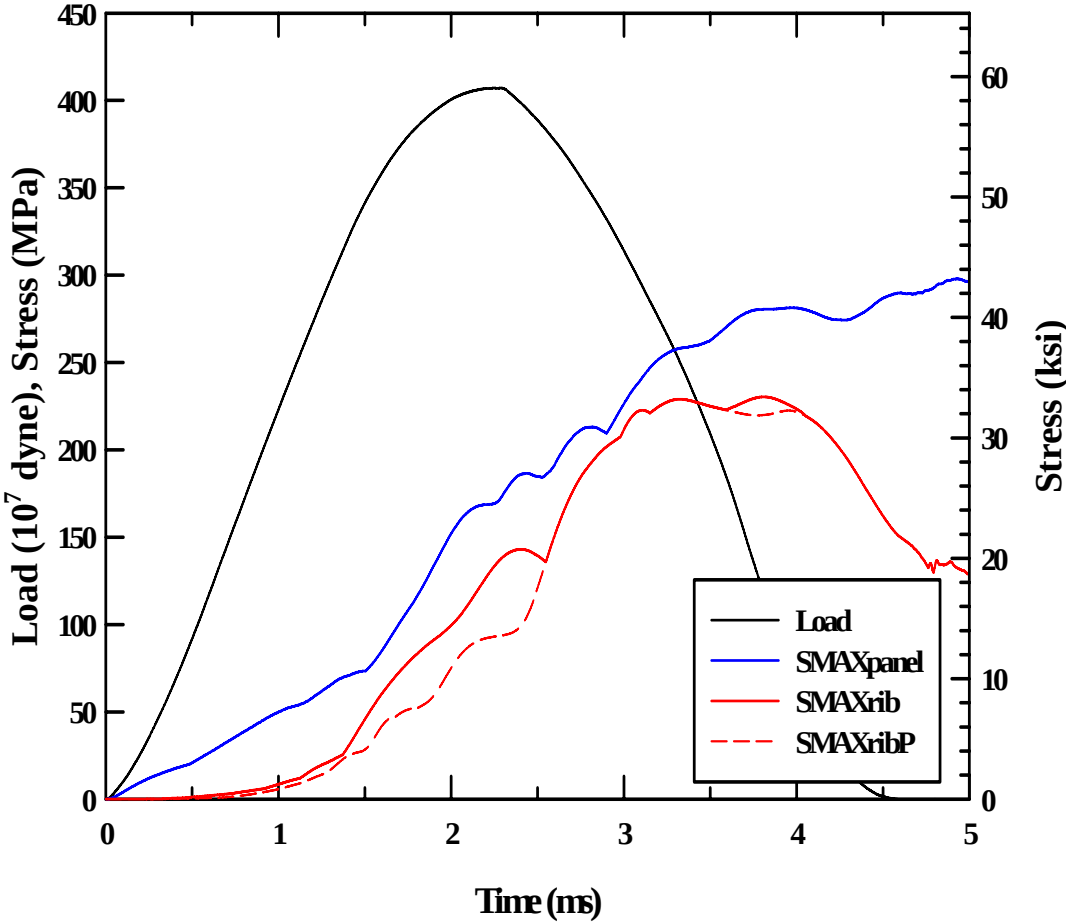

RCC Panel 8

Investigation Conclusions

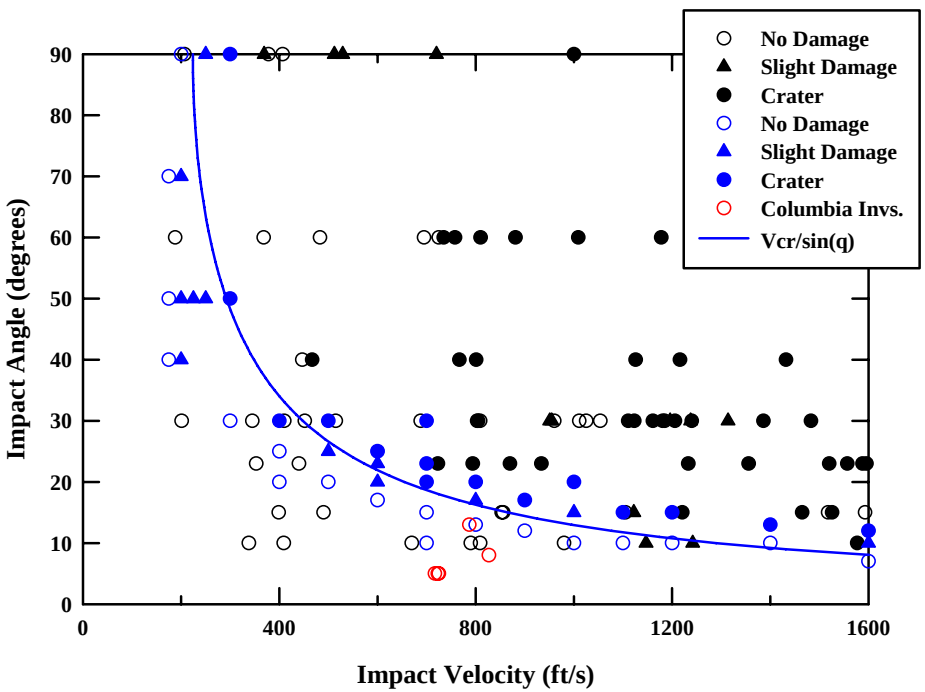

- The component of velocity normal to the impact surface determines the local loading pressure.
- Modeling and experiments showed that an impact on the underside of the wing was not the cause of the accident.
- Forensics, experiments and modeling showed that the loss of *Columbia* was due to a foam impact on RCC panel 8.

The Physical Cause

The physical cause of the loss of Columbia and its crew was a breach in the Thermal Protection System on the leading edge of the left wing. The breach was initiated by a piece of insulating foam that separated from the left bipod ramp of the External Tank and struck the wing in the vicinity of the lower half of Reinforced Carbon-Carbon panel 8 at 81.9 seconds after launch. During re-entry, this breach in the Thermal Protection System allowed superheated air to penetrate the leading-edge insulation and progressively melt the aluminum structure of the left wing, resulting in a weakening of the structure until increasing aerodynamic forces caused loss of control, failure of the wing, and breakup of the Orbiter.

SwRI Three-Pronged Approach

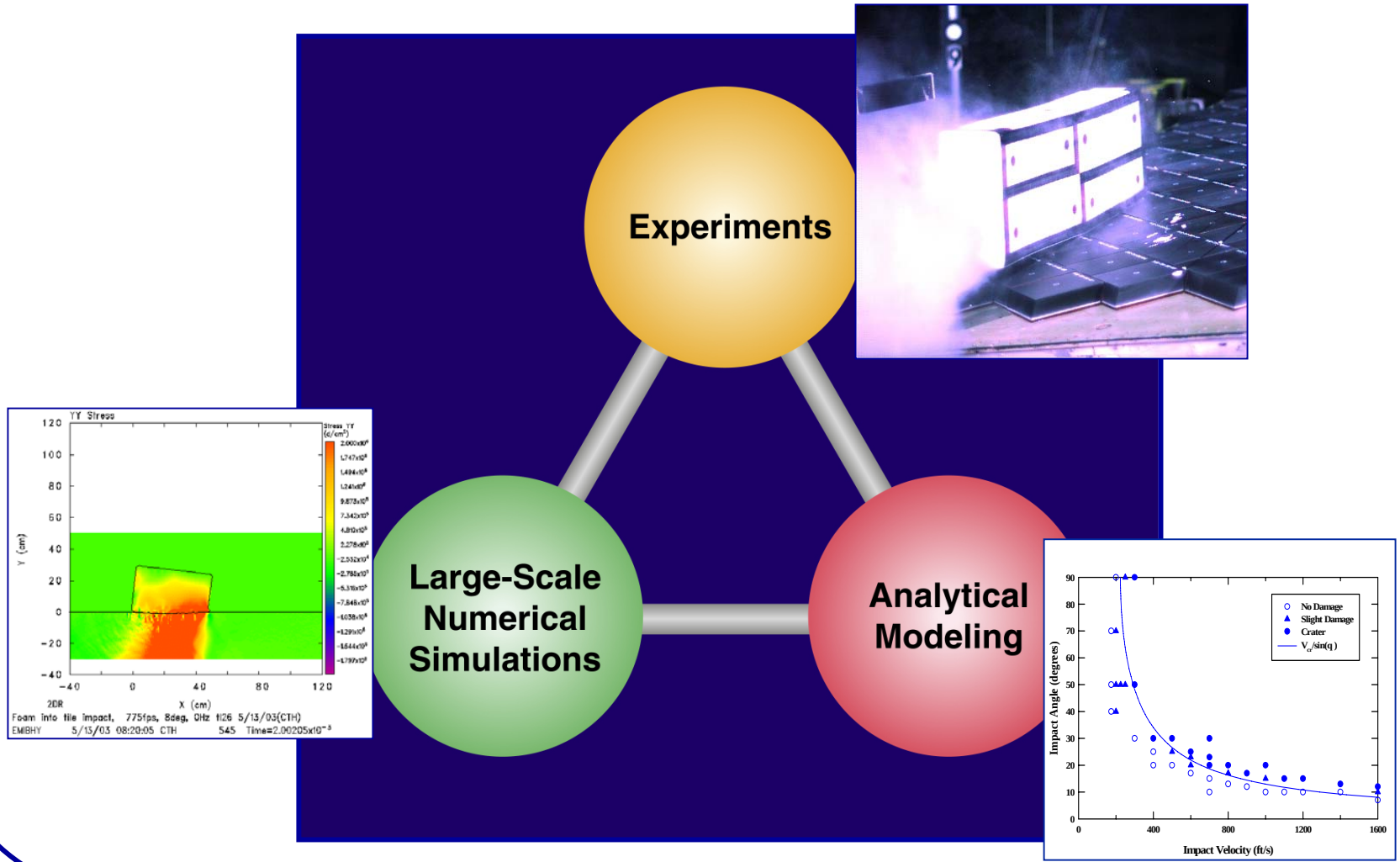

Return to Flight

CAIB Recommendations R3.2-2 Estimate Risk

- Initiate a program designed to increase the Orbiter's ability to sustain minor debris damage by measures such as improved impact-resistant Reinforced Carbon-Carbon and acreage tiles. This program should determine the actual impact resistance of current materials and the effect of likely debris strikes. [RTF]

CAIB Recommendation R3.8-2
Impact Damage Models

- Develop, validate, and maintain physics-based computer models to evaluate Thermal Protection System damage from debris impacts. These tools should provide realistic and timely estimates of any impact damage from possible debris from any source that may ultimately impact the Orbiter. Establish impact damage thresholds that trigger responsive corrective action, such as on-orbit inspection and repair, when indicated.

Foam and Ice on the External Tank

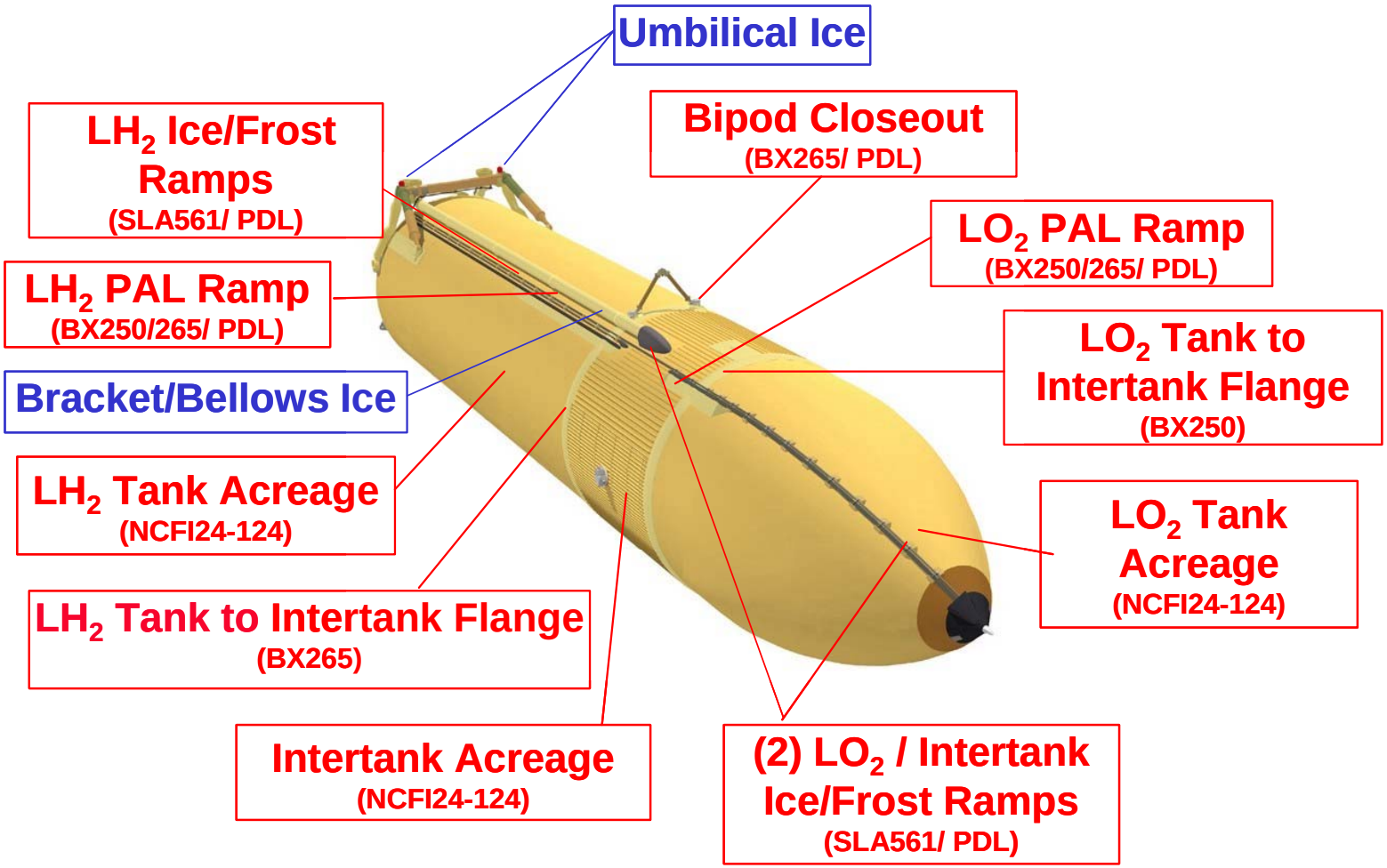

Impacts into Thermal Tiles

Physics-Based Impact Models: Inputs and Outputs

<u>Specific Impact Event Input:</u>

Impactor denstity: ρ_p

Impactor Dimensions:
Length L, Width W, Height H

Impact Velocity V and Angle θ

Large compression crush-up curve required (foam)

Projectile fracture (ice)

<u>Tile Material Properties:</u>

Large compression crush-up curve required (stress vs. strain in compression up to 90% compression)

Foam, Ice and Ablator Impact Models

<u>Output: Computed Crater Dimensions</u>

Depth, Length, Width

Our Validation Triangle

When experiments, large-scale numerical simulations and the analytical physics-based model agree, the physics-based model is assumed to be validated.

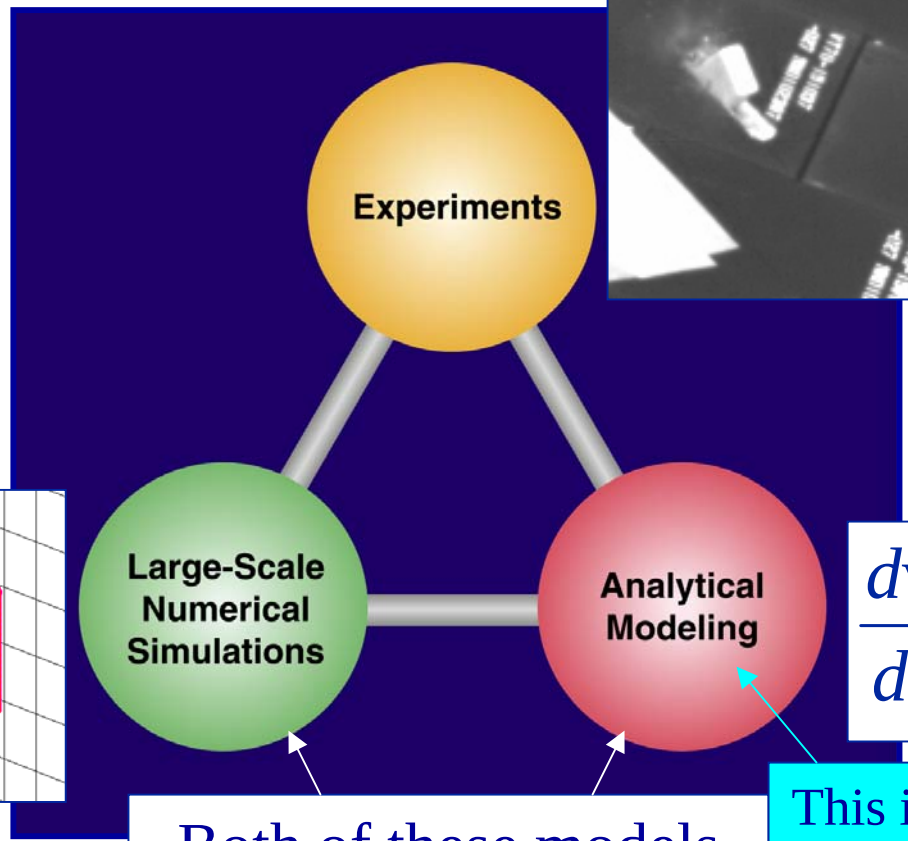

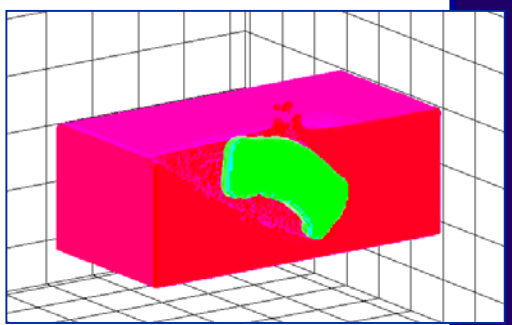

$$\frac{dv}{dt} = -\frac{\sigma_{zz}(v)}{\rho_p L}$$

Both of these models are Physics Based

This is our fast-running, physics-based model for flight

Powerful Feature of the Models

- For both the fast-running physics-based model and CTH
  - *The model coding is exactly the same for all the different cases that will be shown – only the input material properties are changed.*
- Thus, it is not a different model for ice or low density ice, it is not a different model for LI-900 or FRCI-12; the impact model is exactly the same, only the input material properties change.
- As will be shown, excellent agreement between models and test data exists for all impact cases.

Material Properties for Tiles

Thermal Tiles (LI-900)

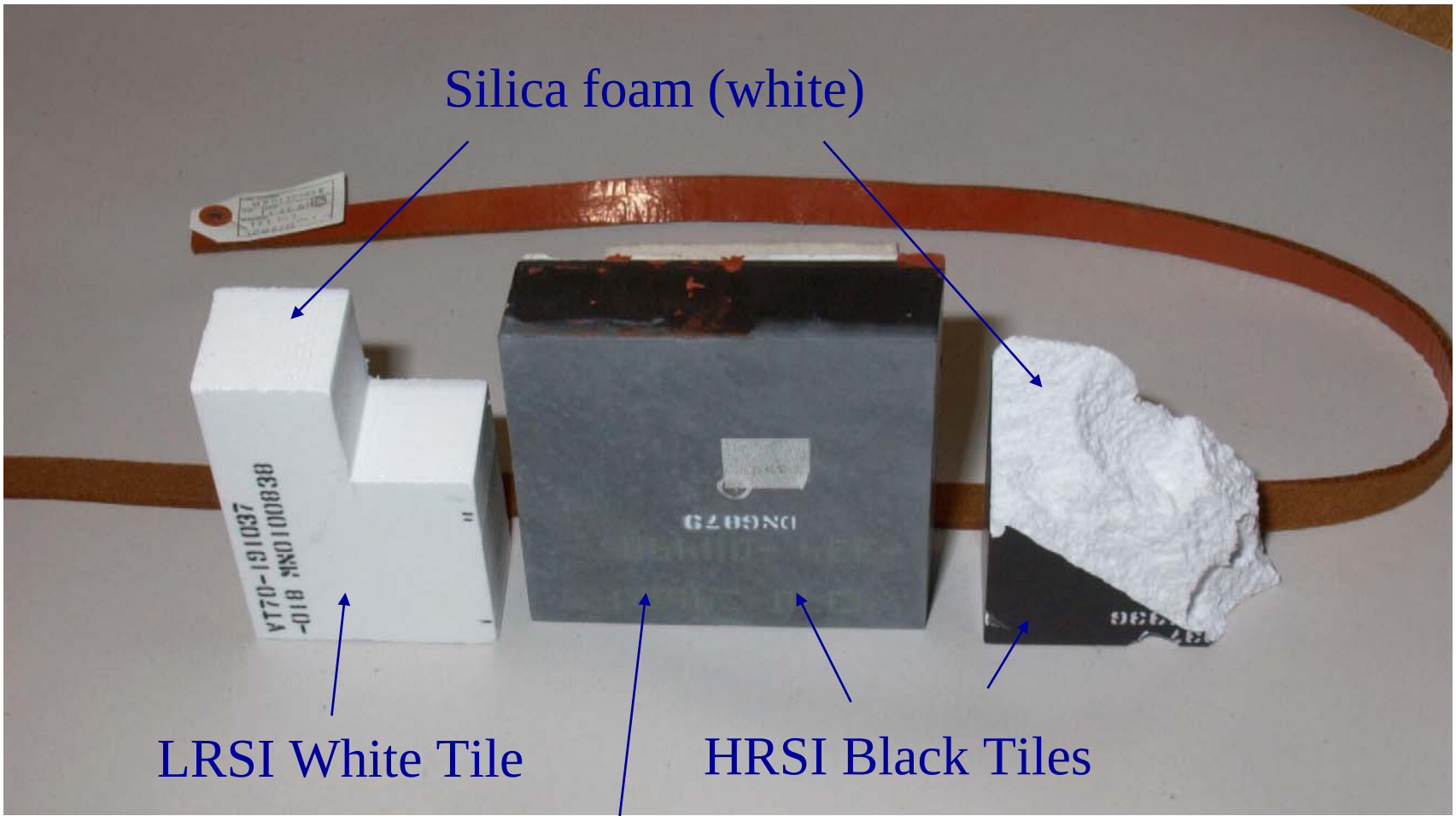

Thermal Tiles

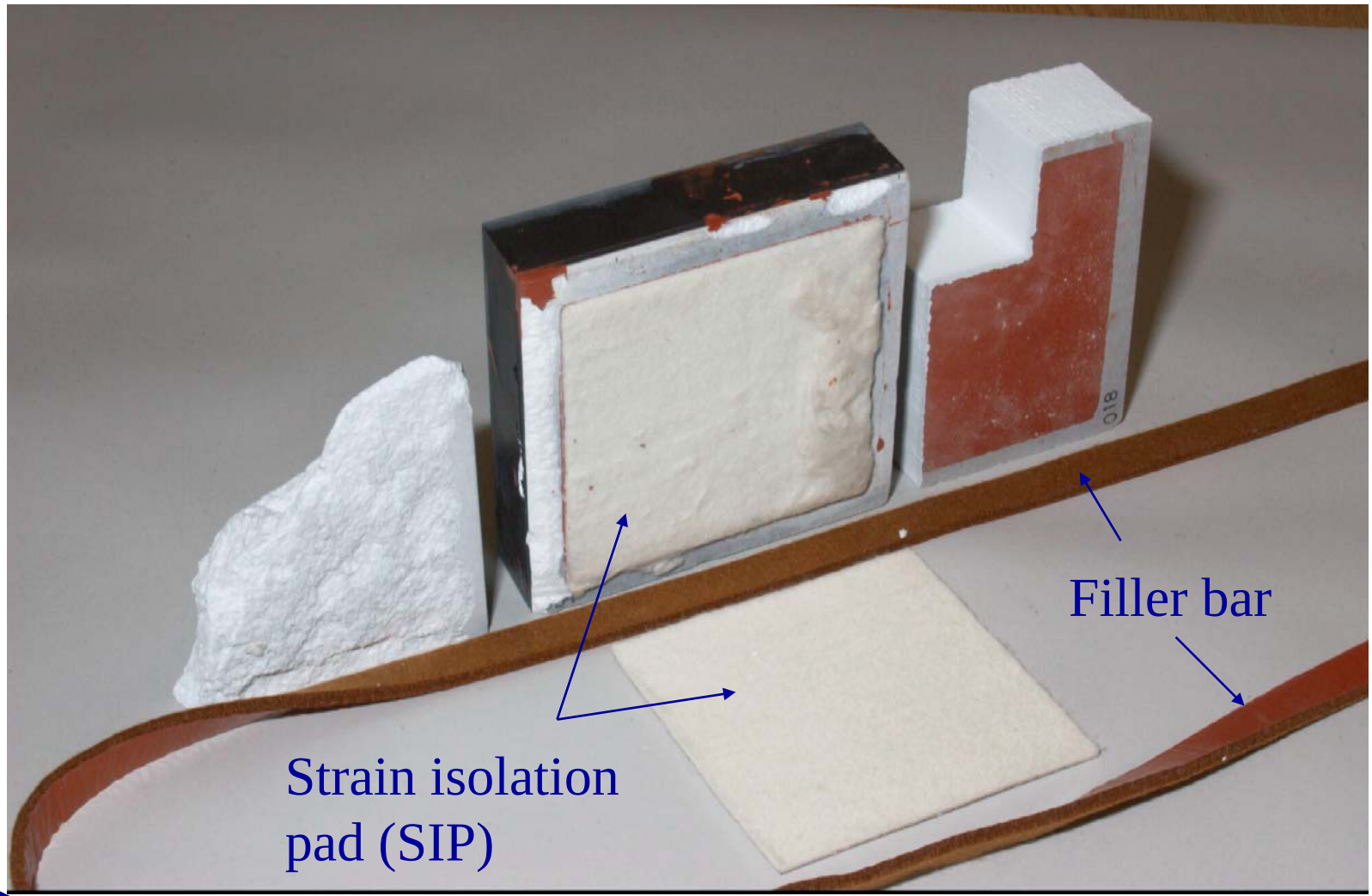

Larger strain behavior based on Crush-in-a-Box Uniaxial Strain Test Data

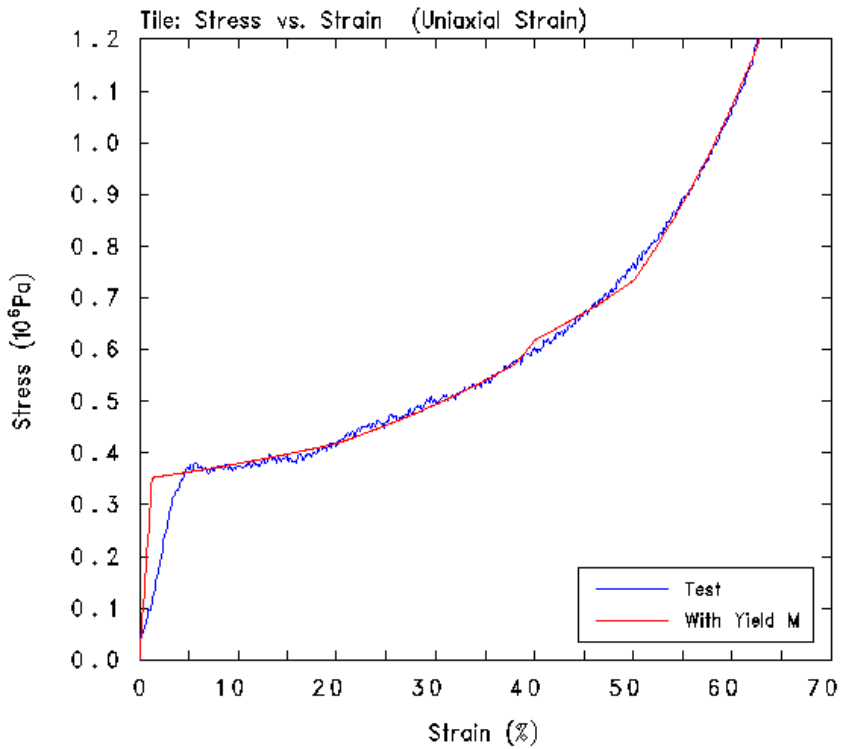

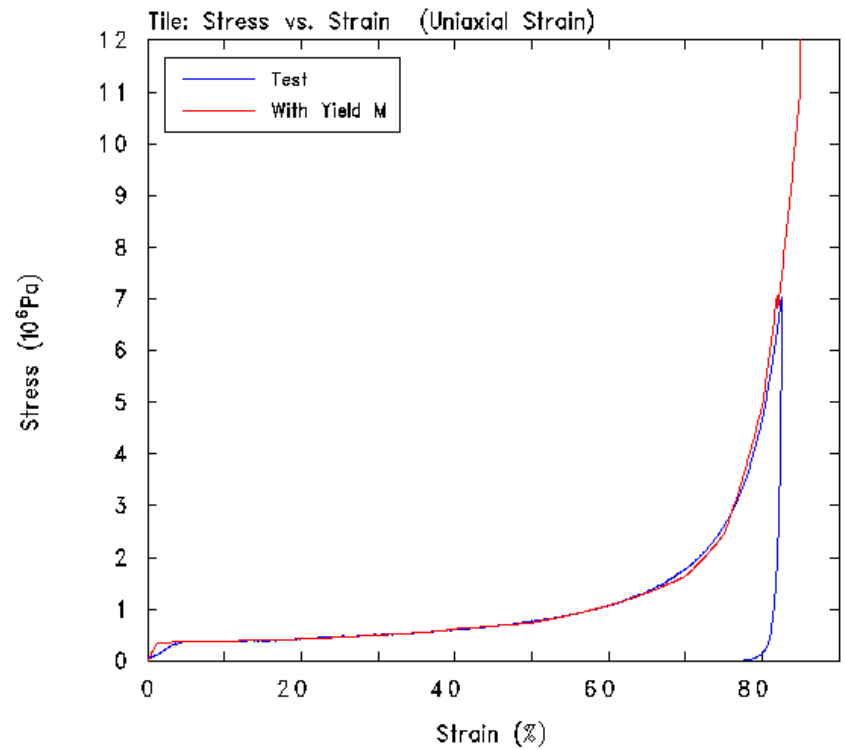

- Test performed with a cylinder from same tile specimen confined with a steel ring.
- Data placed into new tile model within CTH. Model includes a yield at 550 kPa.

Material Properties for Impactors

Ice Physical Properties

- The modeling assumed the following properties for ice (obtained from typical values found in the literature):
  - Modulus of Elasticity (E) = 8000 MPa
  - Shear Modulus (G) = 3000 MPa
  - Density = 0.914 g/cc (57 lb/ft^3)
  - Poisson's ratio = 0.33
  - Flow stress = 2.0 MPa
  - Tensile strength = 1.0 MPa
  - Sound speed (c_0) = 2954 m/s

RT-455 Ablator Model Developed for CTH

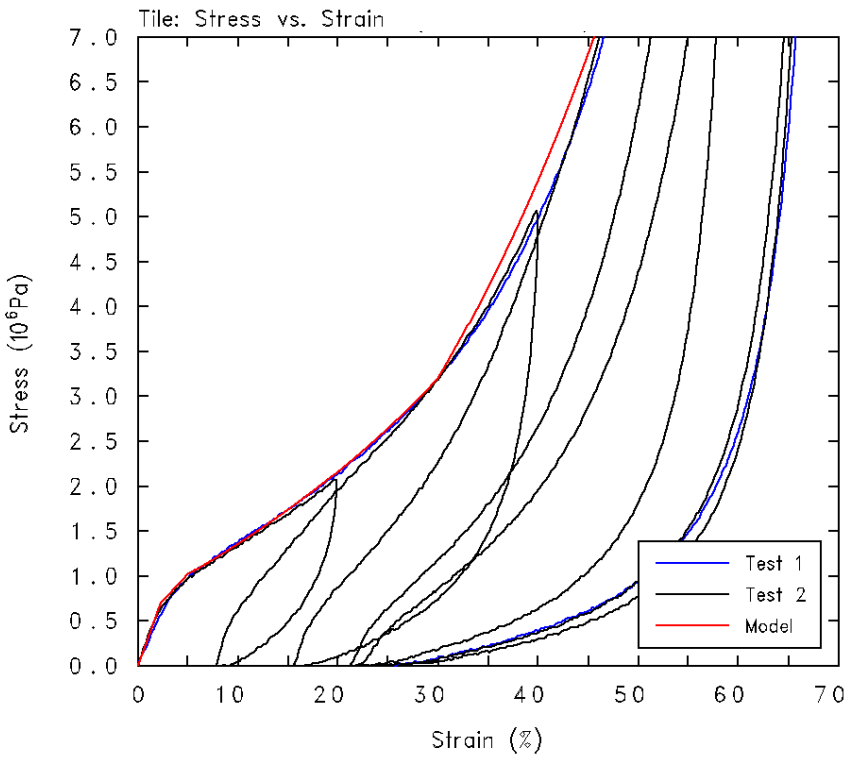

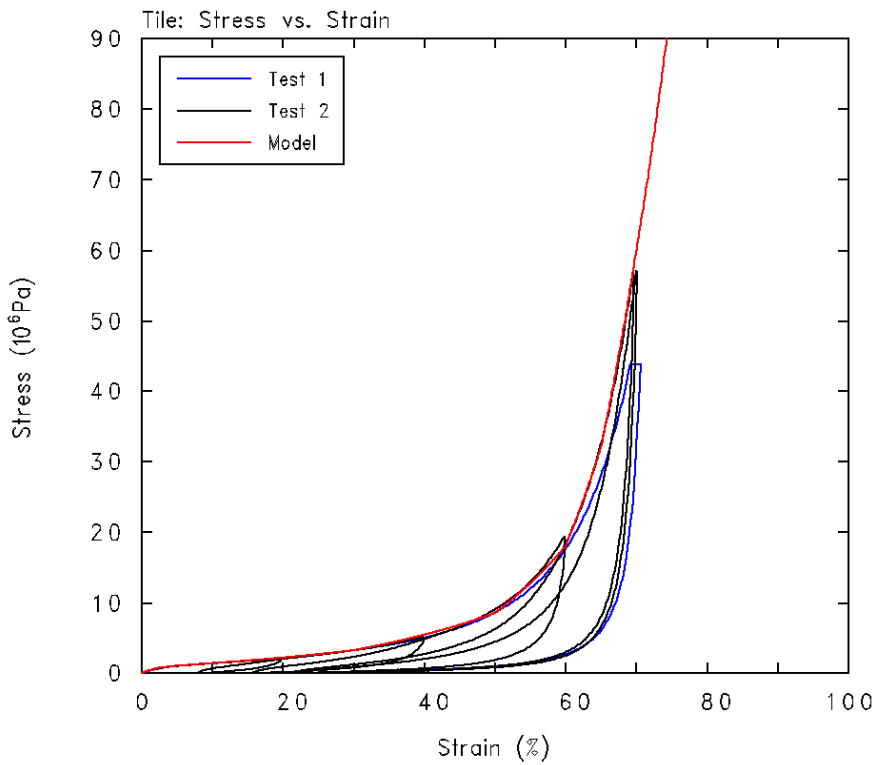

Initial density 0.66 g/cm^3

PDL Model for CTH

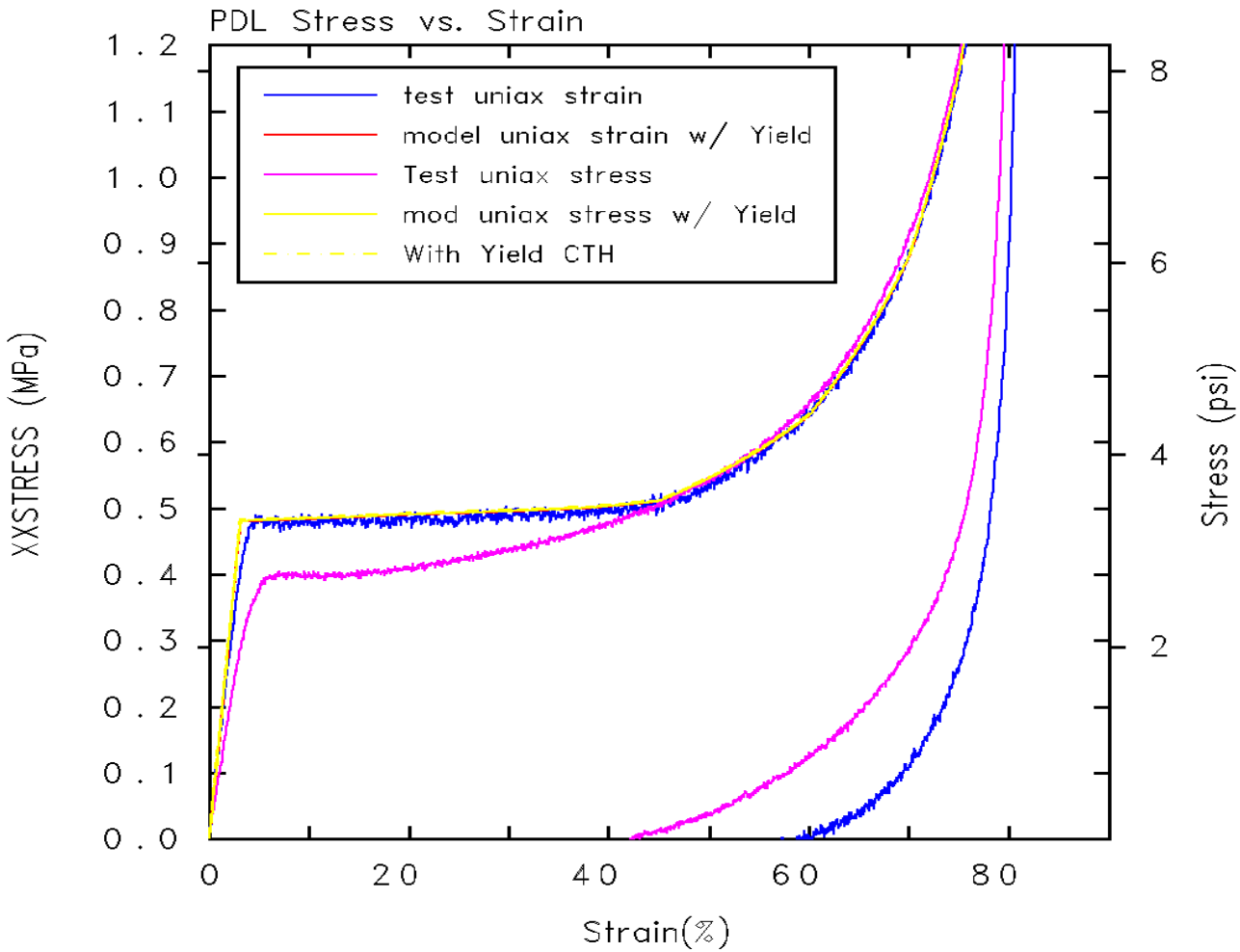

Ice into Tile

Physics-Based Ice into Tile Model

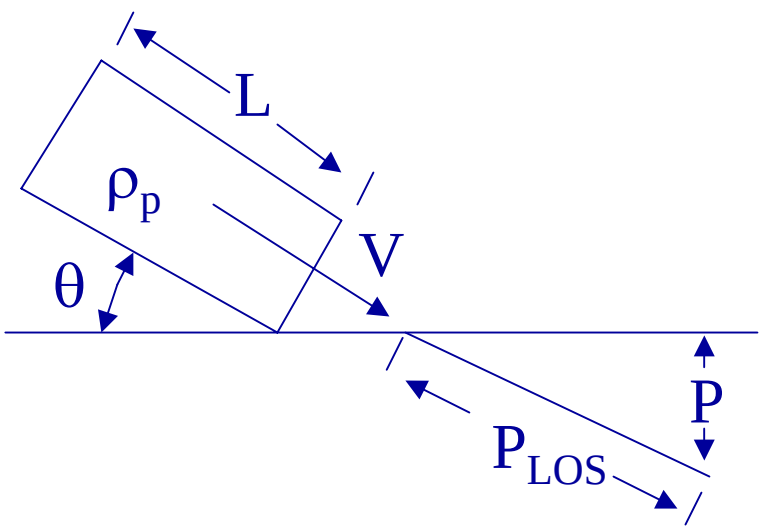

- Given the tile crush-up behavior, the model solves the Riemann problem to find the stress in the tile versus velocity, $\sigma_{zz}(v)$. A shear term is also included.
- Given this information, $F = ma$ qualitatively translates into

$$\frac{dv}{dt} = -\frac{\sigma_{zz}(v)}{\rho_p L}$$

(see the rest of these charts for exactly how the full equations appear).

- The depth of penetration is calculated by integrating this equation with a numerical scheme to produce a line-of-sight depth of penetration P_{LOS}.

Tile Resistance to Penetration

- The model computes a penetration resistance stress of the form

$$\sigma_{zz}(v) = \sigma_{Hugoniot}(v) + \frac{7}{3}\sigma_{crush}\ln(\alpha)$$

- Here,
  - $\sigma_{Hugoniot}(v)$ is the stress as a function of particle velocity along the Hugoniot (the idealized one-dimensional planar impact). This function is computed based on the large-strain compression curves and the Hugoniot jump conditions. It is stored as a table for rapid look-up during the computation.
  - σ_{crush} is the crushing strength of the tile
  - $\alpha(v)$ is the extent of the deforming region within the tile, and is computed with a cavity expansion expression. It depends on the material properties of the tile and the penetration velocity.

The Hugoniot Contribution to the Resistance

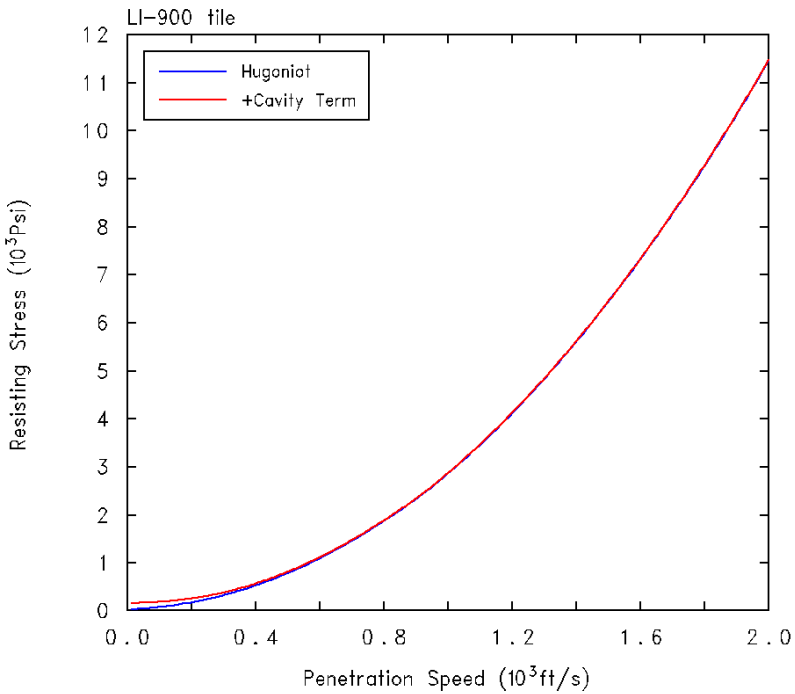

- The model solves the Riemann problem to find the stress in the tile versus velocity, $\sigma_{Hugoniot}(v)$.
- This term is found by simultaneously solving the Hugoniot jump conditions using the tabular data of tile properties

$$\frac{\rho_0}{\rho} = 1 - \frac{u}{U}$$

$$\sigma_{Hugoniot} = \rho_0 U u$$

where U is the shock speed and u is the penetration speed (U is solved for also).

- The plot shows the value of the $\sigma_{Hugoniot}(v)$ term (blue) as well as the total resisting stress including the shear resistance term (red) in terms of penetration velocity through the tile.

Embedment Phase

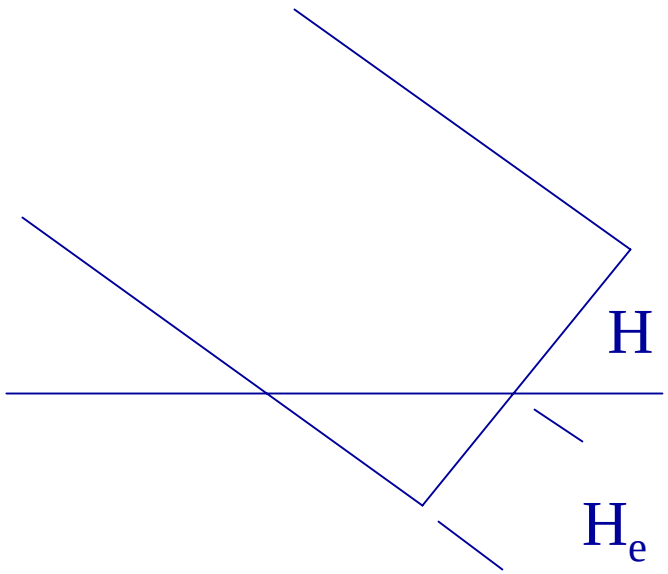

- When the projectile embeds itself into the target, only part of the face of the projectile is loaded by the target. Thus, the force on the face is reduced by the appropriate factor:

$$f = \frac{H_e}{H}$$

- where

$$\frac{dv}{dt} = -f\,\frac{\sigma_{zz}(v)}{\rho_p L}$$

Equations of Motion

- For completeness, we write the full equations of motion, where *x* is the direction along the surface of the tile and *y* is the normal direction into the tile:

$$\frac{d\mathrm{v}_{\mathrm{x}}}{dt} = -f\,\frac{\sigma_{\mathrm{zz}}(\mathrm{v})}{\rho_p L}\cos(\theta) + \frac{F_n}{\rho_p LHW}\sin(\theta)$$

$$\frac{d\mathrm{v}_{\mathrm{y}}}{dt} = -f\,\frac{\sigma_{\mathrm{zz}}(\mathrm{v})}{\rho_p L}\sin(\theta) - \frac{F_n}{\rho_p LHW}\cos(\theta)$$

$$\mathrm{v} = \sqrt{\mathrm{v}_{\mathrm{x}}^2 + \mathrm{v}_{\mathrm{y}}^2}$$

- These equations are integrated forward in time until either the impactor speed v drops below the speed required to crush tile (i.e., it comes to rest) or the impactor is forced back to the tile surface (i.e., it ricochets).

Developing the 95% Bounding Model

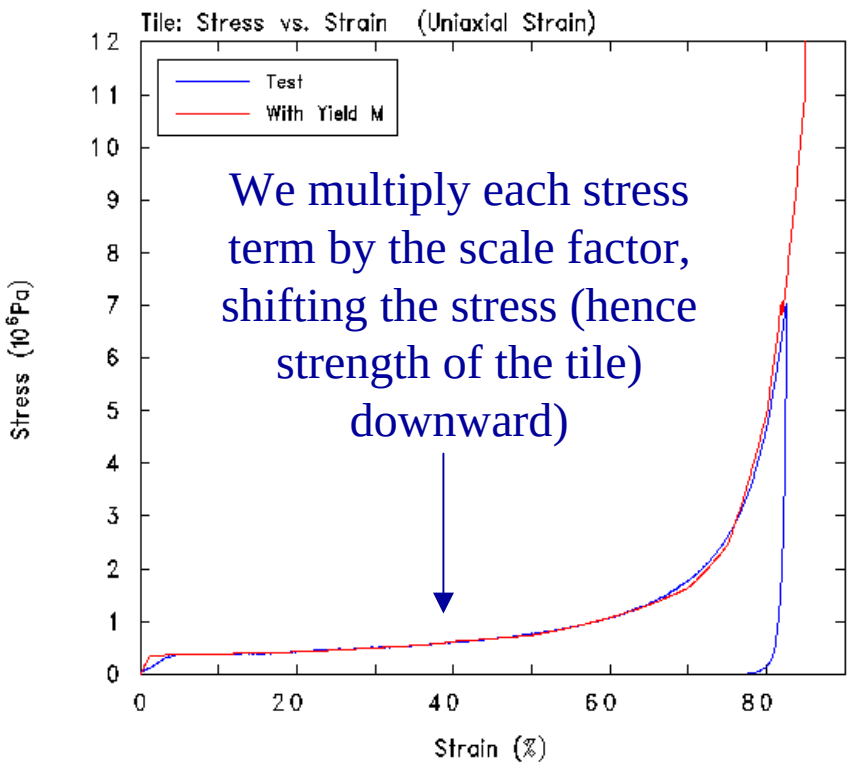

- Since the fast-running physics-based model is based on material properties, the only way to adjust the model is by adjusting those material properties.
- We provide a "bounding model" by adjusting the tile strength – that is, making the tile weaker.
- In particular, each point in the data curve is shifted down by the multiplicative scale factor, and then the Hugoniot and shear terms are recomputed.

Bounding Model: 95% Bounding

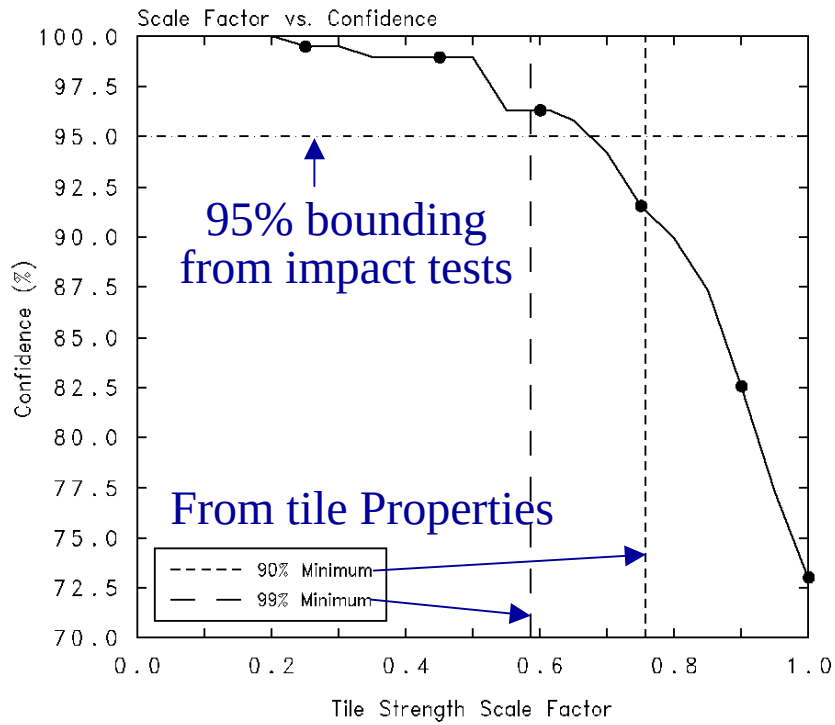

- Based on the experimental data, 95% bounding is achieved when only 9 data points lie above the curve.
- With the earlier version of the model, this level of bounding was achieved with a scale factor of 0.615. We have chosen to stick with this scale factor. For the updated model, at a scale factor of 0.615, 7 points lie above the curve.
- On page 13 of Material Properties Data, Volume 3, Thermal Protection System Materials Data, the in-plane compressive strength of the LI-900 tile material is listed:
  - average is 70 psi,
  - 90% minimum is 53 psi, corresponding to a scale factor of 0.76
  - 99% minimum is 41 psi, corresponding to a scale factor of 0.59.
- Thus, the scale factors from the material testing are in reasonable agreement with that found from the ice impact tests.

F: L=0.5” W= 0.5” H =0. 5” 30°

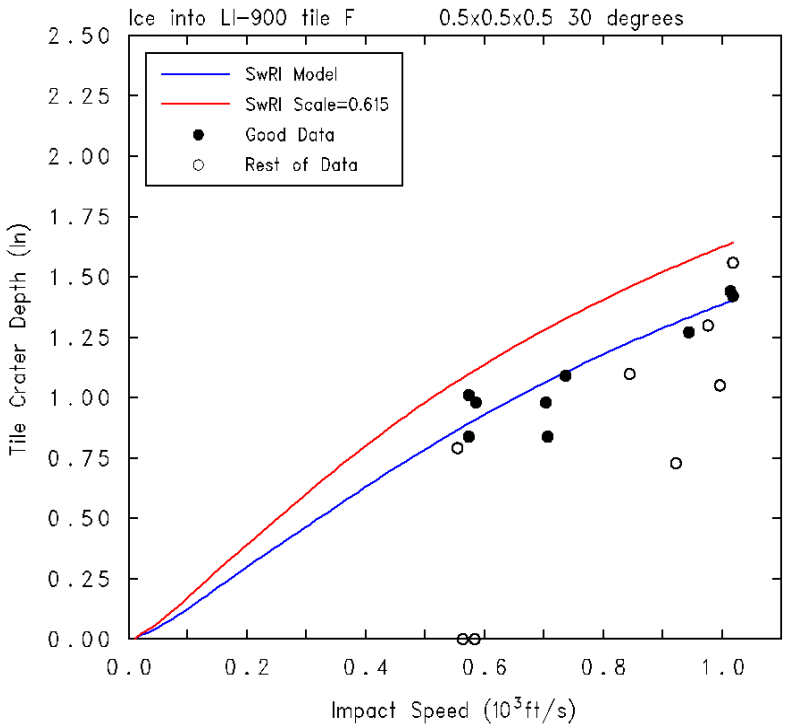

Depth

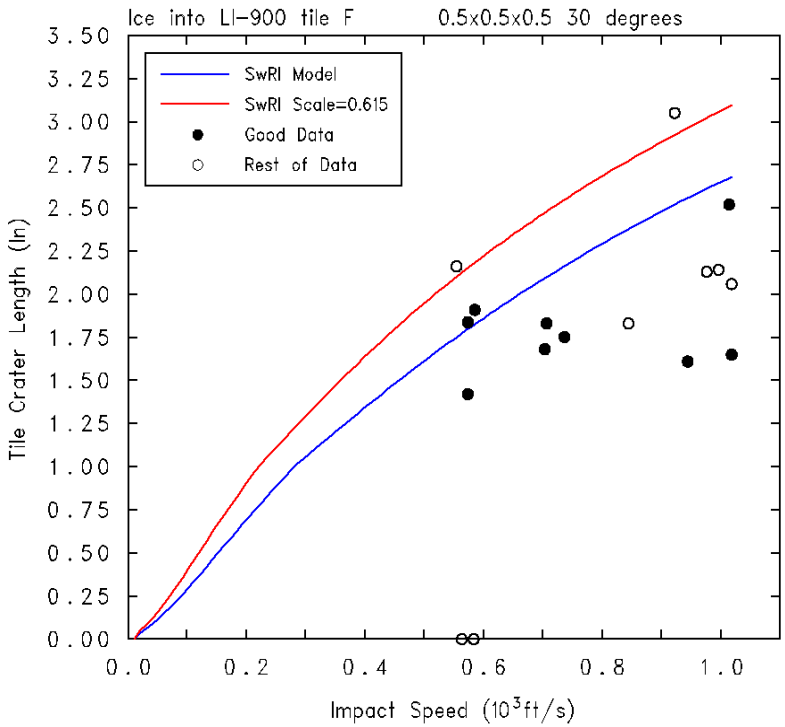

Length

CTH calculations of Ice impact into LI-900 Tile

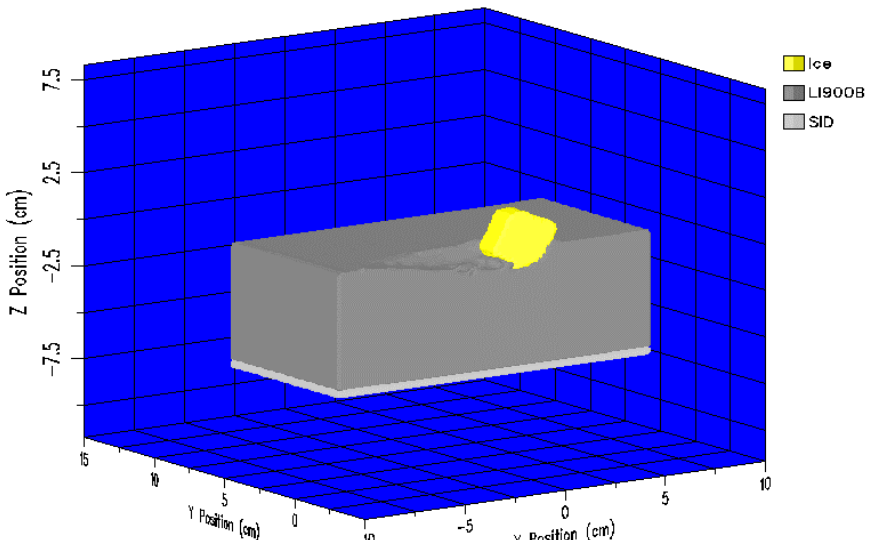

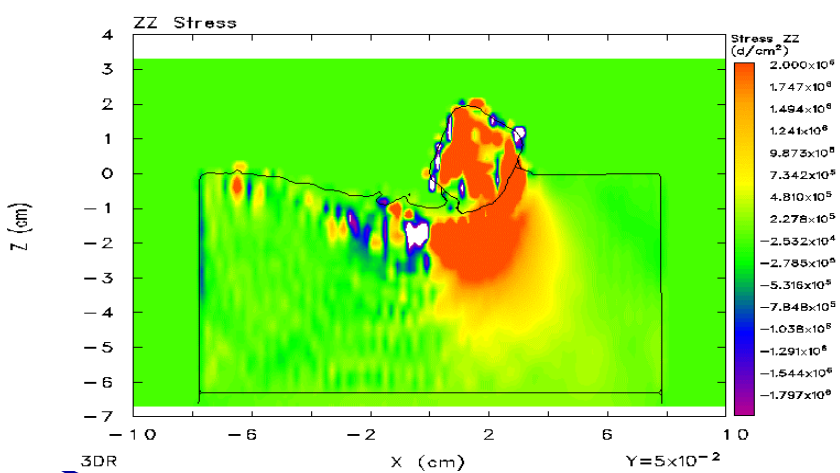

- Work has focused on 3-D computations of ice impact into LI-900 tile using new subroutines in CTH.
- Approximately 350 computations completed to date.
- Six different projectile geometries were examined
- Velocities ranged from 10 to 300 m/s, and impact angles varied from 10 to 30 degrees.

3-D CTH Ice Impact Computations

- 3-D Computations
- 2 upright individual LI900 tiles included in the computation
- 4 mm of SIP material included
- Bottom support is rigid
- Cell size 4 mm (0.016 in.)
- Y=0 is plane of symmetry

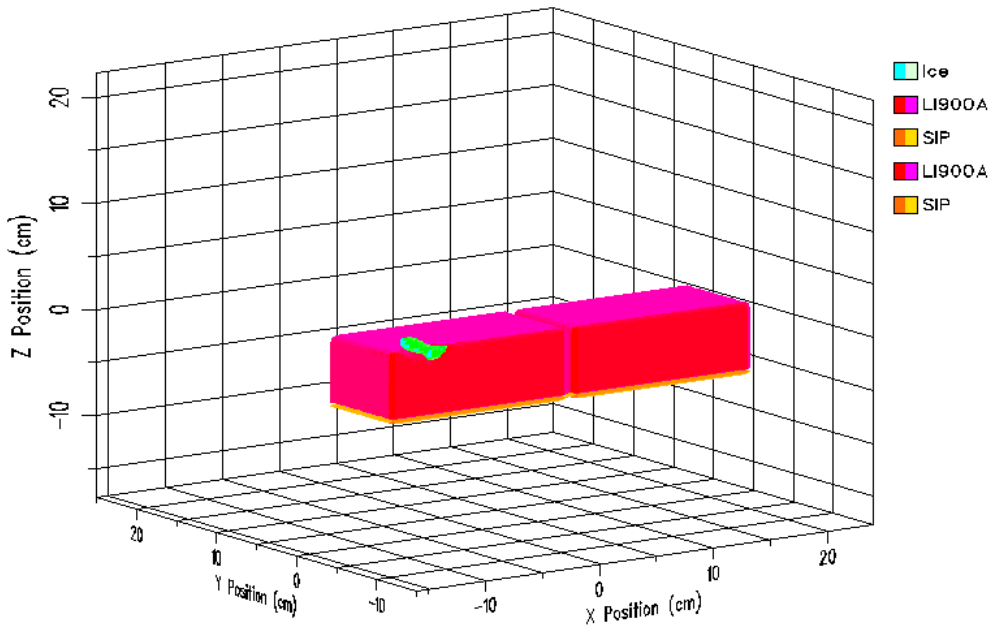

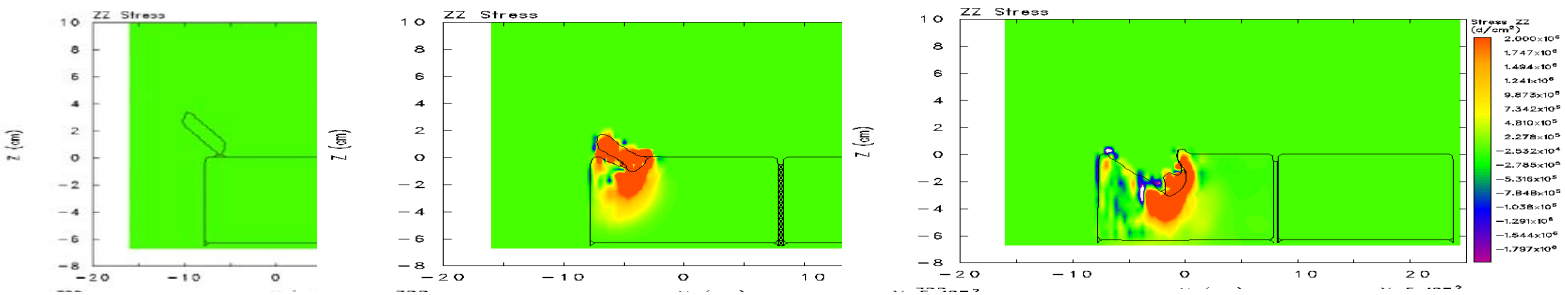

CTH Ablator Numerical Simulations

- Ablator 3’’ x 0.5’’ x 1’’
- Tile 6’’ x 6’’ x 2’’
- 3-D calculations
- Y=0 plane of symmetry
- Ablator and Tile EOS implemented by SwRI.
- No SIP
- 1.5 mm cell size (6 cells across ablator thickness)
- Ran a total of 26 cases
- Two examples follow

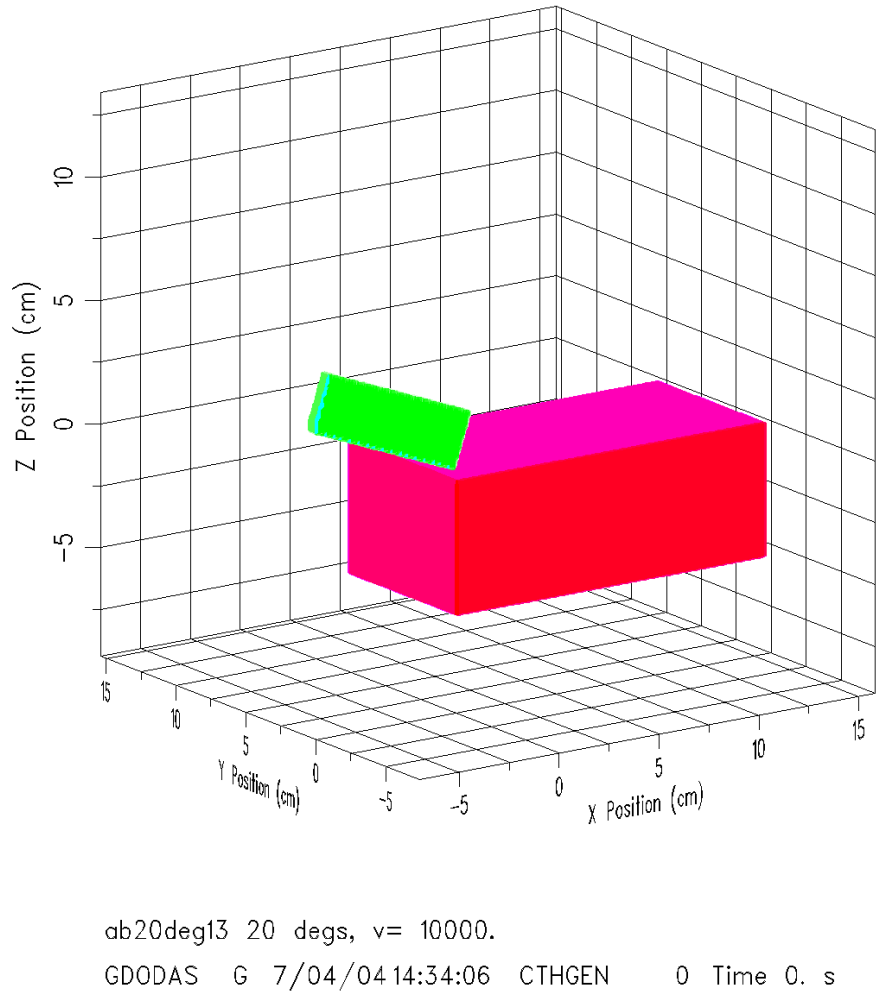

30° Impact at 350 ft/s (P2.11.7-1)

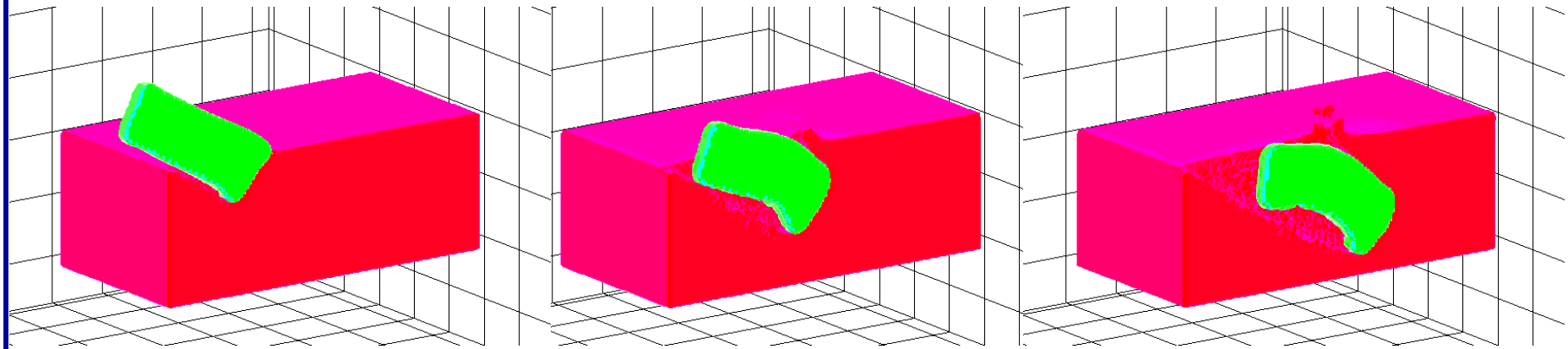

0.5 ms 1.0 ms 1.5 ms

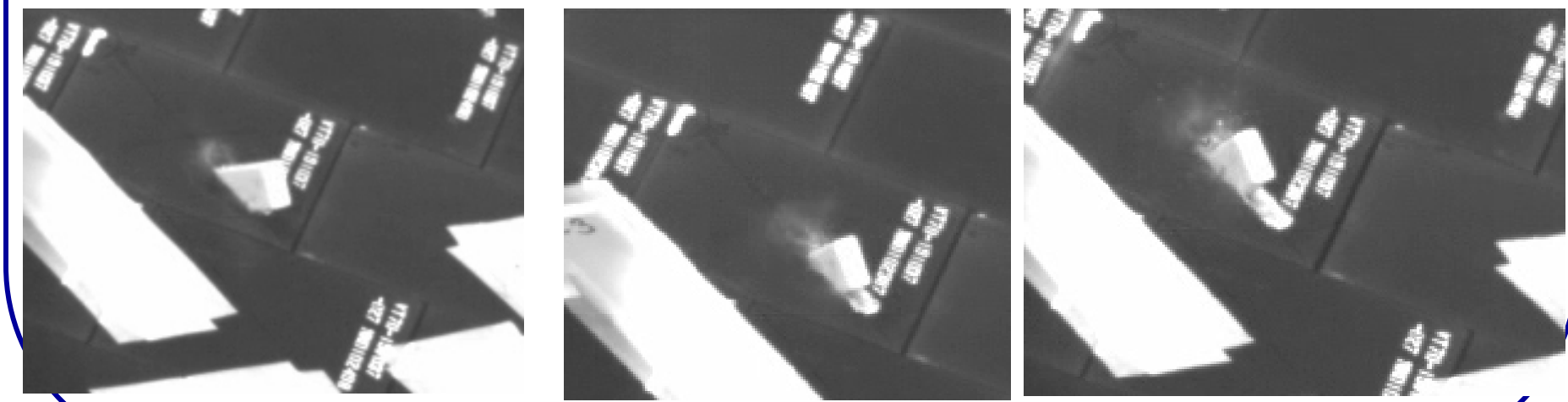

CTH crush-up profiles

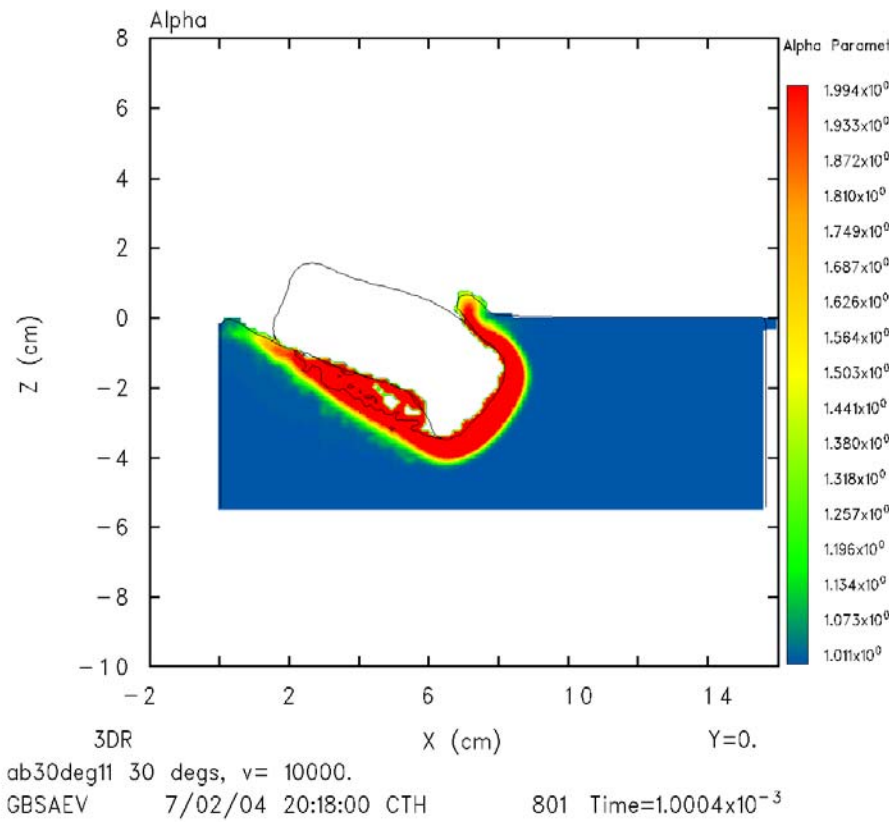

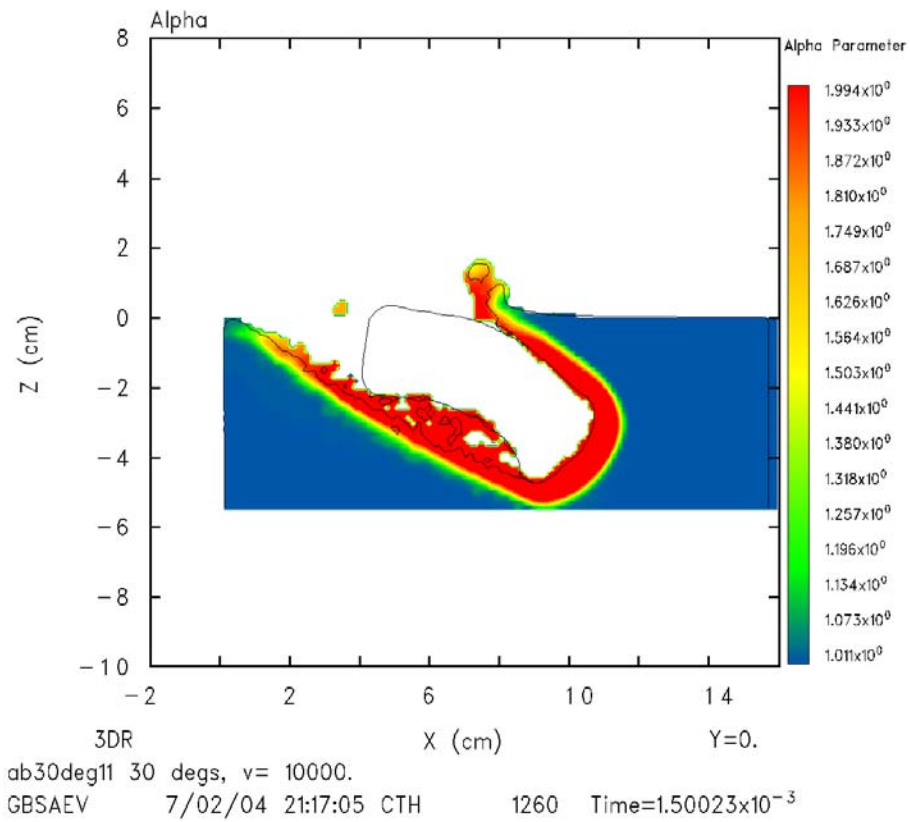

DOP given by the lowest point with alpha = 1.5

Alpha is the current density divided by initial density

Foam into Tile

BX-265 Foam Impactors

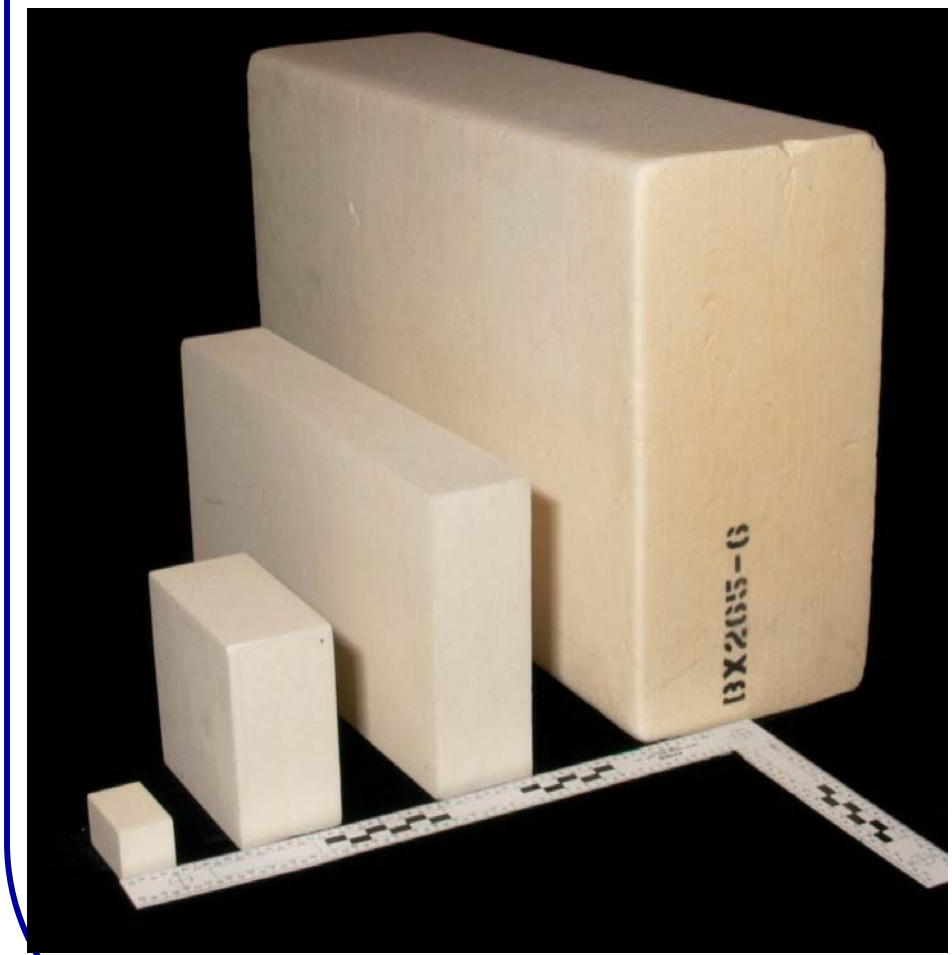

A wide range of projectiles were shot:

- Return to flight:
  - 1.6”×1”×1”; 1 gram (0.0022 lb)
  - 4”×4”×2”; 20 gram (0.044 lb)
  - 12”×6”×2”; 90 gram (0.2 lb)
- *Columbia* Investigation
  - 22”×12”×6”; 750 gram (1.67 lb)

Loading Surfaces

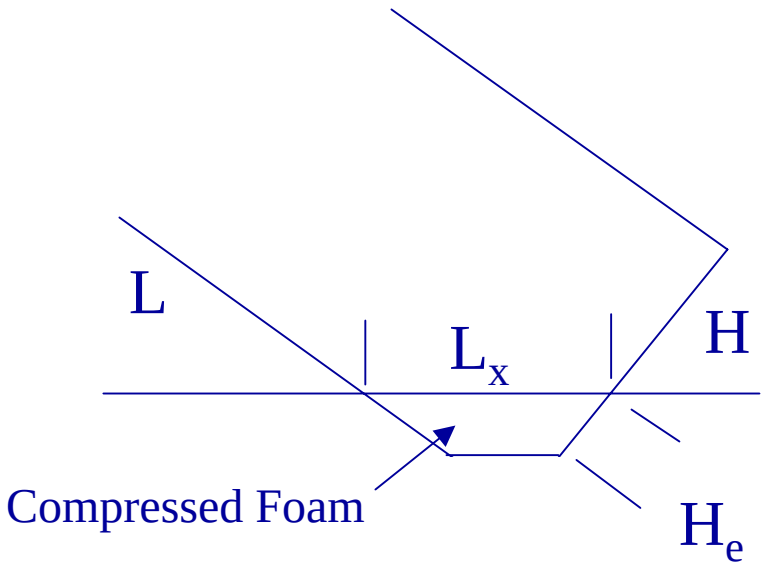

- As the foam projectile impacts the tile, only part of the face of the projectile is loaded by the target. Thus, the force on the face is reduced by the appropriate factor:

$$f = \frac{H_e}{H}$$

- The force on the length of the projectile acting upwards is

$$F_y = L_y W \min(\tilde{\sigma}_H(v_{y0})\cos(\theta) + \tilde{\sigma}_{crush-t}\sin(\theta), \tilde{\sigma}_{crush-t})$$

Equations of Motion

- The equations of motion, where *x* is the direction along the surface of the tile and *y* is the normal direction into the tile:

$$\frac{d\mathrm{v}_{\mathrm{x}}}{dt} = -f\,\frac{\sigma_{\mathrm{zz}}(\mathrm{v})}{\rho_p L}\cos(\theta)$$

$$\frac{d\mathrm{v}_{\mathrm{y}}}{dt} = -f\,\frac{\sigma_{\mathrm{zz}}(\mathrm{v})}{\rho_p L}\sin(\theta) - \frac{F_y}{\rho_p LHW}\cos(\theta)$$

$$\mathrm{v} = \sqrt{\mathrm{v}_{\mathrm{x}}^2 + \mathrm{v}_{\mathrm{y}}^2}$$

- These equations are integrated forward in time until either the impactor speed v drops below the speed required to crush tile (i.e., it comes to rest) or the impactor is forced back to the tile surface (i.e., it ricochets).
- (There is not a sine term in the first equation because the compliance of the foam leads to a nearly flat interface region between the tile and the foam.)

Tile Resistance to Penetration

- The resisting stress is of the form

$$\sigma_{zz}(v) = \sigma_{Hugoniot}(v)$$

- $\sigma_{Hugoniot}(v)$ is the stress as a function of particle velocity along the Hugoniot (the idealized one-dimensional planar impact). This function is computed based on the large-strain compression curves and the Hugoniot jump conditions. It is stored as a table for rapid look-up during the computation.

Riemann Solver

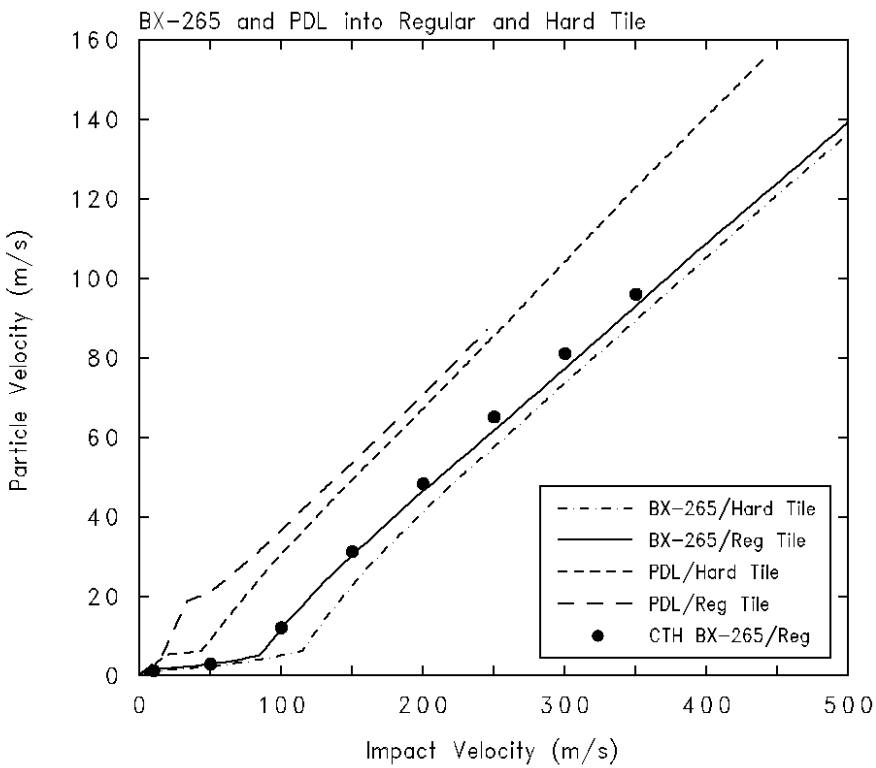

- A centerpiece of the penetration model is a Riemann solver that calculates the penetration speed for various impact speeds, as well as the wave speeds in the material.
- The solver solves the mass and momentum forms of the Hugoniot jump conditions to compute the stress and particle velocity at the interface between the two colliding materials
- The solver uses exactly the same equation-of-state tables used by CTH for modeling the tile and foam.
- The Riemann solver solves 2-, 3- and 4-wave problems, all of which can arise in foam vs. tile impacts.

Damage-No Damage Transition

- Explicit expression for the transition velocity for a 90° impact is

$$V_{crush} = u_{et} + u_{ef} + \left\{ \left(\frac{1}{\rho_{ef}} - \frac{1}{\rho_f(\tilde{\sigma}_{crush-t})} \right) (\tilde{\sigma}_{crush-t} - \tilde{\sigma}_{crush-f}) \right\}^{1/2}$$

- If there were no edge catching, then the transition would be given by

$$\mathrm{v} = \frac{V_{crush}}{\sin(\theta)}$$

Edge Catch

- The tile is pushed down by the foam, which has inertial resistance as well as a spring-like behavior of the SIP (represented by a spring constant *k*):

$$\ddot{y}_{tile} = \frac{L_y W \tilde{\sigma}_y - k A_{tile} y_{tile}}{m_{tile}}$$

- The current critical (transition) velocity is then computed according to

$$\mathrm{v} = \frac{V_{crush}}{\sqrt{\Delta y_{tile} / T_{SIP}} \sin(\pi / 4) + (1 - \sqrt{\Delta y_{tile} / T_{SIP}}) \sin\theta}$$

- If the current velocity is above this value, the edge catches and penetration into the tile begins.

Tile Fracture Algorithm

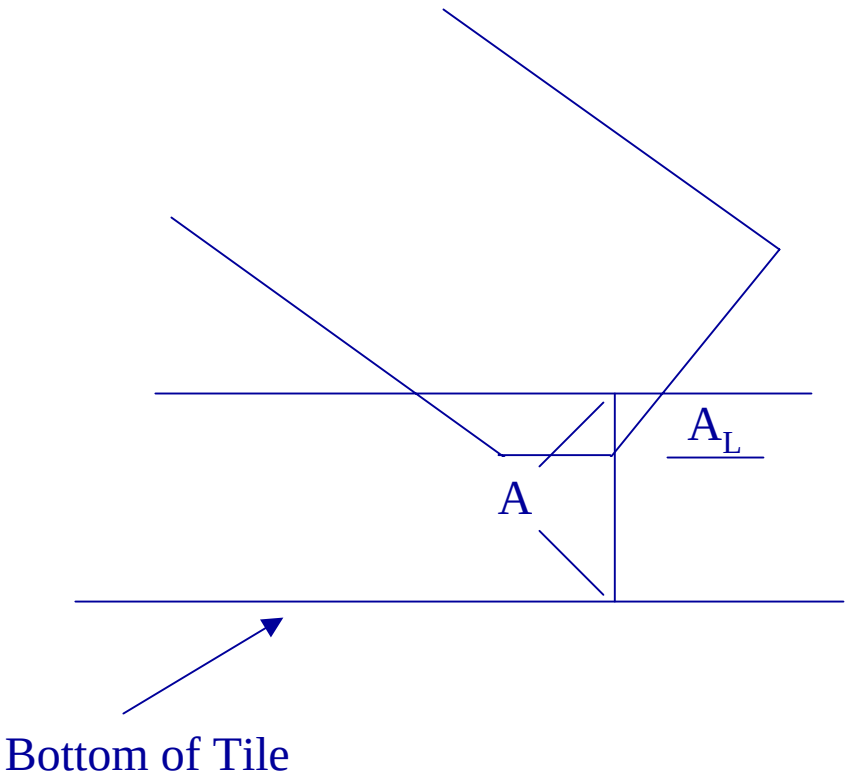

- There is a tile fracture algorithm, in an effort to determine when a tile breaks, as is seen in the shear-out tile failure mode, for example.
- The model is still under examination.
- A cross section is taken through the tile, with area *A*. If the area loaded by the impactor is given by A_L, then the tile breaks if the force exerted by the projectile is greater than the load the tile ligament can support (we assume that the tensile strength of the tile is equal to $\sigma_{crush\text{-}t}$):

$$A_L \sigma(v) > (A - A_L)\, \sigma_{crush-t}$$

Foam Model Examples

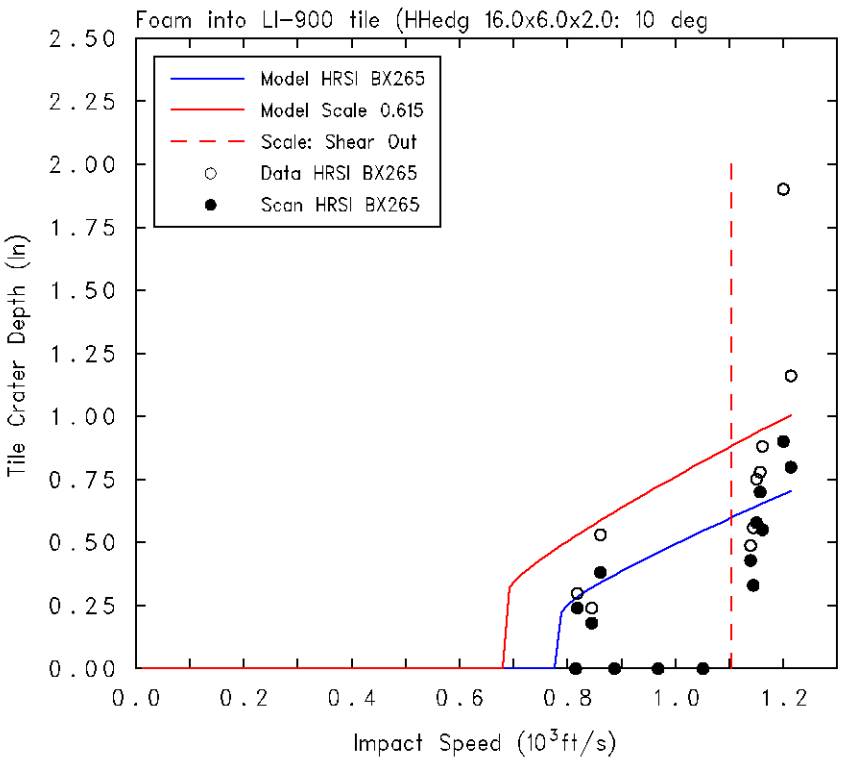

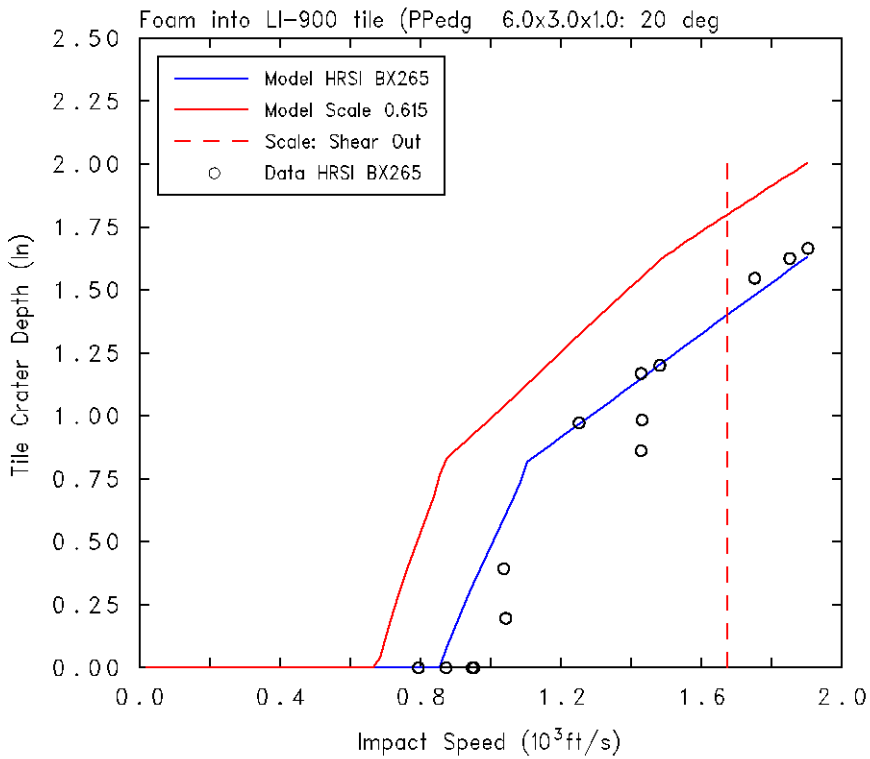

Test 1.1.9-2, 30 degs, 220 m/s (718 fps)

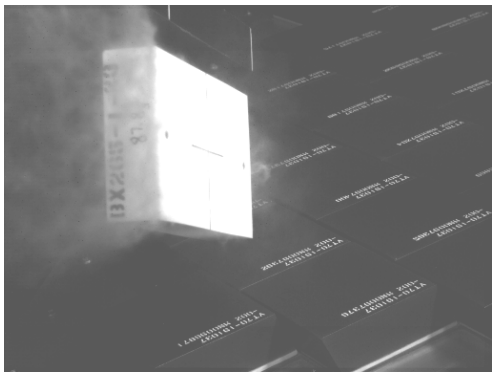

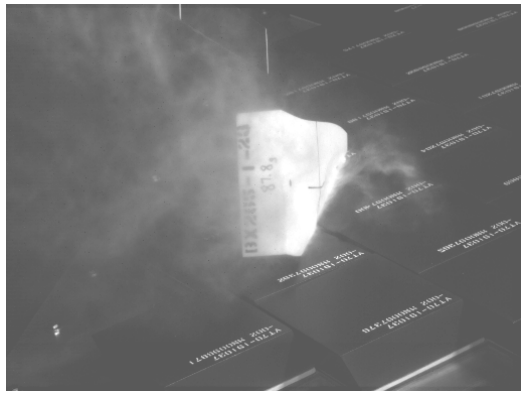

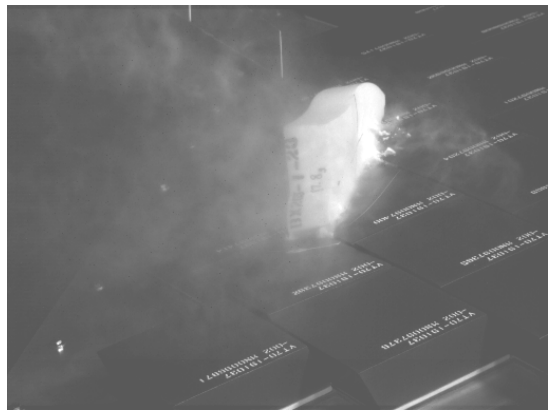

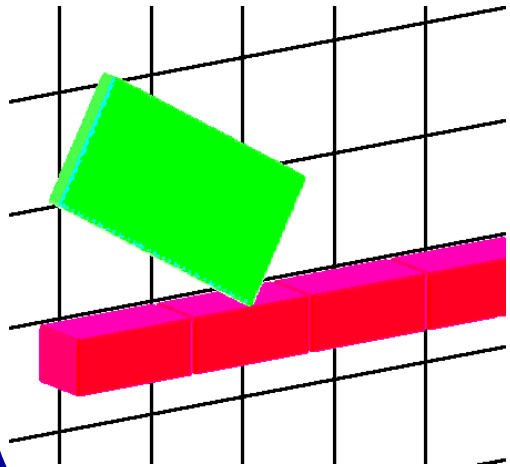

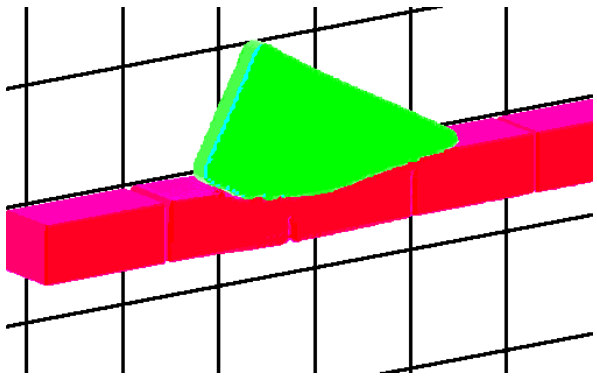

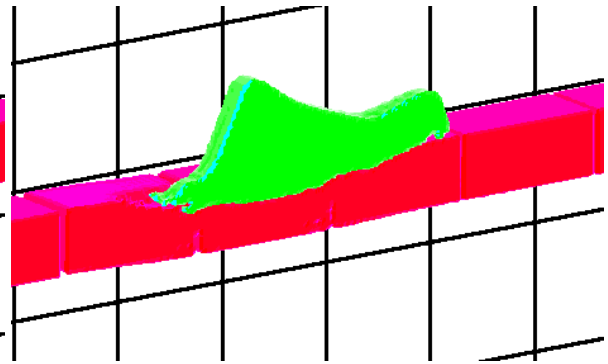

Tile-Out or Pop-Off

Tile Crush-Up at Bottom of Tile

- In 3d CTH computations, we do not quantitatively see as much crush-up at the bottom layer as we see in one-dimensional computations (to be shown later) (i.e., α is less): presumably this is due to the larger cell size in 3D.
- However, we do see crush-up all along the bottom of the tile.
- For example (next three charts)...

BX-265 vs. Tile CTH Computations

- 3-D Computations
- 9 upright individual LI-900 tiles included in the computation
- SIP simulated as a 4 mm (0.016 in.) gap
- Bottom support is rigid
- Cell size 4 mm (0.016 in.)
- Y=0 is plane of symmetry

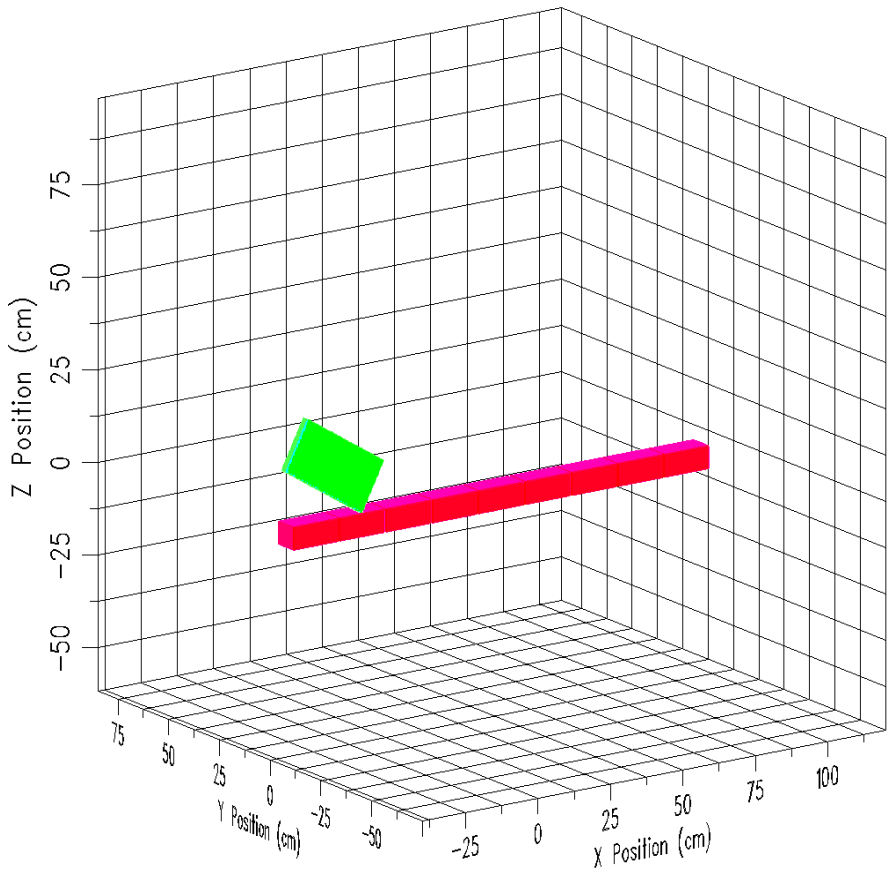

Simulation of P1.1.2-4: V=957 ft/s, θ = 20°
Crush-up plots in plane of symmetry

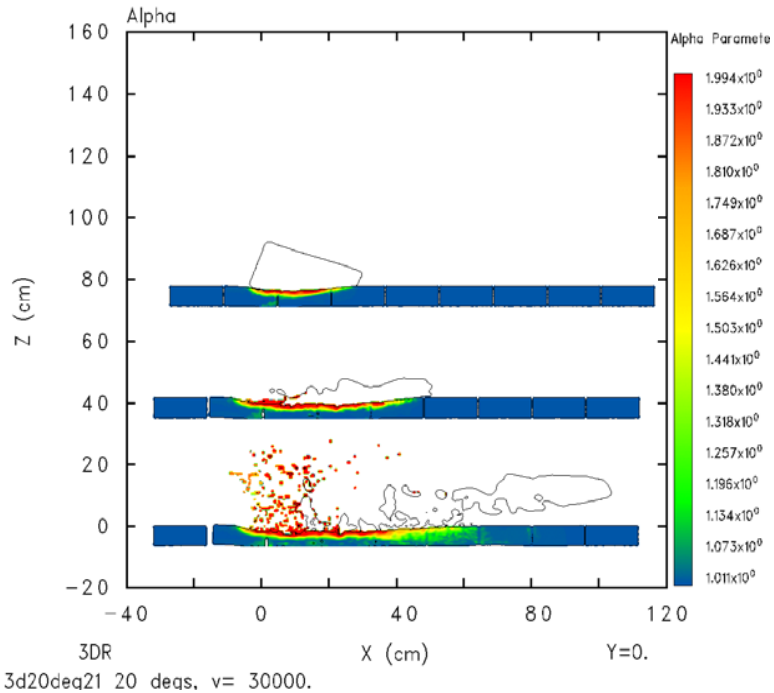

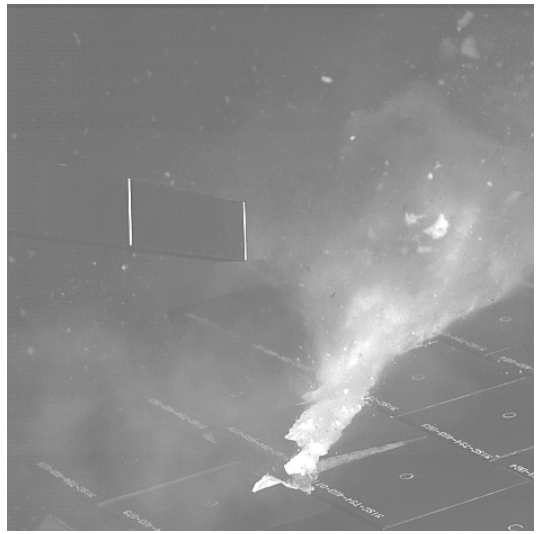

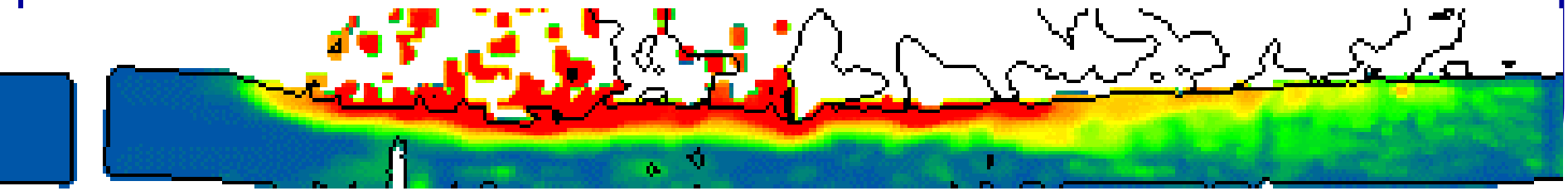

Simulation of P1.1.2-4: V=957 ft/s, θ = 20°
Crush-up plots in planes perpendicular to impact
(High resolution)

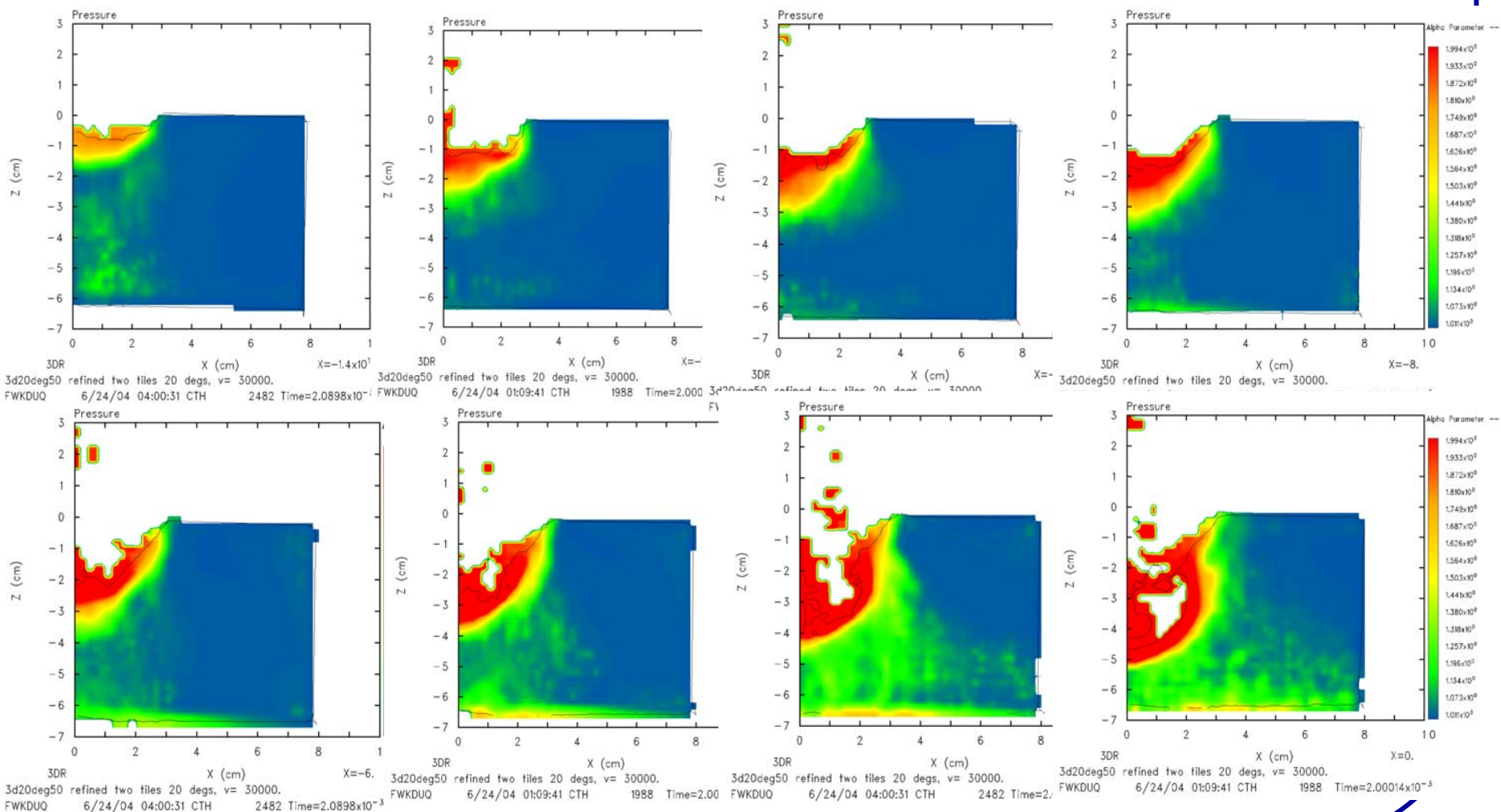

Simulation of P1.1.2-4: V=957 ft/s, θ = 20°
Crush-up plots in planes perpendicular to impact
(High resolution)

Yellow at bottom is crushed tile material

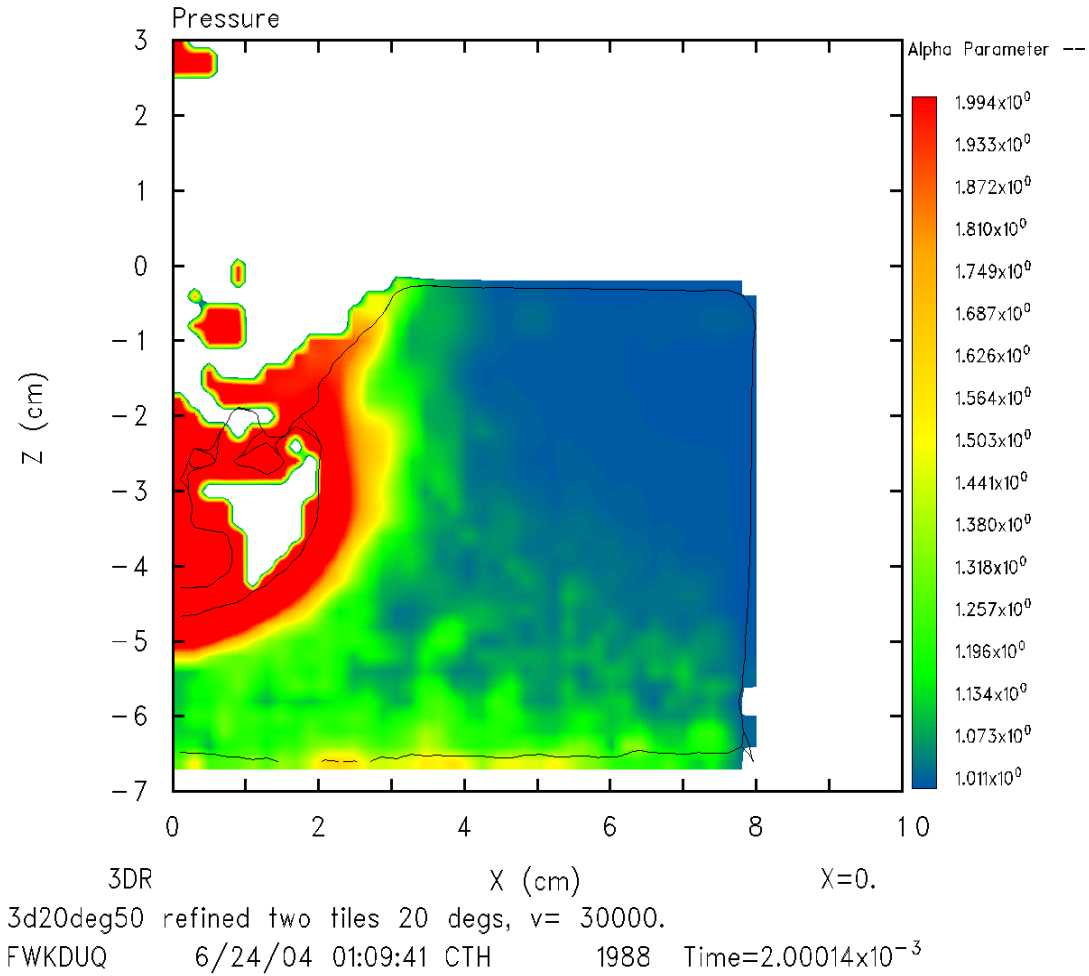

RCC Impact Testing

CAIB Recommendation R3.3-4
RCC Properties

- In order to understand the true material characteristics of Reinforced Carbon-Carbon components, develop a comprehensive database of flown Reinforced Carbon-Carbon material characteristics by destructive testing and evaluation.

Aramis System Allows Direct Measurement of Dynamic Displacements

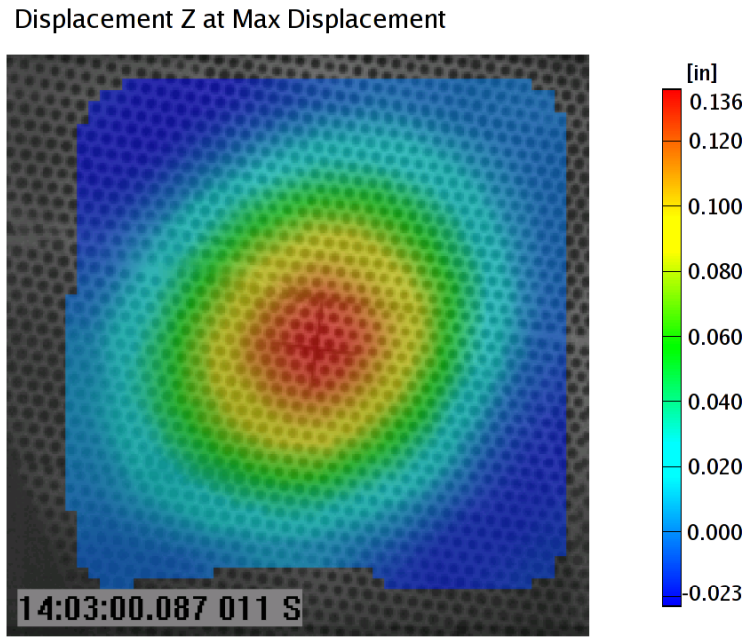

Strains can then be computed, and both displacements and strains can be compared to DYNA Team computations.

Return to Flight by *Discovery*

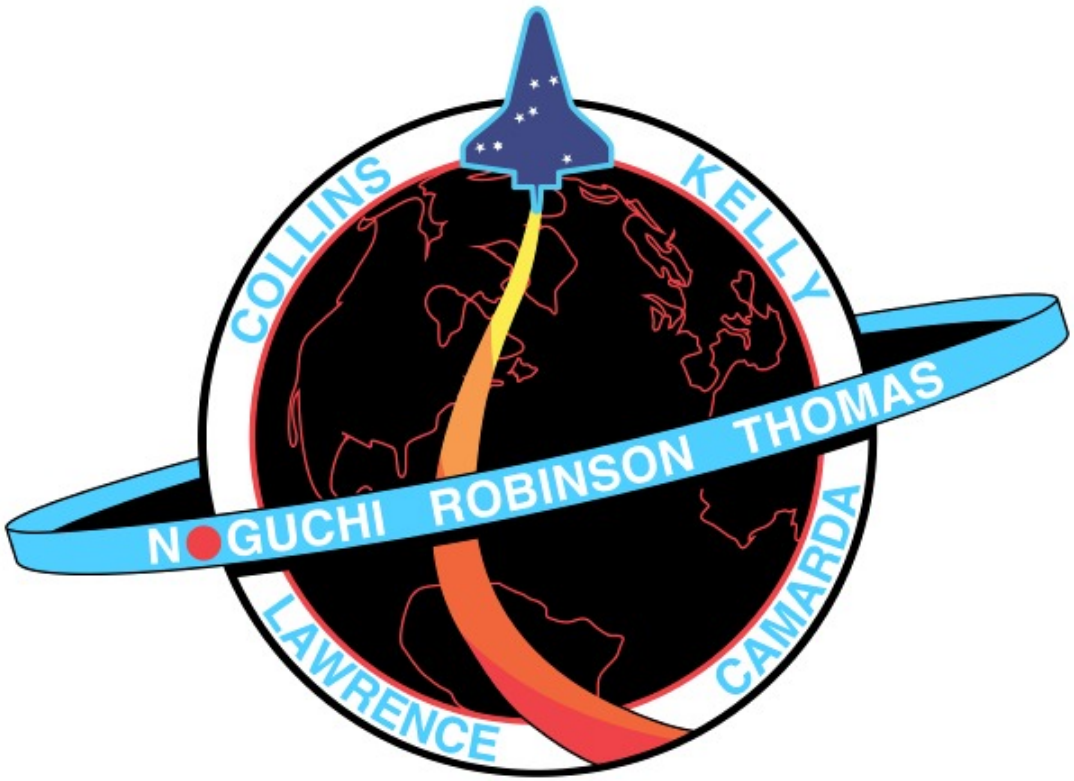

STS-114

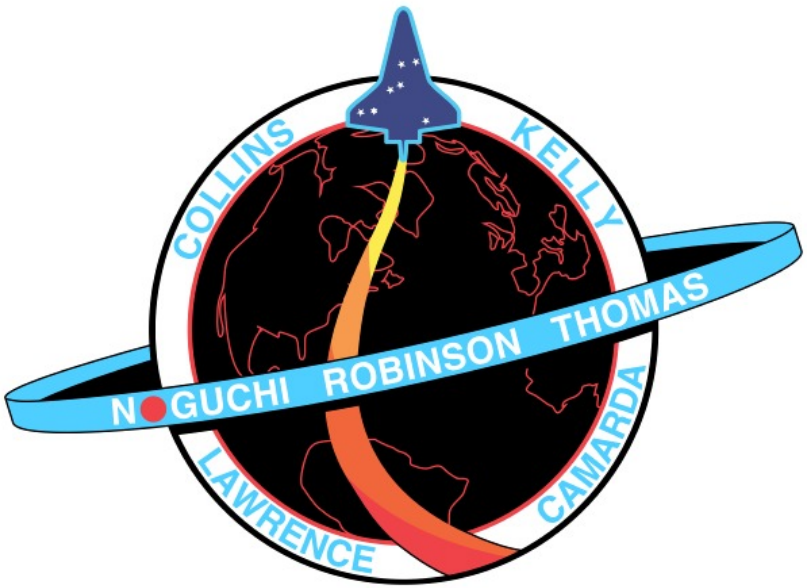

- 114th flight of the Space Shuttle Program
- 31st flight of *Discovery*
- *Discovery* first flew in August, 1984 (it is now the oldest operational shuttle, as well as the most flown)
- Mission: Tuesday, July 26 – Tuesday, August 9, 2005
- Crewed by
  - Eileen Collins
  - Jim Kelly
  - Charlie Camarda
  - Wendy Lawrence
  - Steve Robinson
  - Andy Thomas
  - Soichi Noguchi

Prelaunch Ice Formation

The Plots

- The following plots from the ice model are for four masses:
  - Set Length (1.5” or 2”)
    - L=1.5”, H=W=0.767”, mass = 13.2 gram = 0.029 lb
    - L=2.0”, H=W=1.02”, mass = 31.2 gram = 0.069 lb
  - Length/Width ratio = 2.5
    - L=1.77”, H=W=0.707”, mass = 13.2 gram = 0.029 lb
    - L=2.35”, H=W=0.94”, mass = 31.1 gram = 0.069 lb
- Impact speed in plots goes from 0 to 200 ft/s. **Understand that the model has only been baselined for speeds of 80 ft/s** to 1500 ft/s. The concern is that ice may not fracture at the lower velocities, and so there may be larger depths of penetration than the model predicts (the model assumes the ice fractures).
- Impact angles range from 5° to 55° in 5° increments.
- Blue curves are the nominal model, red curves are the 95% bounding curves.
- (If you want, you can pull the picture out of the presentation and enlarge it.)

L=1.5” W= 0.767” H =0.767” 5° - 55°
Mass = 13.2 gram = 0.029 lb

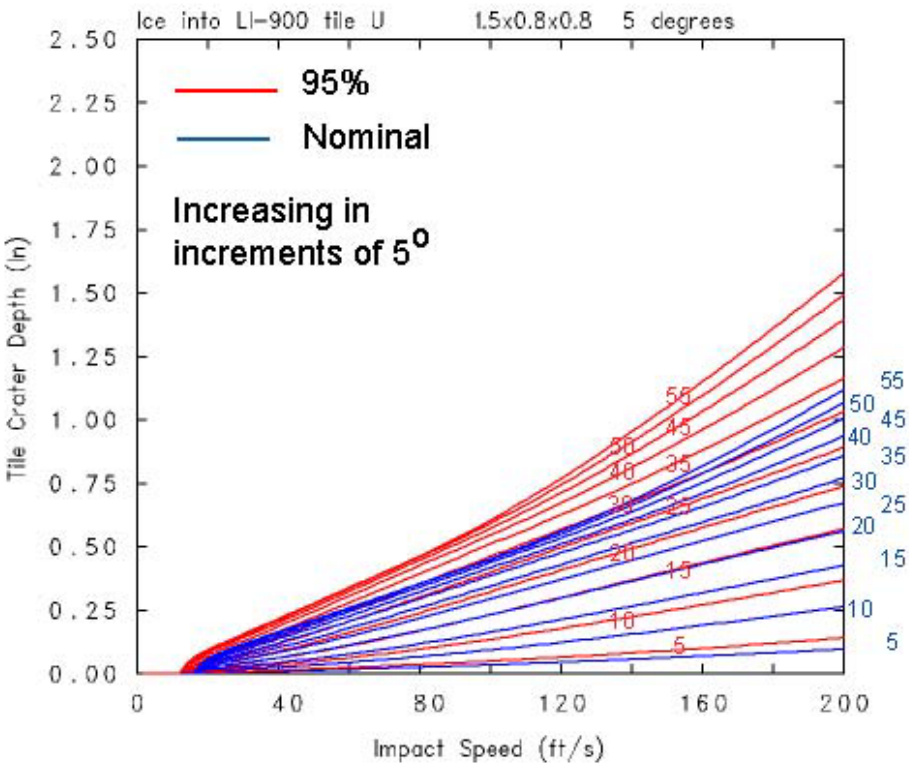

Depth

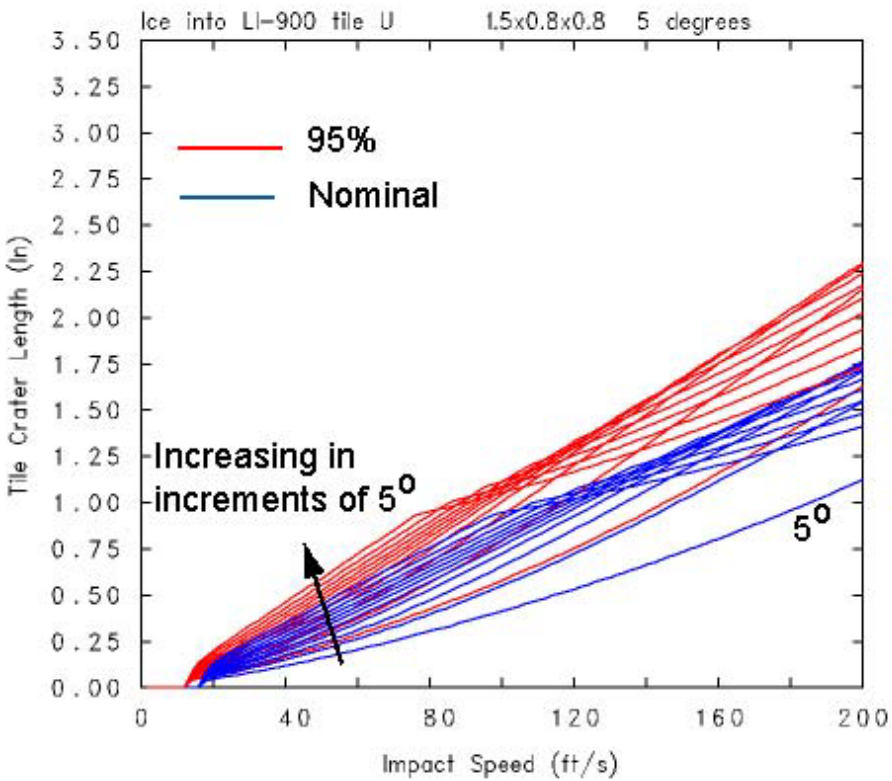

Length

L=2.0” W= 1.02” H =1.02” 5° - 55°
Mass = 31.2 gram = 0.069 lb

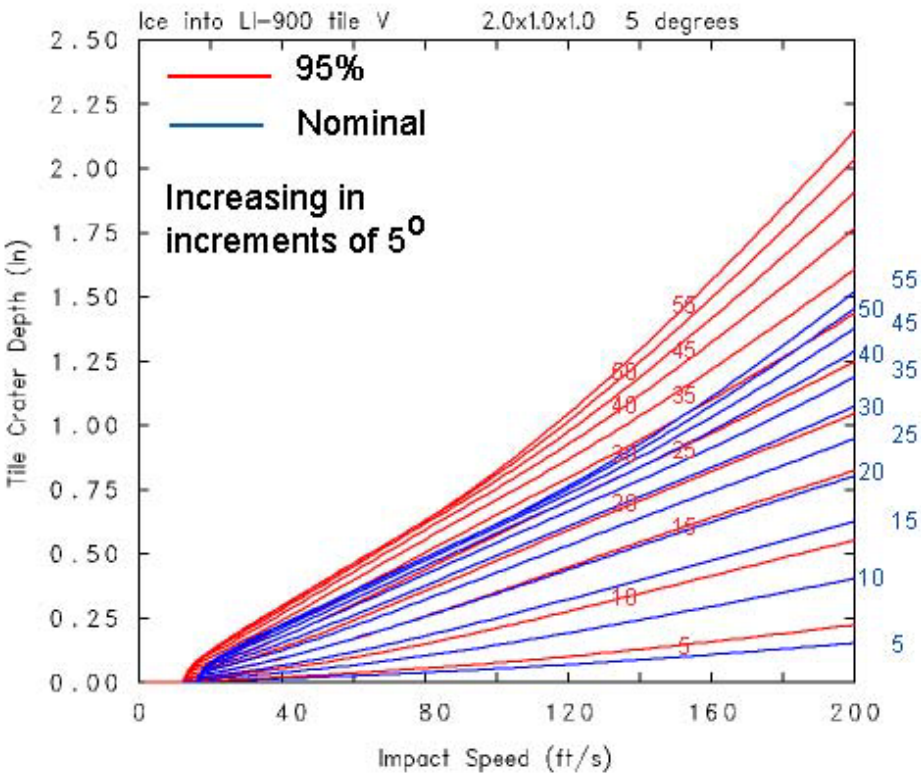

Depth

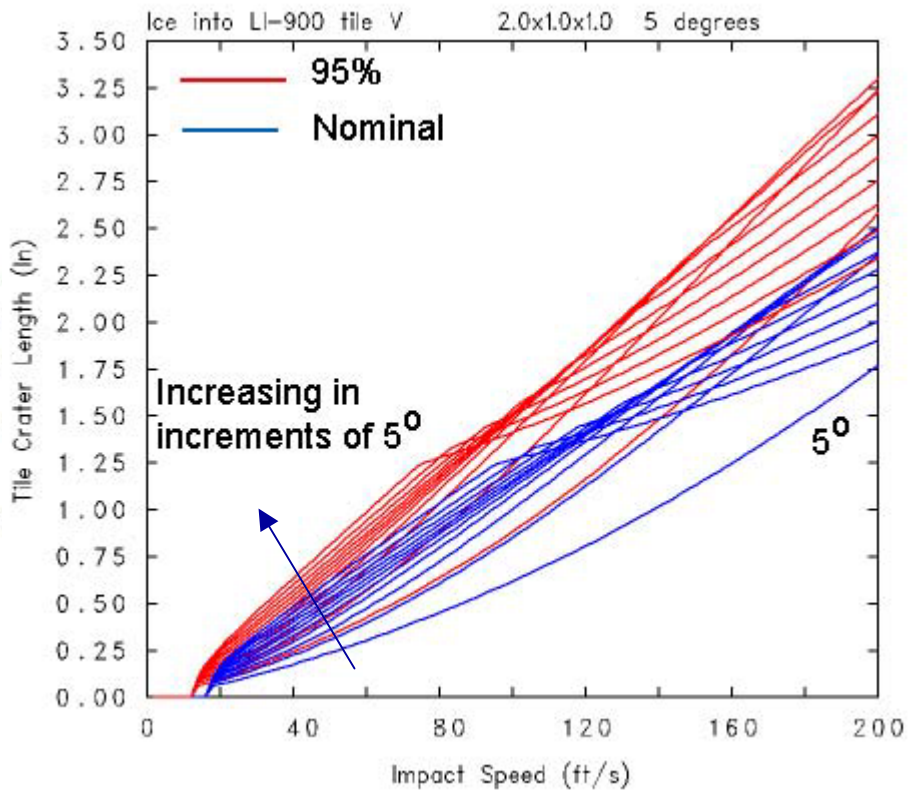

Length

Torn Thermal Blanket

Impact of Thermal Blanket on Speed Brake

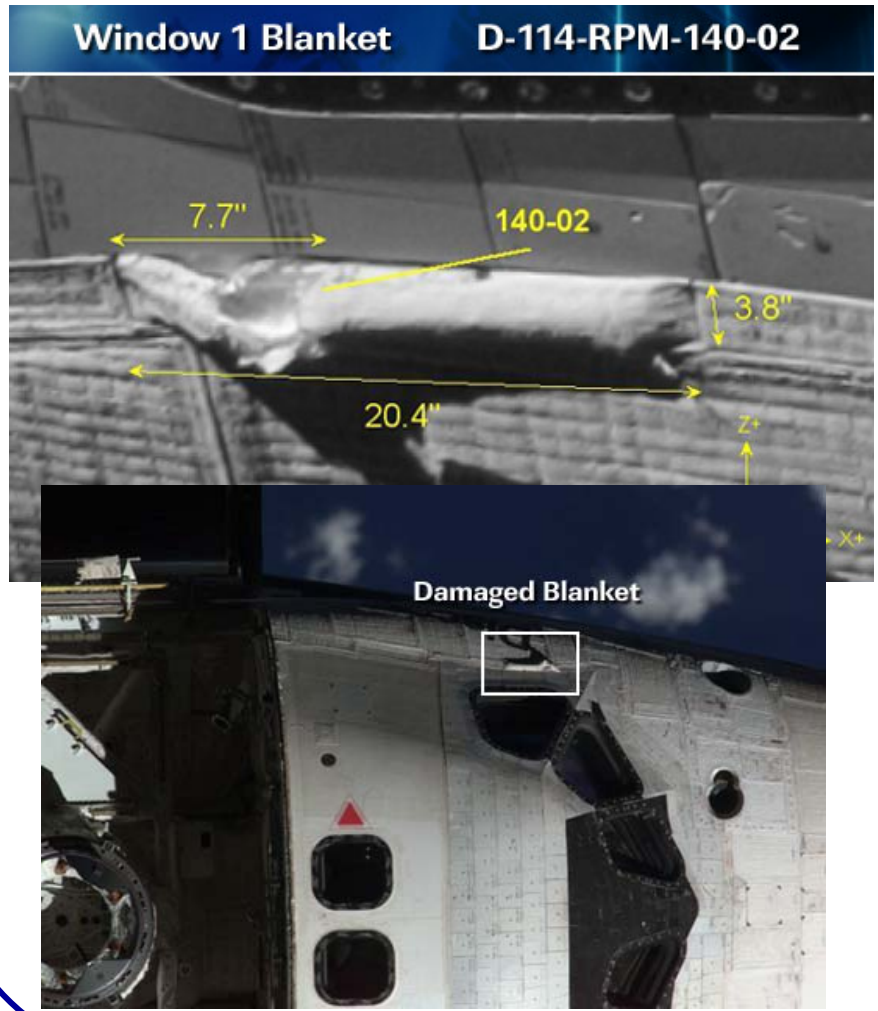

- We performed computations to examine the impact of the thermal blanket were it to tear free during re-entry for STS-114 and strike the speed brake.
- Computations were performed with the hydrocode CTH.
- The impact computations were performed for a velocity of 1600 ft/s.
- “Conservative” issues related to the modeling were explored with LS-DYNA.

Ribbon Fabric Projectile: 12.7” × 3.8” × 0.18” (.053lb) impacting thermal blanket and speed brake at 1600 ft/s

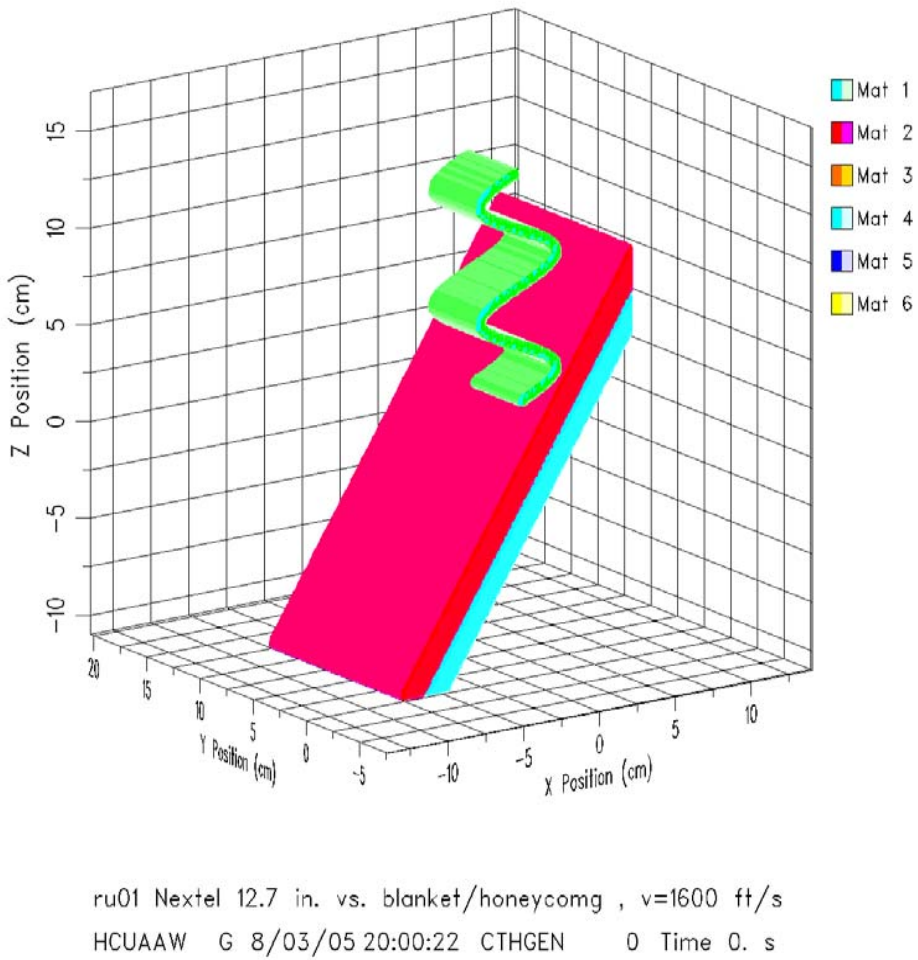

Ribbon Fabric Projectile: 12.7” × 3.8” × 0.18” (.053lb) impacting thermal blanket and speed brake at 1600 ft/s

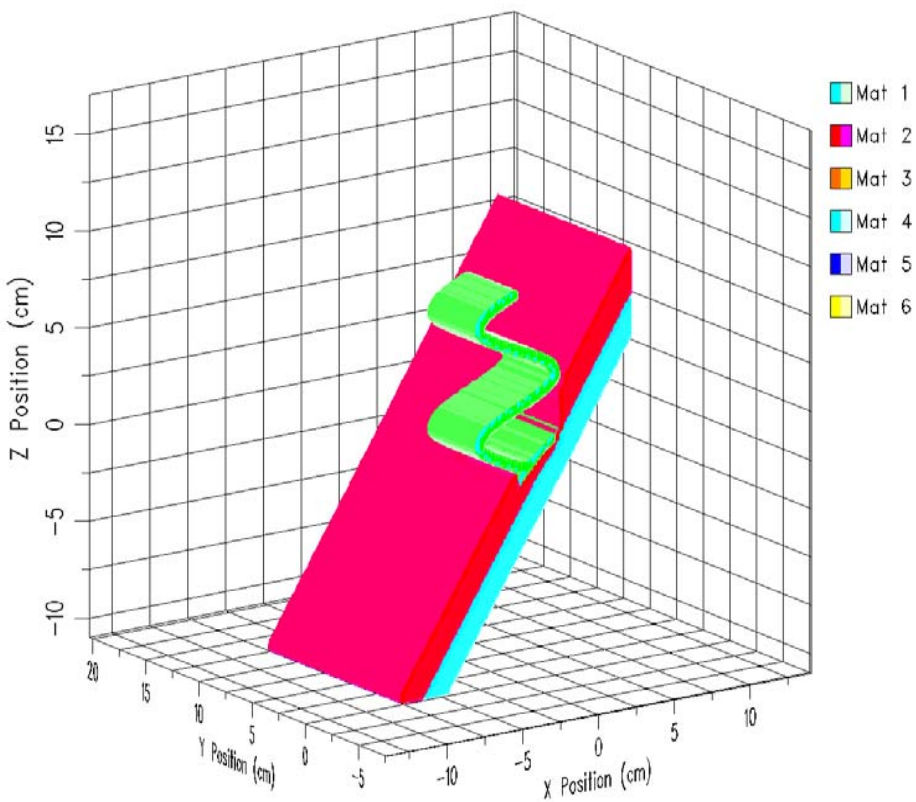

ru01 Nextel 12.7 in. vs. blanket/honeycomg , v=1600 ft/s

HCUAEA 8/03/05 20:48:46 CTH 261 Time 1.253×10^{-4} s

Ribbon Fabric Projectile: 12.7” × 3.8” × 0.18” (.053lb) impacting thermal blanket and speed brake at 1600 ft/s

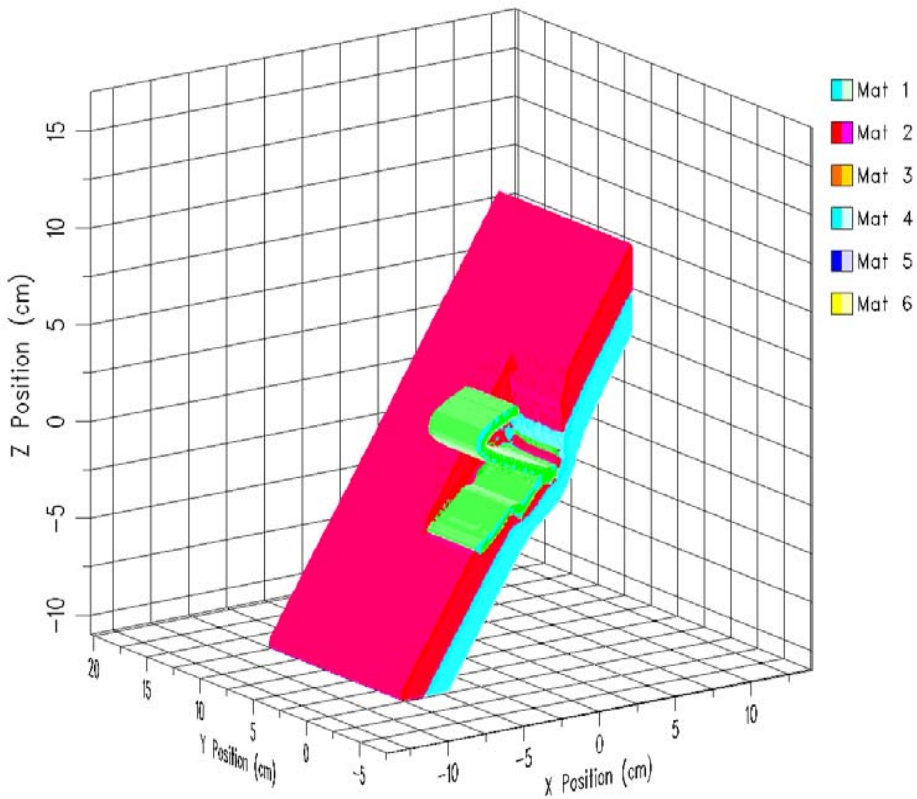

ru01 Nextel 12.7 in. vs. blanket/honeycomg , v=1600 ft/s

HCUAEA 8/03/05 21:25:07 CTH 481 Time 2.5024×10^{-4} s

Ribbon Fabric Projectile: 12.7” × 3.8” × 0.18” (.053lb) impacting thermal blanket and speed brake at 1600 ft/s

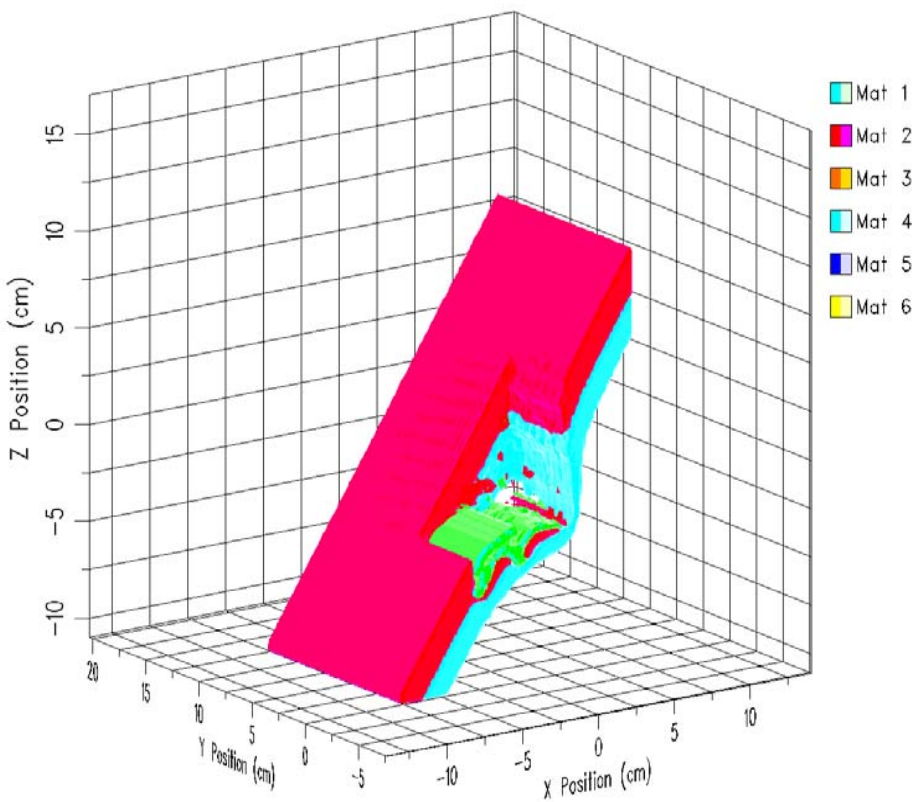

ru01 Nextel 12.7 in. vs. blanket/honeycomg , v=1600 ft/s

HCUAEA 8/03/05 21:59:46 CTH 692 Time 3.7543×10^{-4} s

Ribbon Fabric Projectile: 12.7” × 3.8” × 0.18” (.053lb) impacting thermal blanket and speed brake at 1600 ft/s

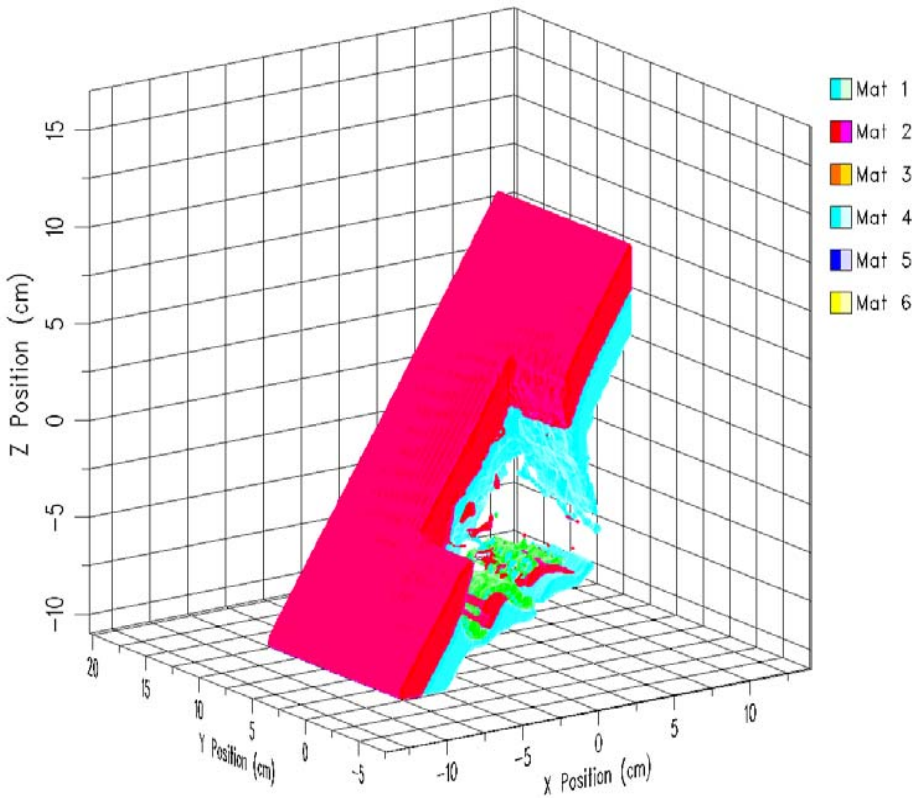

(Last)

ru01 Nextel 12.7 in. vs. blanket/honeycomg , v=1600 ft/s

HCUAEA 8/03/05 22:34:28 CTH 892 Time 5.0023×10^{-4} s

Initial Geometry
Impact speed: 1600 ft/s

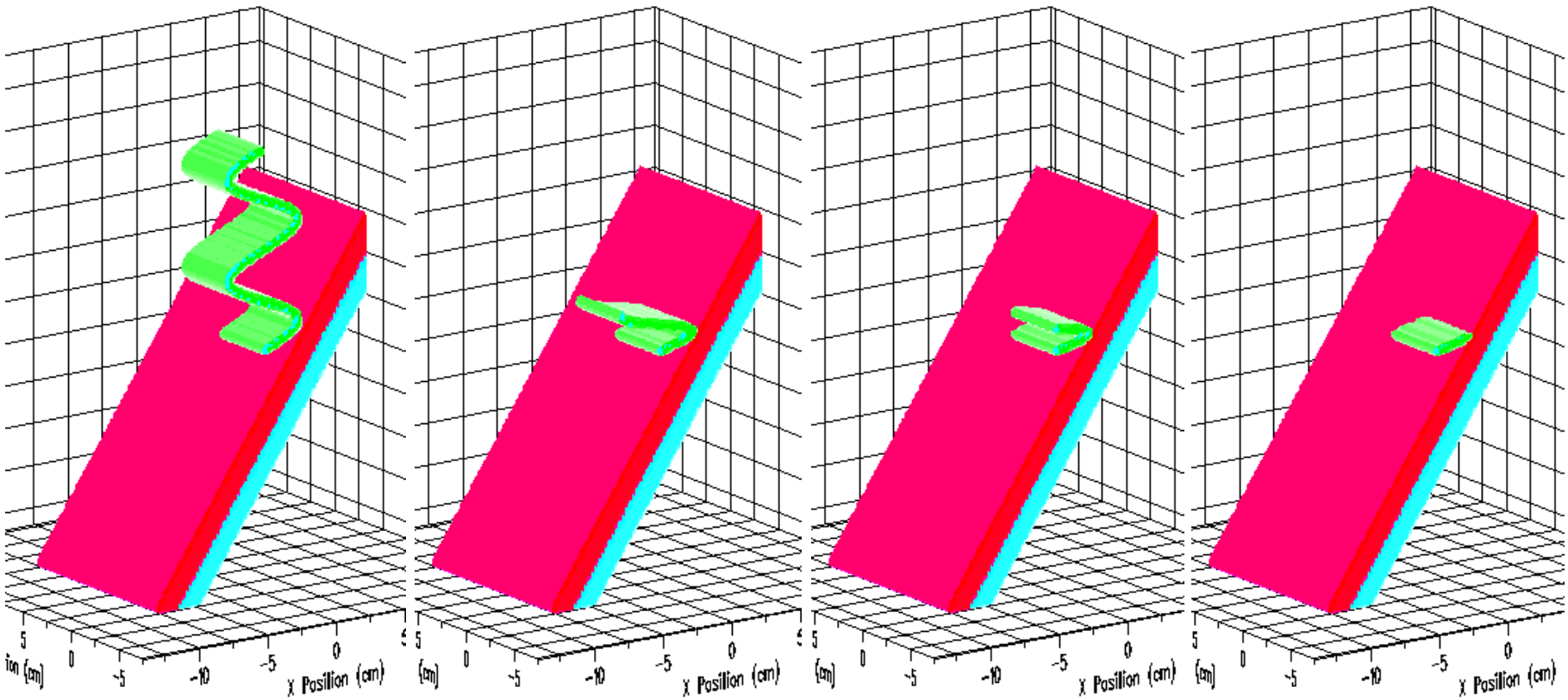

0.053 lb / 24 g	0.0177 lb / 8 g	0.0106 lb / 4.8 g	0.0053 lb / 2.4 g
12.7”×3.8”×0.18”	4.23”×3.8”×0.18”	2.54”×3.8”×0.18”	1.27”×3.8”×0.18”

Post Impact Geometry
Impact speed: 1600 ft/s

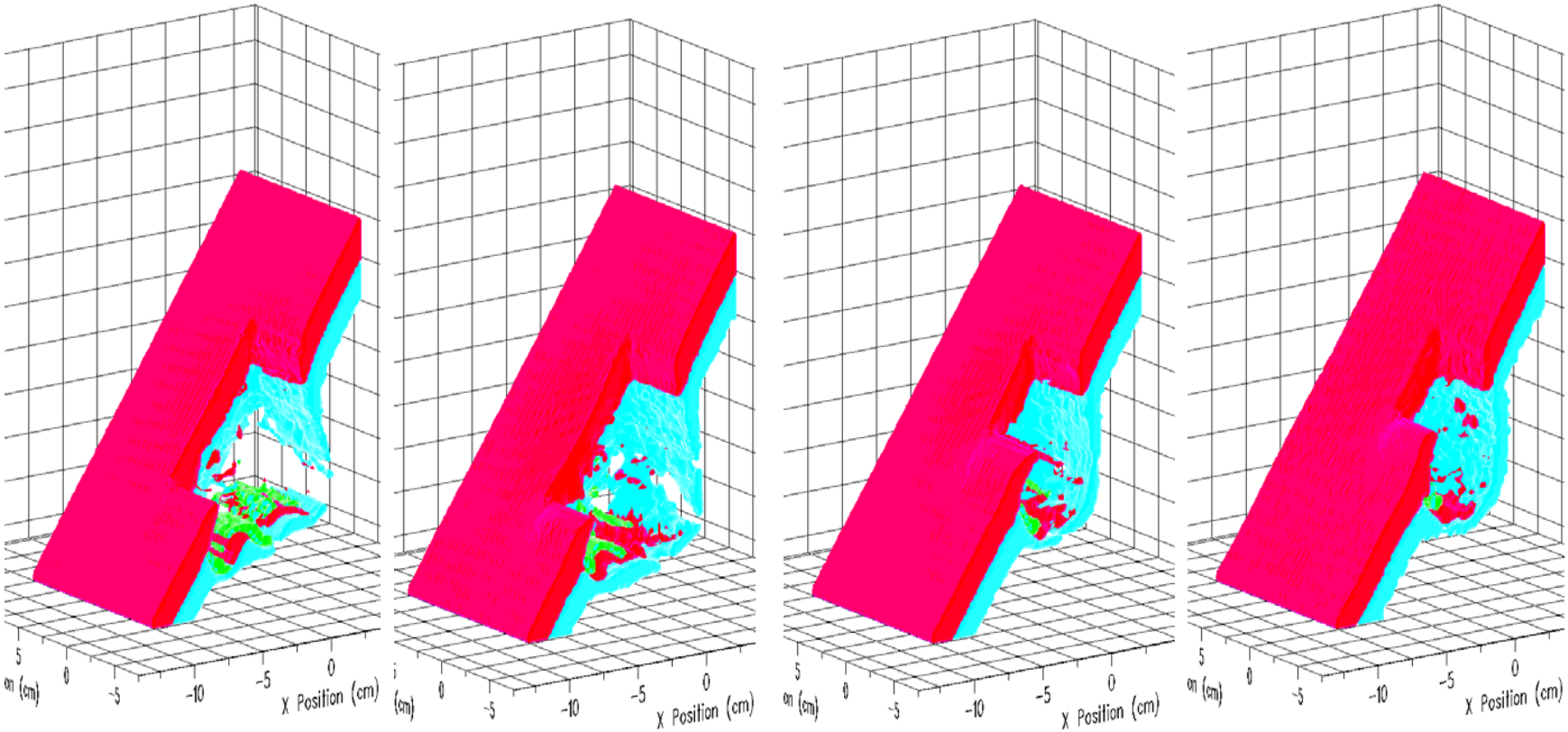

0.053 lb / 24 g	0.0177 lb / 8 g	0.0106 lb / 4.8 g	0.0053 lb / 2.4 g
12.7”×3.8”×0.18”	4.23”×3.8”×0.18”	2.54”×3.8”×0.18”	1.27”×3.8”×0.18”

Examining an “Conservatism” in Our Honeycomb Modeling

- Modeling the aluminum honeycomb is difficult.
- In the Eulerian code CTH, we are unable to resolve the structure of the front and back sheets of the honeycomb, since our computational cell size is 2.5 mm and the thickness of the aluminum sheet is 0.11” (0.3 mm).
- To see if the honeycomb fails much more easily than it should, a series of computations were performed in DYNA to explore with a honeycomb we built out of shell elements.

Conclusions

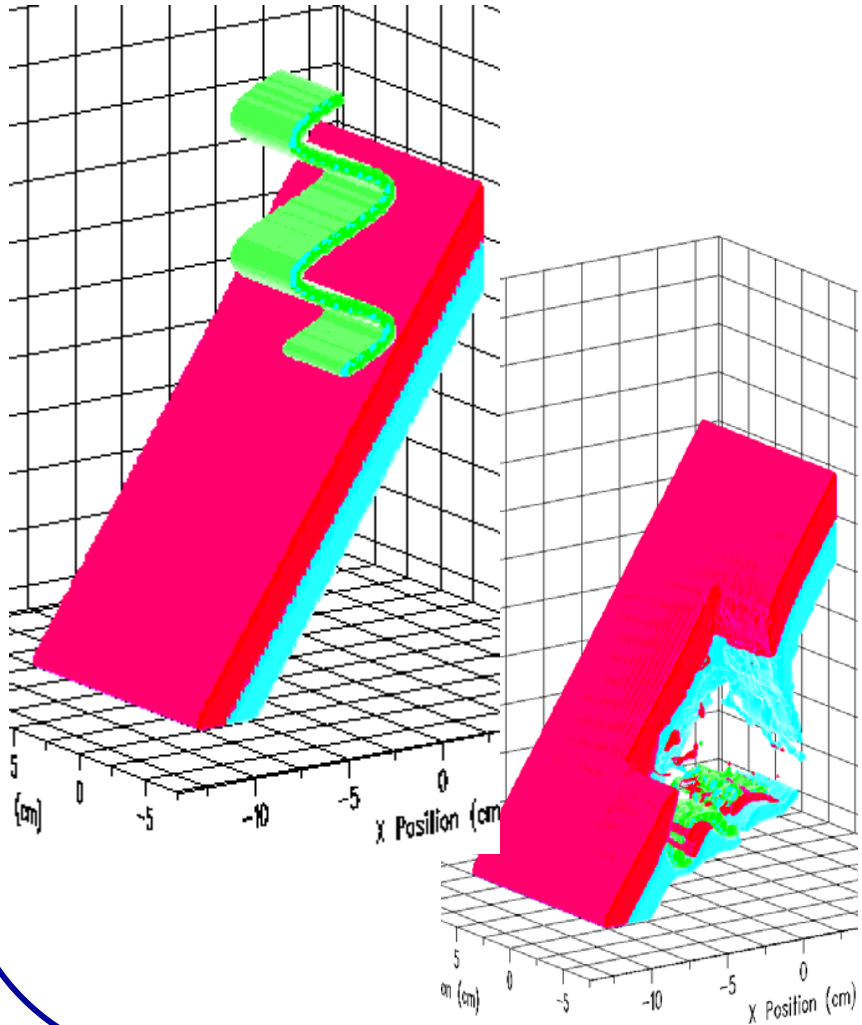

- Thermal blanket impact into the speed brake was modeled using current impact tools.
- It was assumed the fabric behaved similarly to LRSI LI-900 tiles (the density is similar).
- The blanket on the outside of the speed brake was modeled as an HRSI LI-900 tile.
- The honeycomb skin of the speed break was modeled with newly-created homogenized honeycomb material properties placed in the foam model.
- All impacts modeled in CTH (at 1600 ft/s) resulted in penetration of the tile and honeycomb.
- LS-DYNA honeycomb model contained a 0.0135 (6.1 g) impact (0.053/4).

Post Flight Inspection

Starboard Underside of Shuttle

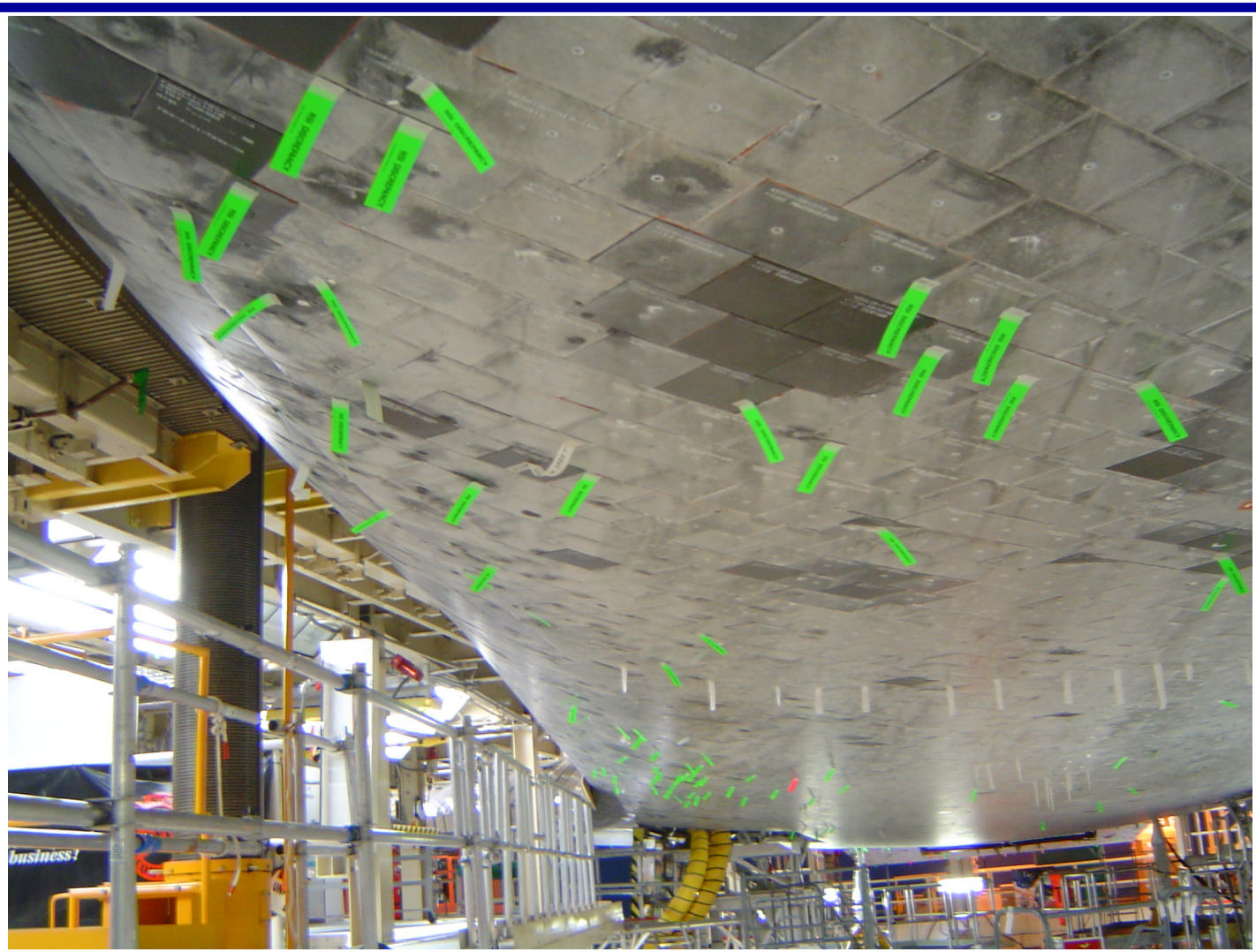

Impact Damage to Tile

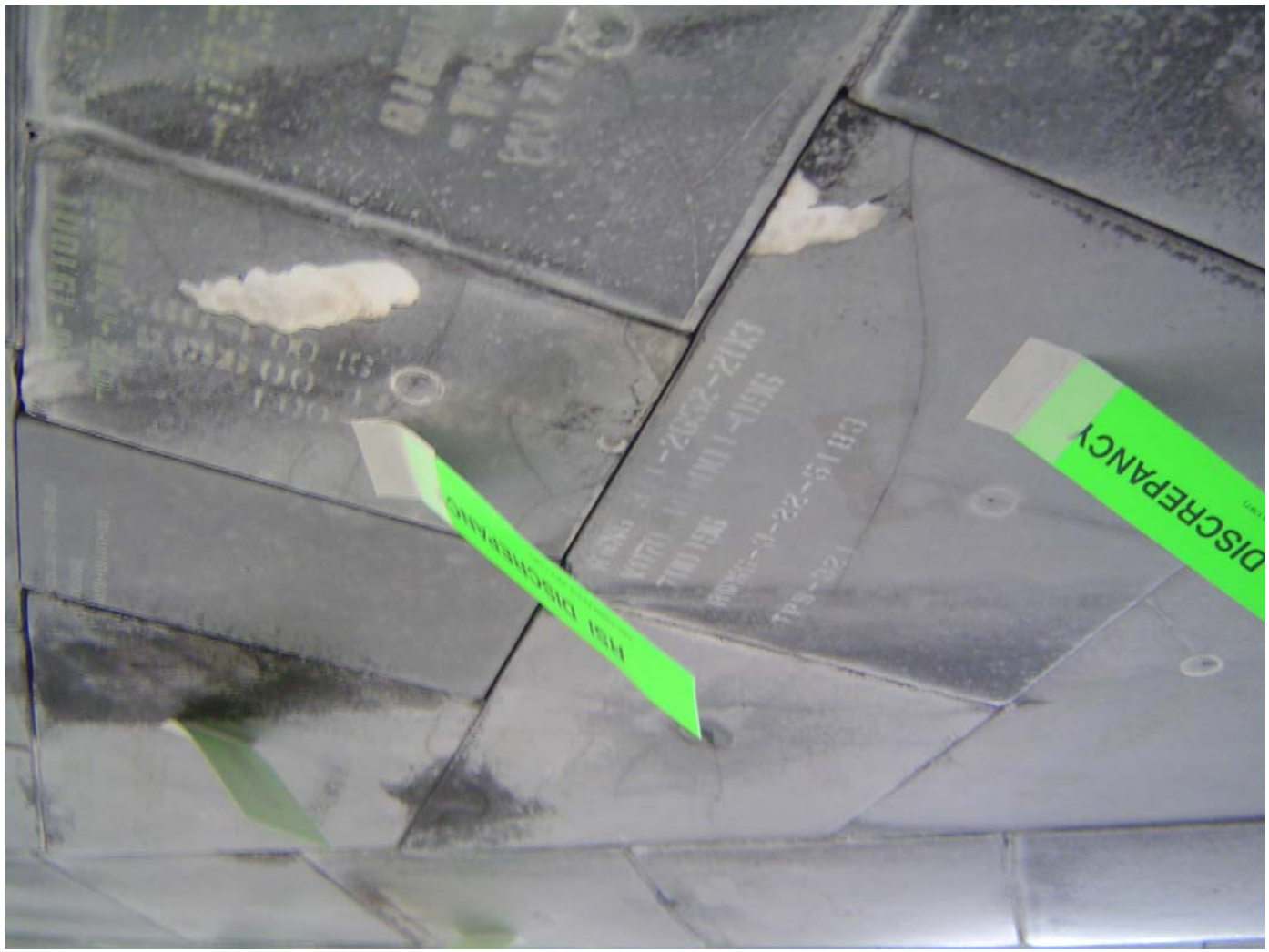

Charts to Estimate Debris Environment from Ice Damage

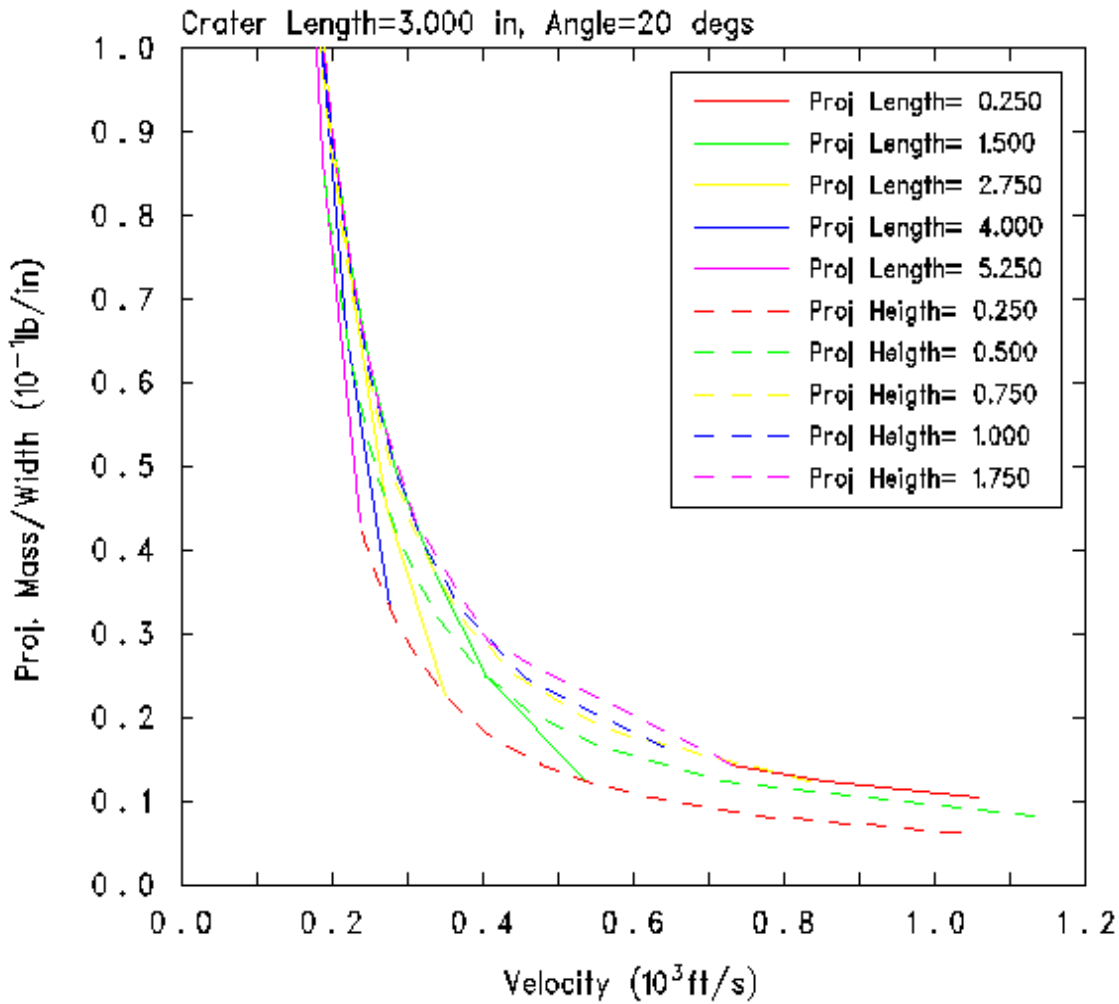

Charts to Estimate Debris Environment from Foam Damage

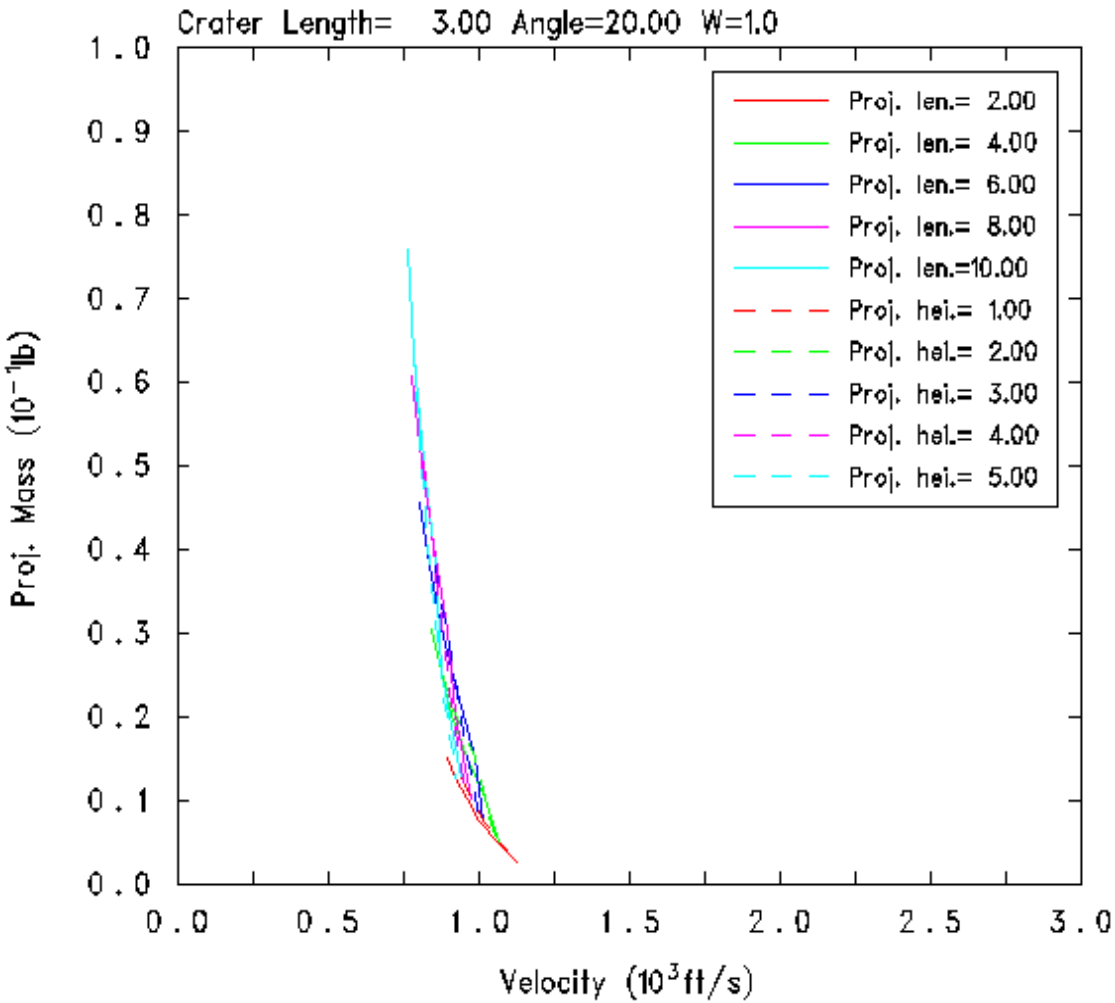

CAIB Recommendations R3.2-1,2 Reduce Damage and Risk

- Initiate an aggressive program to eliminate all External Tank Thermal Protection System debris-shedding at the source with particular emphasis on the region where the bipod struts attach to the External Tank. [RTF]
- Initiate a program designed to increase the Orbiter's ability to sustain minor debris damage by measures such as improved impact-resistant Reinforced Carbon-Carbon and acreage tiles. This program should determine the actual impact resistance of current materials and the effect of likely debris strikes. [RTF]

STS-121

- 115th flight of the Space Shuttle Program
- 32nd flight of *Discovery*
- *Discovery* first flew in 1984
- Projected Launch: May 2006
- Crewed by
  - Steve Lindsey
  - Mark Kelly
  - Michael Fossum
  - Lisa M. Nowak
  - Piers Sellers
  - Stephanie Wilson
  - Thomas Reiter

Our Approach to Understanding and Our Validation Triangle

When experiments, large-scale numerical simulations and the analytical physics-based model agree, the physics-based model is assumed to be validated.

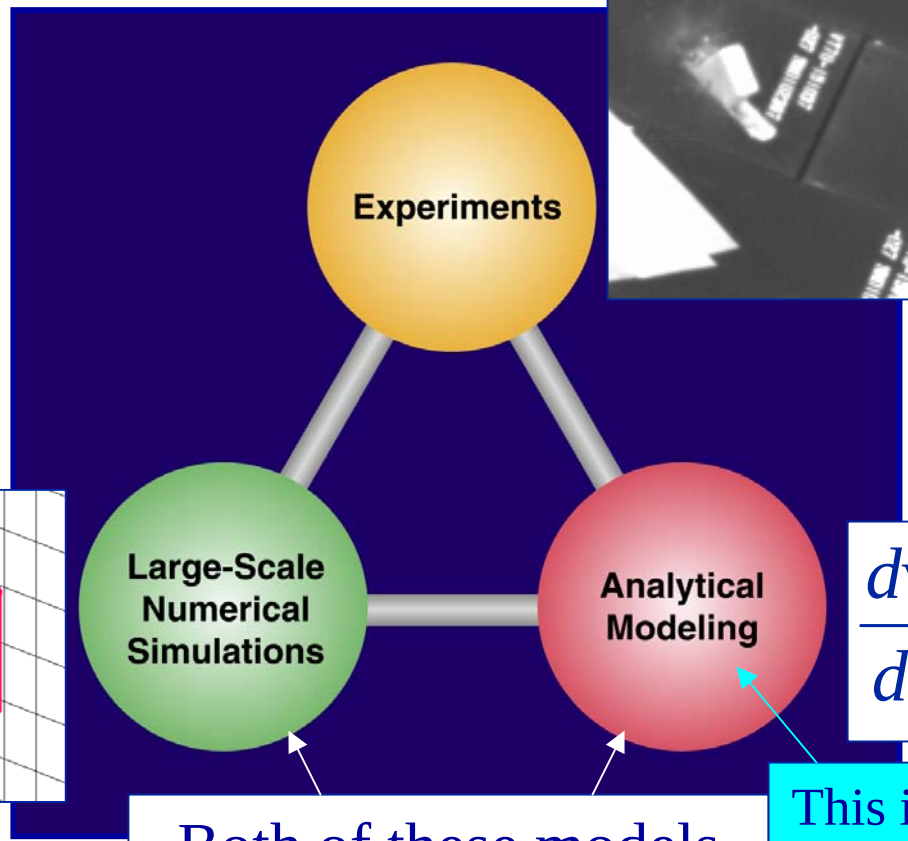

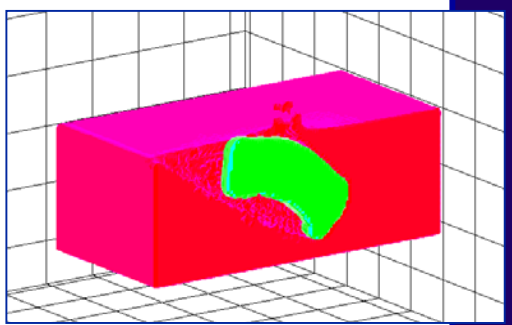

$$\frac{dv}{dt} = -\frac{\sigma_{zz}(v)}{\rho_p L}$$

Both of these models are Physics Based

This is our fast-running, physics-based model for flight

End of Charts